1-7-2021

Ontogenetic Variation in Sciaenid Otolith Morphometry with Fish Size from the Northern Gulf of Mexico

Thomas C. Ingalls
Nova Southeastern University

Thesis of
Thomas C. Ingalls

Submitted in Partial Fulfillment of the Requirements for the Degree of

Master of Science
Marine Science

Nova Southeastern University
Halmos College of Arts and Sciences

January 2021

Approved:
Thesis Committee

Major Professor: Rosanna J. Milligan, Ph.D.

Committee Member: Paul Arena, Ph.D.

Committee Member: Philip Matich, Ph.D.

HALMOS COLLEGE OF ARTS AND SCIENCES

Ontogenetic Variation in Sciaenid Otolith Morphometry with Fish Size from the Northern Gulf of Mexico

By

Thomas C. Ingalls

Submitted to the Faculty of

Halmos College of Arts and Sciences in

partial fulfillment of the requirements for the

degree of Master of Science with a specialty in:

Marine Biology

Nova Southeastern University

2021

Thesis of

Thomas C. Ingalls

Submitted in Partial Fulfillment of the Requirements for the Degree of

Master of Science

M.S. Marine Biology

Nova Southeastern University

Halmos College of Arts and Sciences

January 2021

Approved:

Thesis Committee

Major Professor: Dr. Rosanna J. Milligan

Committee Member: Dr. Paul Arena

Committee Member: Dr. Philip Matich

ABSTRACT

Sciaenids are a diverse family of coastal fishes and their fisheries are an important industry in the United States. In the northern Gulf of Mexico this industry is dominated by six species, specifically, red drum (*Sciaenops ocellatus*), black drum (*Pogonias cromis*), spotted seatrout (*Cynoscion nebulosus*), sand seatrout (*C. arenarius*), Atlantic croaker (*Micropogonias undulatus*), and spot (*Leiostomus xathurus*). Sagittal otoliths of all species were evaluated for changes in size and shape in relation to changes in fish total length and age across a variety of seasons and habitats. Evaluation of otolith morphology was done through computer-aided image analysis, specifically the R package ShapeR, and conventional shape descriptors. Results showed there were strong ontogenetic changes in otolith size and shape in all species. Otolith length and width were among the best predictors of fish total length in all species. Furthermore, otolith size metrics (i.e., otolith length, width, perimeter, area and mass) were used to determine the fish species with high accuracy (95.2%). Otolith shape was not a great predictor of fish total length nor species identification, as the development of protuberances on the surface of the otoliths over the lives of the fishes induced a wide range of shape complexities. The results provide a preliminary framework for using otolith morphology to evaluate the fish size and age in sciaenids and how the environment impacts their otolith morphology. This work is the first of its kind to be conducted on sciaenids in the northern Gulf of Mexico and improves upon our biologic and ecologic knowledge of these socioeconomically important fishes.

Keywords: Sciaenidae, Otolith, Morphology, Growth, Elliptic-Fourier, ShapeR

ACKNOWLEDGEMENTS

First and foremost, I would like to thank my advisor Dr. Rosanna Milligan for all of her advice and guidance throughout this project and my time at NSU. I would also like to thank my committee members, Dr. Paul Arena and Dr. Philip Matich for their advice and encouragement throughout my thesis research. I would also like to give extra gratitude to Dr. Matich for his willingness to give me the opportunity work with the study samples and be willing to collaborate with a budding young scientist. I would like to give thanks to Drs. Amy Hirons and Dave Kerstetter for their assistance during the early works of my thesis project. During my time at NSU I have had the privilege to work and collaborate with expert researchers, for which I will forever be a better scientist and grateful for wisdom that they imparted on me. Finally, thank you to all of my friends and family for the support they have given me during my graduate studies and my thesis research.

Table of Contents

List of Tables

List of Figures

INTRODUCTION

Otoliths

Otoliths are small, hardened structures in the heads of all teleost fishes (Campana and Thorrold 2001) that are used to understand the life history of fishes, chiefly fish size and age. The bony fish, class Osteichthyes, have three pairs of otoliths: sagittae, asterisci, and lapilli. The sagittae is generally the largest and most morphologically diverse pair, followed by the lapilli and then asterisci (Kumar 2012). The three pairs of otoliths are located in the skull, just behind the brain (Campana and Thorrold 2001).

In composition, otoliths are composed mostly of calcium carbonate (~95% by weight), giving them the common milky white appearance (Carlström 1963, Oliveira et al. 1996, Campana 1999). Accretion of calcium carbonate and the proteinaceous matrix occurs on the otolith's outer surfaces in a one-way process. Otoliths in larval fish tend to be featureless spherical or oblate structures, that develop into distinct species specific shapes as adults (Campana 1989, 2004). The development of the otolith through biomineralization of new material is controlled largely by metabolism and temperature, with accretion rates varying with time of day (e.g., night and day) and season (e.g., summer and winter, wet and dry) (Campana 1999, Campana and Thorrold 2001, Fablet et al. 2011, Wu et al. 2011). Unlike other biological structures (e.g., scales and bones) accreted material is rarely reabsorbed even in periods of heavy stress (Mugiya and Watabe 1977).

Otoliths function as sensory receptors of the surrounding environment (Mosegaar 2000, Popper and Lu 2000). The chambers that otoliths reside in are filled with endolymph fluid, allowing the otolith to 'float' inside. A sensory epithelium (macula) connects the otolith to the wall of the chamber via an otolithic membrane. Shifts in location of the otolith in the endolymph fluid, relative to the surrounding chamber, helps orientate fishes within the water column (Popper and Platt 1993). Furthermore, bundles of hair cells in the macula allow fishes to register amplitude, frequency, and direction of sound (Mosegaar 2000). While the lapilli and asterisci are generally associated with balance and orientation, and sagittae with sound detection, all three pairs interact to form part of a multi-functional sensory system (Popper and Platt 1993, Mosegaar 2000).

Because of the environmental sensory properties of otoliths, the size and shape of the otolith changes in relation to the needs of the species. For instance, pelagic fishes (e.g., tuna, mackerel, swordfish) that predominantly swim in straight lines in the open ocean, and do not rely

heavily on auditory cues for information gathering, tend to have very small otoliths in relation to body size (Vanderkoov 2009). Conversely, many nearshore species living in highly structured and turbid waters have larger and denser otoliths, in relation to body size (Vanderkoov 2009).

Through studying the changes in the development and structure of otoliths, with respect to the functions they provide to fishes, researchers have been able to utilize otoliths as biological and ecological archives to study an individuals' life history. The cyclic process of calcium carbonate accretion produces daily and yearly (referred to as annuli) rings, that has been used to estimate the age of a fish (Pannella 1971, Campana 1999). The changes to otolith morphology induced by environmental differences (e.g., water temperature) has allowed for the use of stock discrimination within the same species by way of otolith shape analysis (Schade 2019). In addition, the inert nature of otoliths and resistance to degradation is so strong that otoliths recovered from stomach contents, feces, and fossilized sediments have been used to reconstruct past diet and trophic profiles, historic fish assemblages, and even past climate regimes (Patterson 1993, 1999, Campana 2004, Byrd 2020).

Traditionally, most ecological studies using otoliths have focused on investigating the internal features of the otolith (e.g., annuli, chemical composition, and density) (Campana and Thorrold 2001, Mendoza 2006). In recent years, focus has shifted towards more external, or trait based, studies to help describe fish populations and their responses to natural or anthropogenic changes (Caillon et al. 2018, Taylor 2020). A prominent subfield in trait-based studies is morphometric analysis. The ability to use external features to extract information (e.g., age and stock) without having to modify or destroy the tissue (e.g., section the otolith) has increased its appeal as a biological and ecological evaluation method (Afanasyev 2017).

Otolith morphometrics have been used to estimate fish lengths (Hunt 1992, Zorica 2010, Bermejo 2007, 2014), discriminate between species (Tuset 2003, Kumar 2012, He et al. 2018), discriminate between stocks (Stransky et al. 2008, Ramírez-Pérez et al. 2010, Hűssy et al. 2016, Song et al. 2020), differentiate species ecological niches (Schulz-Mirbach et al. 2008, Sadighzadeh et al. 2014, Jaramillo et al. 2014), identify spatial biodiversity (Tuset 2016), and aid in diet reconstruction (Bal 2018). Additionally, otolith morphology has been used to estimate fish age by establishing patterns between number of annuli and the morphology of the otolith and has been

used to successfully estimate age in both tropical (Newman 1996, Pilling 2003, Lou 2005, Steward 2009) and temperate fish species (Doering-Aries 2008, Lepak 2012, Britton and Blackburn 2014).

Morphometry & Image Analysis

Otolith morphology can be analyzed using either metric (continuous) or meristic (discrete) traits, with metric traits (e.g., length and width) being predominantly favored for explaining size changes in otoliths. For explaining changes in the shape of otoliths, metrics alone tend to do a poor job of explaining differences in shape as there are often strong correlations between metrics that leads to redundancies in analysis (Tatsuta 2018). To better explain otolith shape, and how that shape changes over the life of an individual, an array of mathematical approaches have been applied, some of the most common of which are shape descriptors (e.g., circularity, rectangularity, ellipticity) and Elliptic Fourier analysis (EFA) (Zengin 2015, Caillon et al. 2018, Qamar 2019).

Shape descriptors are equations that use size metrics to describe the shape of otoliths. For example, the shape descriptor termed circularity uses the size metrics perimeter and area to evaluate how circular an otolith is. Shape descriptors are good for general descriptions of otolith shape (e.g., how circular the otolith is). Commonly used shape descriptors are form factor (FF), circularity (C), roundness (R), rectangularity (RC), ellipticity (E), aspect ratio (AR), and compactness (CP) (Zengin 2015, Qamar 2019, Taylor 2020). Form factor, circularity, and roundness primarily describe how close the shape of an otolith is to that of a perfect circle. In describing more of how the otolith shape is stretched and pulled in one direction, descriptors of rectangularity, ellipticity, and aspect ratio are used. Compactness indicates the smoothness of the shape's outline, with increasing development of protuberances and lobes on the edges of the otolith increasing the perimeter to area ratio (Taylor 2020). Decreases in CP can be thought of as increases in shape complexity. A limitation of shape descriptors is that different size values can be used to generate the same descriptor value, allowing for some ambiguity in what the otolith shape may actually be. In addition, different shapes may generate the same descriptor value. For instance, a result of one in AR (which uses the metrics of otolith length and width) could indicate that the otolith is either a perfect circle or a square. To avoid potential vagueness of shape descriptors more complex equations, like those used in EFA, are used to better explain the shape of the otolith.

EFA describes an otolith's shape by generating vectors from a point of origin (generally the center of the otolith) to outlying plane coordinates, and then applying a one-dimensional Fourier transformation. The vectors, termed coefficients, are then compiled into a continuous sequence (ordered from 0-360°) which then produces an estimated outline of the otolith (Rohlf 1988). Additionally, the EFA coefficients can be used as quantitative variables of otolith shape and analyzed using multivariate tests to connect otolith shape to other factors (e.g., fish size, age, and environment) (Caillon et al. 2018).

Complementing the growing field of otolith morphometric analysis is the expansion and improvement in computer-aided analyses. For a computer, or more specifically a program, to analyze otolith morphology (i.e., size and shape) the software must 1) be able to correctly identify the otolith in the image, 2) isolate the otolith from the background, and 3) know where to take measurements on the otolith.

Programs can identify and isolate an otolith from an image by classifying the pixels that make up the image into groups based on similar levels of brightness and color. The software groups the pixels based on difference thresholds (e.g., any pixel 20% different in brightness are grouped separately), typically set by the investigator. To aid in otolith identification and isolation in the image, post processing techniques (e.g., contrast enhancement, adjusting highlights and shadows, varying exposure) can be used to enhance the photograph to help the software detect the outline of the otolith (Rohlf 1988). However, it should be noted that post processing is merely a tool to help enrich photographs for desired characteristics (e.g., contrast between otolith and background), and does not fix photographs where the otolith is not orientated or illuminated properly. Therefore, it is important that time be taken to plan out the photo design to correspond to what descriptive features (e.g., length, width, perimeter, and area) are wanting to be extracted from the otolith.

To get descriptive information of the otolith most programs are coded to know how to 'read' the image (i.e., top from bottom, left from right) and which points it should measure between (e.g., points furthest distance from one another). Measurement values are generated by calibrating the image, often by connecting the number of pixels that correspond to a set physical distance (e.g., 100 pixels is equivalent to 1mm).

To assess some of the applications of computer aided otolith morphometric analysis, otoliths from members of the family Sciaenidae were investigated for size and shape differences across fish size. This family of fish is well known for having high morphological diversity in otolith size and shape (Taylor 2020) which make members of the family good candidates for morphometric comparison work.

Study Species

Marine fish in family Sciaenidae (Cuvier 1829) are ubiquitous in temperate and tropical coastal waters of the western Atlantic and eastern Pacific oceans. Worldwide, Sciaenidae contains approximately 70 genera and 270 species (Odell et al. 2017). Genera of sciaenids found in coastal waters of the United States include drums (*Sciaenops* and *Pogonias*), seatrouts (*Cynascion*), croakers (*Micropogonias*, *Roncador*, and *Umbrina*), kingfish (*Menticirrhus*), and spot (*Leiostomus xanthurus*) (Weinstein 1981). This study focused on six species of sciaenids that dominate estuarine habitats in the northern Gulf of Mexico (GOM). The species of interest were red drum (*Sciaenops ocellatus*), black drum (*Pogonias cromis*), spotted seatrout (*Cynoscion nebulosus*), sand seatrout (*C. arenarius*), Atlantic croaker (*Micropogonias undulatus*), and spot (*Leiostomus xathurus*) (Figure 1).

The study species can be categorized into three board groups, the drums, seatrouts, and croakers (Figure 1). The drums (red drum and black drum) are heavier bodied than species in the other two groups. Red drums and black drums are similar in appearance, both with elongated backs (more pronounced in black drum) leading to sub-terminal mouths. Red drums can be distinguished from black drums by the lack of barbels under the mouth, a large black spot on the upper portion of the caudal peduncle, and the lack of bars on the side of the body (Robbins 1986) (Figure 1).

Seatrouts comprise the sub-family Otolithinae. A defining characteristic of this sub-family is a larger terminal mouth with two pronounced canine teeth in the upper jaw (Weinstein 1981). Spotted seatrouts and sand seatrouts have elongated fusiform body shapes, characteristic of fast swimming fish (Weinstein 1981) (Figure 1). Spotted seatrouts can be distinguished from sand seatrouts by the presence of numerous black spots scattered on the dorsal side of the body (Robbins 1986) (Figure 1).

The croaker group is made up of the Atlantic croaker and spot. Atlantic croaker can appear similar to black drum in overall body shape (Figure 1), but can be distinguished by the presence of a prominent lateral line and a less robust body (Robbins 1996). Additionally, spot can be distinguished from Atlantic croaker by the presence of a black spot on the upper edge of the gill cover and the lack of barbels on the chin (Johnson 1978). The variations in external body morphology allow for fish to be identified correctly and ensure that the internal structures of focus (e.g., otoliths) do indeed come from the desired species.

Habitats

Being an estuary-dependent family, sciaenids are found in shallow coastal waters, estuaries, bays, and into river systems (Odell et al. 2017). The general habitat preference for the study species are sandy and muddy seafloors, which contain their preferred, infaunal prey (e.g., crustaceans, bivalves, and polychaetes) (Frimodt 1995, Odell et al. 2017). Black drums and sand seatrouts show preference for areas with higher water movement, that being large river runoffs and surf zones, respectively (Frimodt 1995). Spotted seatrouts have been known to inhabit a wider range of habitat types than other species in this study, including seagrass beds, salt marshes, and tidal pools (Frimodt 1995). Due to the wide range of physical conditions in estuarine environments, the species of this study have all adapted to a wide range of temperatures, salinities, and dissolved oxygen concentrations that vary spatially and temporally, depending on weather and seasons. The movement of sciaenids between habitats varies with seasons and life stages, that correlate with changing environmental conditions and prey abundance (White and Chittenden 1977, Weinstein 1981, Odell et al. 2017). Knowing the species habitat preferences is important in studying changes to otolith morphology as the environment the animal lives in changes the formation and eventual structure of the otolith (Campana 2004).

Size & Growth

The size and growth of each varies between species and group (Odell et al. 2017). The drum group contains the largest species in this study, in terms of both length and weight, and the species that live the longest. Red drum can reach lengths of 1550mm TL and weigh upwards of 45kg (Chao 1978, Frimodt 1995). The maximum reported age for a red drum was 50 years old

(Ross 1995). In the first three years of life, red drum generally reach lengths of 300, 530, and 700mm TL, respectively (Pearson 1929, Miles 1950, Simmons and Breuer 1962). Black drums have been recorded reaching lengths of 1700mm TL and weighing upwards of 51kg (Robbins 1986, IGFA 1991). Black drums have been reported to live upwards of 43 years (Beckman 1990). Average lengths reached in the first three years of life for black drum are 180, 330, and 430mm TL, respectively (Simmons and Breuer 1962, Richards 1973, Weinstein 1981).

Spotted seatrouts have been known to reach lengths of 1000mm TL and weigh upwards of 7.9kg (IGFA 2001). Spotted seatrouts have been reported to live upwards of 18 years (Hugg 1996). Maceina et al. (1987) found sex affected the lengths spotted seatrouts reached in the first few years of life. Averaging 227, 372, 429mm TL for males for the first three years of life, respectively (Murphy and Taylor 1994). Female spotted seatrouts are smaller in the first year but tend to be bigger in subsequent years (Murphy and Taylor 1994). The sand seatrout has been recorded to grow up to 635mm TL and weigh upwards of 2.8kg (IGFA 2001). The sand seatrout is one of the shortest-lived species in this study, only living up to five years of age (Nemeth et al. 2006). Sand seatrouts reach around 250, 425, and 573mm TL in the first three years of life, respectively (Ditty et al. 1991).

The smallest group of the study, in terms of length and weight, are the croakers. Atlantic croaker can reach lengths up to 550mm TL and weigh upwards of 2.6kg (IGFA 2001). Atlantic croakers are known to live upwards of eight years (Barger 1985). White and Chittenden (1977) found northern populations of Atlantic croaker (i.e., populations not in the GOM or south of the Carolinas') generally reach greater sizes and live longer. Atlantic croakers have been found to reach average total lengths of 201, 263, and 274mm in the first three years of life, respectively. (Barbieri 1994). The smallest species in this study was spot. Spots have been measured up to 360mm TL and weighing upwards of 450g (IGFA 2001, Robbins 1986). Spots have been reported to live up to five years (DeVries 1982). In the first three years of life spot reach approximately 150, 220, and 280mm TL, respectively (Welsh and Breder 1923, Townsend 1956, McRae et al. 1997).

Maturity

Sciaenids are seasonal broadcast spawners, producing large numbers of eggs that are released directly into the water column over extended periods of time (e.g., months, seasons). Passive mechanisms (i.e., wind, tides, and Ekman transport) are primarily responsible for the movement of fertilized eggs and larval sciaenids (Odell et al. 2017). To help facilitate the transport of larvae back to inshore nursery grounds, sciaenids will spawn in areas (e.g., tidal inlets) with favorable water movement. Juvenile sciaenid species remain in the estuary until they reach sexual maturity, at which time they migrate as adults to their respective spawning grounds (Weinstein 1981).

Of all the study species, red drum reach sexual maturity the latest, generally around four to five years of age and around 730-750mm TL (Pearson 1929, Simmons and Breuer 1962). Adult red drums spawn in late summer and fall in the mouths of channels and passes (Simmons and Breuer 1962, Peters and McMichael 1987). Simmons and Breuer (1962) found that black drums reach sexual maturity at the end of the second year, around 320 mm TL. Black drum typically spawn between February and March, however, differences in growth rates and gonadal development have suggested that a second spawning event may take place in late June or July (Pearson 1929, Simmons and Breuer 1962, Weinstein 1981). Spawning for black drum takes place near channel inlets.

In the seatrout and croaker groups maturity is reached sooner than drums. Spotted seatrouts can reach maturity in under a year, but more often reach maturity by the first summer after hatching (Miles 1950, Nieland 2002). In the coastal waters of the northern GOM spawning typically starts in March and continues until October, with a peak in April and May for spotted seatrouts (Weinstein 1981). There is strong agreement that spotted seatrouts spawn in shallow protected water within estuarine systems (Pearson 1929, Gunter 1945, Miles 1950, and Tabb 1961). Similarly, in sand seatrout, maturity is reached within the first year, around 140-180mm TL (Sutter and McIlwain 1987). This species has a prolonged spawning season that lasts from early spring to late summer in estuarine and inshore waters (Shlossman and Chittenden 1981, Sutter and McIlwain 1987).

Atlantic croakers generally mature around two years of age between lengths of 200-320mm (Weinstein 1981). However, fish caught south of Cape Hatteras on the Atlantic coast matured around one year of age, approximately 160mm TL (White and Chittenden 1977). In spot, sexual maturity is thought to occur between ages one and two, yet some year classes have been reported not reaching maturity until three years (Dawson 1958, Hales and Van Den Avyle 1989). While Dawson (1958) reported finding mature spot between 170-175mm TL, earlier research of spot found no mature individuals less than 185mm TL (Hildebrand and Cable 1930, Gunter 1945, Townsend 1956). In a review of Atlantic sciaenids, Odell et al. (2017) noted that age at maturity in spot is still not fully understood. The onset of sexual maturity is typically associated with shifts in habitat, metabolism, and body growth rates, all of which then may alter otolith morphogenesis in sciaenids.

Sciaenid Otoliths

As a family, sciaenids undergo considerable ecological and biological changes from juvenile to adults (Weinstein 1981, Taylor 2020). Additionally, through the course of development from larvae to adults, the otoliths of sciaenids also undergo consider morphological changes. Sciaenids produce very large complex otoliths, and in proportion to body size, are some of the largest otoliths of any family (Vanderkooy 2009). It has been postulated that the reason for having exceptionally large otoliths, which are more energetically taxing to produce, is due to this family's reliance on sound production and transduction for purposes of mating, feeding, and signaling arrival of predators (Ramcharitar 2006). Because sciaenids form such large and complex otoliths, they have been the used in a wide range of age, morphology, behavior, and habitat studies (Kumar 2012, Taylor 2020). However, to date, no studies have been conducted assessing the morphological changes in otolith size and shape of study species. This knowledge gap is even more surprising considering these species are of high commercial and recreational importance in GOM fisheries.

Sciaenid Fishery

The sciaenid fishery in the northern GOM primarily targets red drum, black drum, spotted seatrout, sand seatrout, Atlantic croaker, and spot. The closeness to shore has made sciaenids popular to commercial and recreational fishers. Recreationally, sciaenids are heavily targeted by fishers because of the fishes' large size as adults, fighting power when hooked, and quality of meat.

A 2002-03 fishing census showed that 74% of recreational landings in Texas were sciaenids (Boyd 2019). The reported recreational landings of all these targeted species in 2017 totaled over 67.5 million individuals (NMFS 2018a).

In 2017, spotted seatrout, sand seatrout, and Atlantic croaker were in the top five most commonly caught fishes in the GOM (NMFS 2018a). Spotted seatrout and red drum were among the most harvested species by weight in the GOM (NMFS 2018a). The 2017 commercial harvest for Atlantic croaker, spot, spotted seatrout, and sand seatrout totaled over 20,272 MT and was valued at over $10.5 million USD, collectively (NMFS 2018b). No commercial harvest reports for red or black drum were given by the NMFS (2018b), but the 2016 commercial landings of red and black drum in the GOM, reported by NOAA, were 27.4 MT and 2,711.3 MT, respectively. The GOM is a popular fishing destination, with this region seeing roughly 36% of all US based fishing trips (NMFS 2018b).

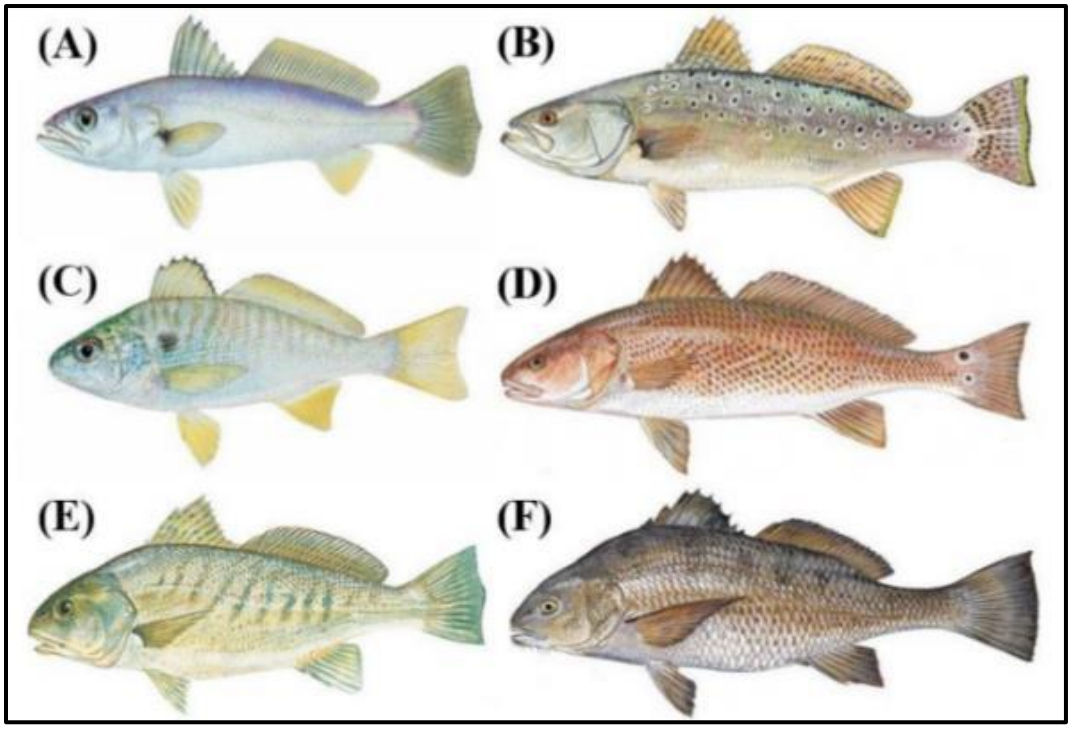

Figure 1. Study species: (A) sand seatrout, *Cynascion arenarius* (B) spotted seatrout, *C. nebulosus*, (C) spot, *Leiostomus xanthurus* (D) red drum, *Sciaenops ocellatus* (E) Atlantic croaker, *Micropogonias undulatus* and (F) black drum, *Pogonias cromis*. The species pictures (B), (D), (E), and (F) are from the South Carolina Department of Natural Resources website: www.dnr.sc.gov/marine/species. Pictures (A) and (C) are from the 'Fishes of Texas' database (Hendrickson 2015).

AIMS

The primary objective of this study was to collect and evaluate otolith morphology data of commercially and recreationally important sciaenids within a defined estuarine region in the northern GOM, specifically Sabine Lake. Comparison of otolith morphologies were made within species to assess the utility of otolith morphology as tool for discriminating fish size, and by extension, age. Focus was placed on 1) the relationship between otolith size (i.e., length, width, mass, perimeter, and area) and fish size (i.e., total length, TL); 2) the relationship between otolith shape (i.e., shape descriptors and EFA) and fish size; and 3) distinguishing between species by way of otolith size and shape. Additionally, for aims one and two, the effects of habitat and season on otolith size and shape were investigated.

MATERIALS & METHODS

Study Area

Sabine Lake is a shallow estuarine lake that straddles the border of Texas and Louisiana (Figure 2) and is formed from the southerly waterflow of the Sabine Basin, primarily the Sabine and Neches rivers. The lake is approximately 24 km in length and 11 km at its widest point, with an average depth of two meters (Wooster 2010). Sabine lake is unique among estuarine systems in Texas as it has the smallest surface area and water volume, 17,798 ha and 0.326 km^3, respectively, but has the largest surrounding marshland, 13,760 ha (Armstrong 1987, McFarlane 1996). Furthermore, this estuary concurrently experiences the least amount of evaporation (112.4 cm/year) with the highest precipitation (151.7 cm/year) (McFarlane 1996). The large flux of fresh water, both from rainfall and river inputs, into the system causes this lake to experience the lowest annual average salinity (2.3 ppt) of any Texas estuary (McFarlane 1996).

Water flows out of Sabine Lake through the tidal inlet known as Sabine Pass. An eight kilometer long waterway that connects Sabine Lake to the northern GOM. This estuarine lake contains all life stages (larval, juvenile, and adult) of all target species. Adult sciaenids use Sabine Lake as foraging and breeding grounds throughout the year. Larval and juvenile sciaenids utilize Sabine Lake as a nursery habitat. The clustering of many age classes in a relatively small area made this lake an ideal location in which to examine changes in otolith morphology.

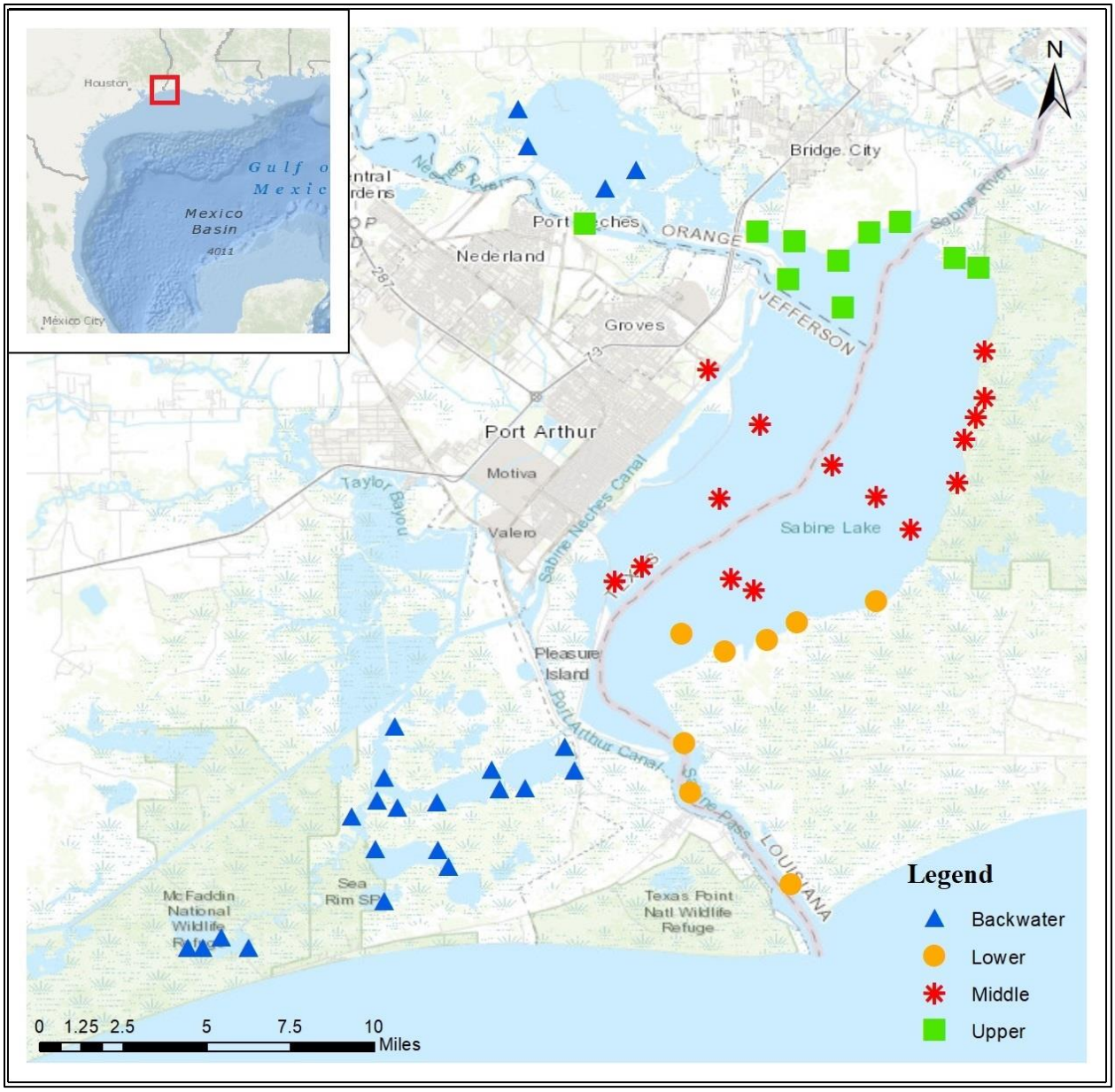

Figure 2. Map of Sabine Lake Texas/Louisiana, with sampling station overlays. The stations are classified on one of the four habitat types surveyed, backwater, lower, middle, and upper.

Sampling

All samples were collected by Texas state resource managers of the Texas Parks and Wildlife Department opportunistically. Sampling was permitted under Sam Houston State University, IACUC 16-02-18-1003-3-01. Fish were captured using monofilament gill nets, bag seines, and otter trawls, to sample nearshore individuals across a range of age classes. Gill nets were 183 m x 1.2 m, comprised of 45.7 m sections of 7.6 cm, 10.2 cm, 12.7 cm, and 15.2 cm stretched mesh tied together in ascending order set perpendicular from the shoreline. Bag seines were 18.3 m x 1.8 m, comprised of 1.3 cm stretched nylon monofilament mesh, pulled along shore for an area sweep of 0.03 hectares. The otter trawls were 6.1 m wide with 38 mm stretched nylon multifilament mesh, towed at 4.8 km $hour^{-1}$ for 10 minutes.

All sampling took place between April and November 2018. Gill net sampling took place between April and June (N=45) and September and November (N=45). Bag seines and otter trawls were pulled 20 times each per month (April to November). Fish were sampled in four different habitat types (backwater, upper, middle, and lower) in and around Sabine Lake (Figure 2). Each specimen was given a unique ID number and the following metadata were recorded: date-of-capture, latitude, longitude, sampling gear, total depth (m), temperature (°C), salinity and dissolved oxygen concentration (ppm). The species identity, standard length (mm), total length (mm), and wet weight (g) of each fish were recorded by Dr. Matich and colleagues.

Size & Body Corrections

For the few individuals that were missing total length (TL) data, the TL was estimated from the standard length (SL) of the collected samples using linear regression equations between SL and TL. Fish body condition was evaluated using Fulton's condition factor (*K*) – calculated by dividing body mass by the cube of TL, multiplied by 1000 to give the units of kg m^{-3} (Stevenson and Woods 2006). Otolith metrics (i.e., length, width, mass, perimeter, and area) were standardized by dividing by fish TL.

Laboratory techniques

Sagittae from all specimens were removed by making a horizontal cross section through the cranium just dorsal of the eye to expose the inner ear chambers that the otoliths are located in

(following the methods of Towne 2018), and the otoliths were removed. Immediately following extraction, the otoliths were cleaned with distilled water to help prevent potential decomposition that could erode the surface of the otolith and alter its morphology (Milton and Chenery 1998). Cleaned otoliths were dried in a drying oven (40^{o}C) for five minutes and then stored in individually labeled, cushioned boxes. Otoliths that were broken (e.g., cracked in half) were removed from analysis.

Imaging

Otoliths are typically measured in one of three planes: anteroposterior (length), dorsoventral (width), and proximodistal (thickness) (Campana and Casselman 1993, Burke 2008). To meet these standards the proximal, distal, and dorsal side of all pairs of otoliths were photographed. A combination of a Nikon D3500 with an 18-55 mm lens and a Canon EOS 77D with a 100 mm F2.8 macro lens were used to capture all otolith images. Otoliths were illuminated either using two 250 watt halogen lights, or three battery powered LED push-lights, and camera flash. The use of some or all the lighting units depended on the otolith being photographed to best illuminate the subject. Best illumination was considered to be creating strong contrast between the otolith and the background, reduction of shadows from the curvature of the otolith, and avoidance of over-proper exposure of the otolith.

For consistent standards in the photographs, the left otolith and right otolith were orientated adjacent to one another , such that when the image was captured of the pair, the left otolith was on the left side of the photograph and the right on its respective side (Figure 3). The left and right otoliths were differentiated from one another by orientation of sulcus groove, consistently located on the proximal side of the otolith. Additionally, the otoliths were orientated with the anterior side facing towards the top of the photo, verified by the position of ostium on the anterior-proximal side of the otolith, and the caudal points of each otolith pointing towards one another (Figure 3). Otolith thickness was not evaluated in the present study because only otoliths with thicknesses greater than 0.90 mm were able to be photographed using the cameras and lenses available, leading to thickness not being uniformly captured across all species. The orientation schemes were reflections of how the otoliths would be generally orientated within the cranium.

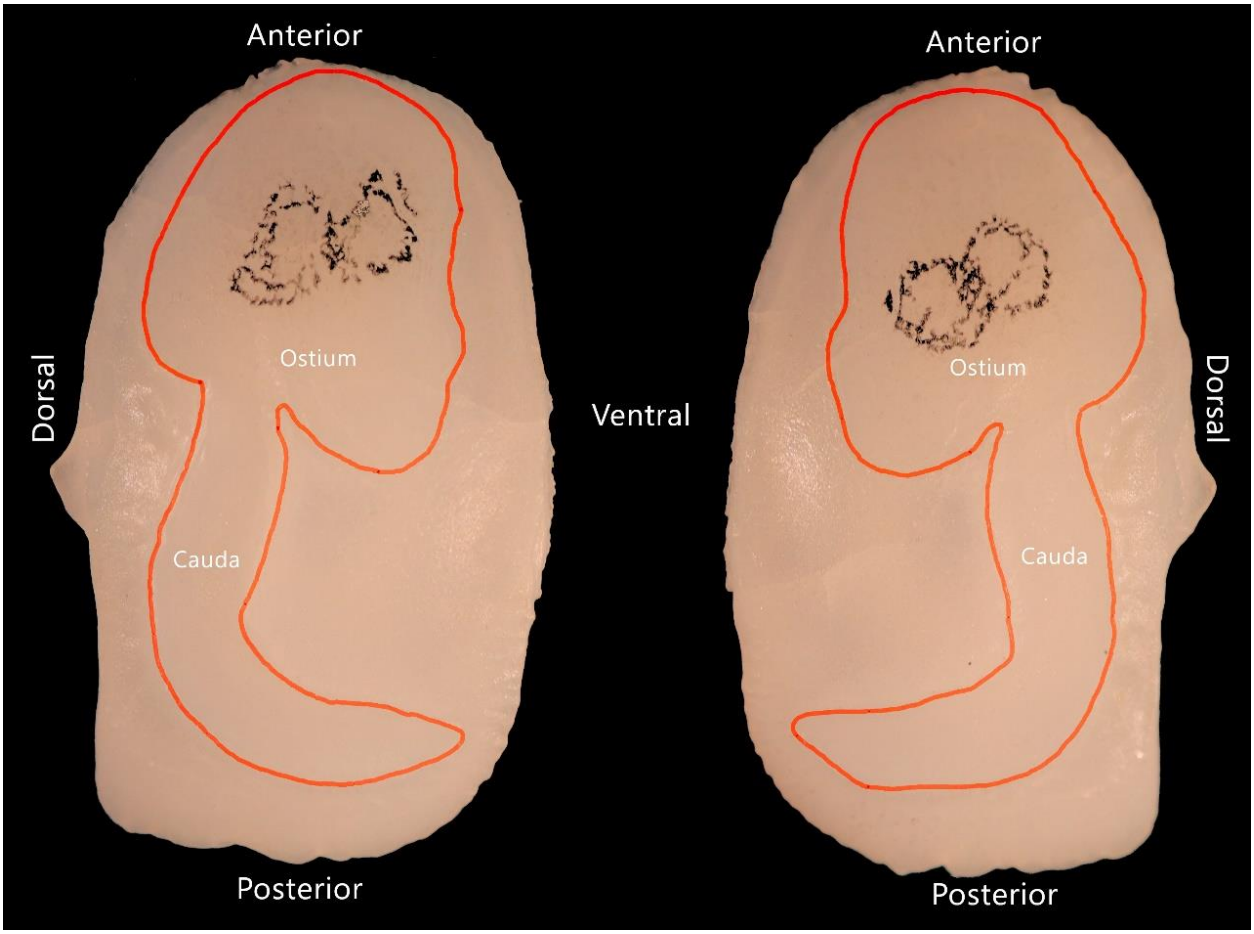

Figure 3. Proximal view of red drum sagittae highlighting the orientation of the otolith with respect to the sulcus, orange outline, comprised of the ostium and cauda.

Photographs were edited using the free image manipulation software GIMP (GNU Image Manipulation Program, ver. 2.10) (GIMP Development Team 2020). GIMP was used to isolate the otolith from the image background and replace it with a pure black color to remove any 'noise' (e.g., dust particles or reflections) that the shape analysis program (ShapeR, Libugnan and Pálsson 2015) may mis-interpret as otolith outlines. Additionally, GIMP was used for photograph calibration that was needed for the ShapeR to measure otolith metrics. Calibration was done by measuring the number of pixels that corresponded to 1mm on a ruler, that was photographed alongside the otoliths.

ShapeR is a package in R software (R Core Team 2020) that was used to extract, visualize, and generate otolith size and shape data through a series of automatic processes pre-built into the

package (Libugnan and Pálsson 2015). The package accomplishes this by first reading a text file in csv format (*.csv) that contained all biological information of the specimens, and all pertinent information of the photographs (i.e., designated folder name, photograph names, and calibration measurements). ShapeR then analyzed each photograph, in the designated folder, extracting size measurements and shape coefficients of the otolith. Following procedures laid out in Libugnan and Pálsson (2015), a second set of photographs was included in the designated folder for the program to perform quality control checks on its interpretation of the otolith. Prior to exporting otolith metrics and Elliptic Fourier coefficients (EFC) from the program, the assigned outlines of each otolith were manually inspected to verify the package had indeed correctly identified the outline of the otolith. It was important that the generated outline matched that of the otolith perimeter as the generated outline is what the program used to interpret all size and shape measurements. Photographs where the otolith was mis-outlined (e.g., the packages overlaying red outline did not match to the otoliths perimeter) were re-ran under different threshold levels until the package correctly outlined the otolith. All data was exported as *.csv files to be used for further analyses.

Otolith Size

Size measurements outputted from ShapeR were otolith length, width, perimeter, and area (Libugnan and Pálsson 2015). ShapeR measured length as the longest point-to-point distance between the anterior and posterior ends of the otolith (Figure 4). Width was measured as the longest point-to-point distance between the dorsal and ventral sides of the otolith that was perpendicular to the length measurement (Figure 4). Otolith perimeter was equal to the distance of the generated outline of the otolith. Area was equal to all the space inside of the produced otolith outline (Figure 4). Otoliths were weighed to the nearest 0.001g on a calibrated digital scale with draught shields, model AMF204. The digital measurements, in addition to otolith mass, were the metrics that were used to explained otolith size.

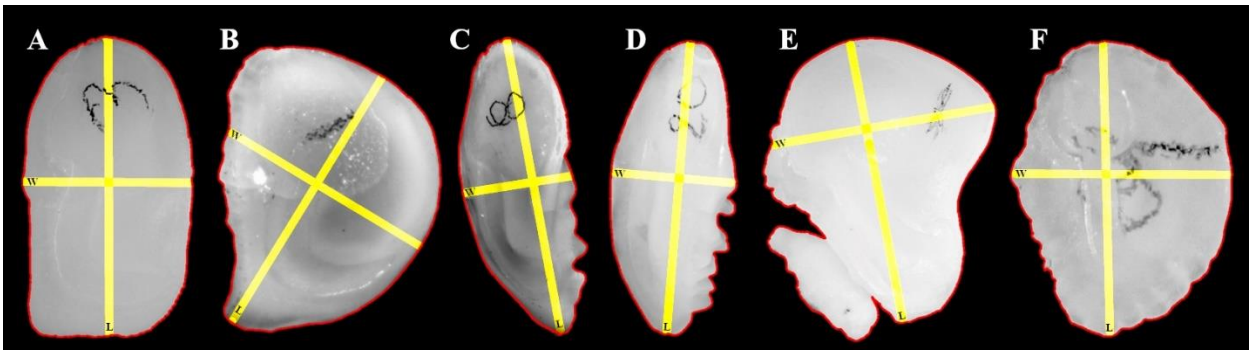

Figure 4. Images produced by ShapeR showing the overlaid outline (red) around the perimeter of the otolith. Yellow lines were added to show the general zones of what the package interpreted as length (L) and width (W). In order from A to F the species were red drum, black drum, spotted seatrout, sand seatrout, Atlantic croaker, and spot, respectively.

Otolith Shape

Otolith shape was evaluated using shape descriptors and EFC. The shape descriptors were form factor (FF), circularity (C), roundness (R), rectangularity (RC), ellipticity (E), aspect ratio (AR), and compactness (CP) . The equations used to measure these shape descriptors are listed below. The equations for FF, C, and R were taken from Zengin (2015), RC, E, and AR were taken from Qamar (2019), and CP was taken from Taylor (2020). Size metrics used in the equations were otolith length (OL), otolith width (OW), area (OA), and perimeter (OP).

$$FF = \frac{(4\pi OA)}{OP^2} \qquad C = \frac{P^2}{OA}$$

$$R = \frac{4OA}{\pi OL^2} \qquad RC = \frac{OA}{(OL)(OW)}$$

$$E = \frac{(OL - OW)}{(OL + OW)} \qquad AR = \frac{OL}{OW}$$

$$CP = \frac{OP}{OA}$$

ShapeR is coded to generate 48 normalized Elliptic Fourier coefficients for each otolith. Three coefficients are automatically excluded from the results, by the package, because they were used to standardize the starting point, rotation, and size of the otolith (Libungan and Pálsson 2015). Of the 45 coefficients that remained, any coefficients that significantly covary were then removed

by ShapeR. Depending on the number of coefficients that were the removed by the package, the remaining number of coefficients available for analysis were $n \leq 45$. The remaining EFC were exported from ShapeR and analyzed in PRIMER v7 (Primer Development Team 2020) for differences in shape across changing size in the samples.

Aging

Due to access and time constraints of laboratory space from the COVID-19 pandemic, it was not possible to age the specimens by way of traditional aging methods (e.g., increment analysis). As such, ages of fishes were estimated from TL based on general length-at-age from the literature. Mean age of each species was estimated from the mean TL of the species.

Data Analyses

Abiotic Variables

Abiotic variables (i.e., depth, temperature, salinity, and dissolved oxygen (DO)) were analyzed for differences between habitat and season by means of two-way analysis of similarities (ANOSIM) to examine environmental changes over the study period.

Fish Size & Body Condition

A one-way analysis of variance (ANOVA) was used to test for significant differences in TL, wet weight, and body condition between species. Body condition was evaluated using Fulton's condition factor (*K*). A one-way analysis of variance (ANOVA) was used to test for significant differences between *K* and species.

Otolith Size

Otolith length, width, perimeter, area, and mass (hereafter 'metrics') were tested against fish TL using linear regressions ($y = mx + b$). Area and mass were transformed when plotted against TL, square-rooted and logged, respectively. For comparison of metrics between species, the metrics were standardized by dividing by fish TL.

Otolith Shape Descriptors

Form factor, roundness, circularity, ellipticity, rectangularity, and aspect ratio (hereafter 'descriptors') were tested against fish TL using linear regressions ($y = mx + b$). Compactness was tested against fish TL using power regressions ($y = a(x^b)$).

Elliptic Fourier Coefficients

Elliptic Fourier coefficients (hereafter 'EFC') of all species were visually assessed using non-metric multi-dimensional scaling (nMDS) plots to identify potential shape clustering. The variable tested in the nMDS plots was fish size (i.e., TL). Linkage tree analysis (LINKTREE) and literature analysis of species size and growth were used to approximate how to best sub-group the variable fish size. One-way ANOSIM's were conducted to test for significant differences in EFC between fish size groups. Two-way ANOSIM's were conducted to see if there were significant differences between EFC and seasons and habitats.

Species Prediction

Canonical Analysis of Principle Coordinates (CAP) was conducted to assess whether the different measures of otolith size and shape could be used to correctly predict species identity. A CAP was conducted, separately, for otolith metrics, descriptors, and EFC, to evaluate the predictive power of each method.

RESULTS

Abiotic Variables

Abiotic variables are summarized in Table 1. Water depth increased, on average, the closer the habitat (e.g., lower basin) was to the tidal inlet of Sabine Lake. The water depth was significantly deeper in the southern region of Sabine Lake compared to the northern region, $p = 2.2 \times 10^{-16}$ (Table 1). Water temperature changed over the course of sampling – peaking in summer months (Figure 5). Between habitats and seasons, water temperature was significantly different, $p = 4.7 \times 10^{-4}$ and $p = 2.2 \times 10^{-16}$, respectively (Table 1). Salinity was more dynamic over the course of sampling than temperature (Figure 6). There were significant differences in salinity between habitats and seasons, $p = 5.3 \times 10^{-14}$ and $p = 2.2 \times 10^{-16}$, respectively (Table 1). The dissolved oxygen (DO) levels appeared to vary inversely with water temperature over the course of the study (Figure 7). DO was not significantly different between habitats but was significantly different between seasons, $p = 0.21$ and $p = 5.1 \times 10^{-9}$, respectively (Table 1).

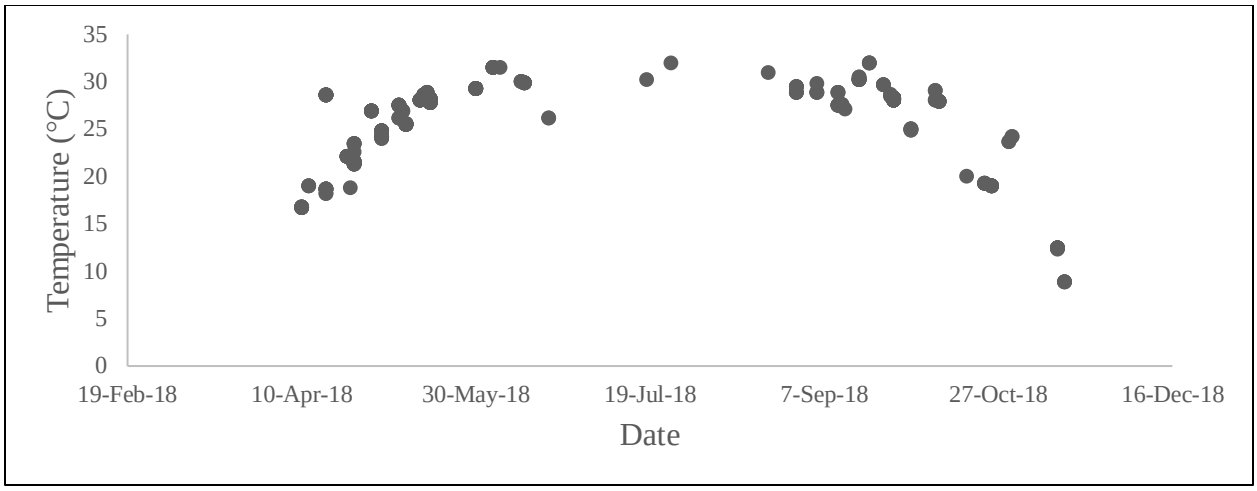

Figure 5. Water temperature at time of capture across sampling period.

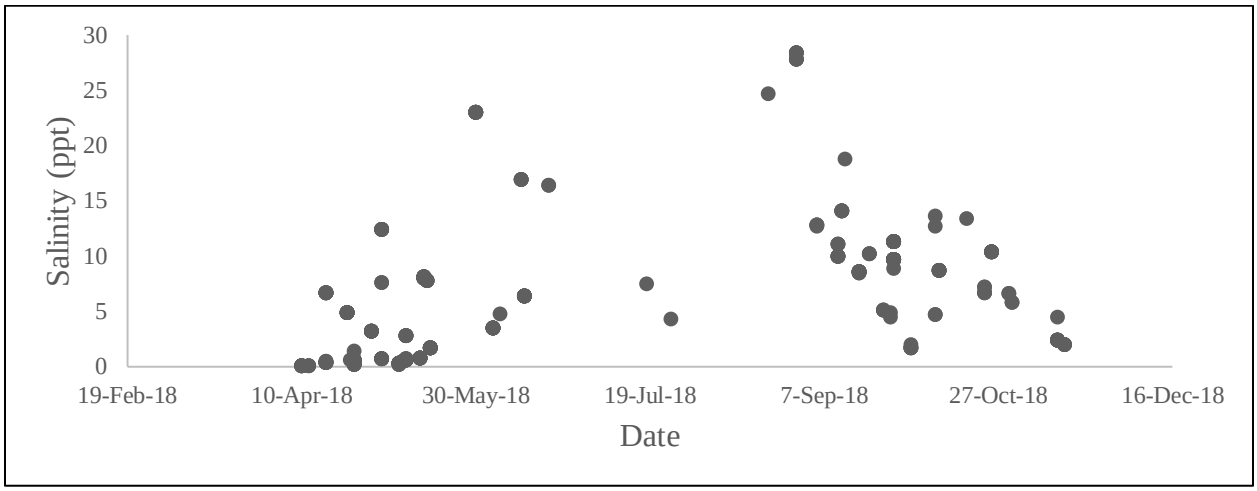

Figure 6. Salinity at time of capture across sampling period.

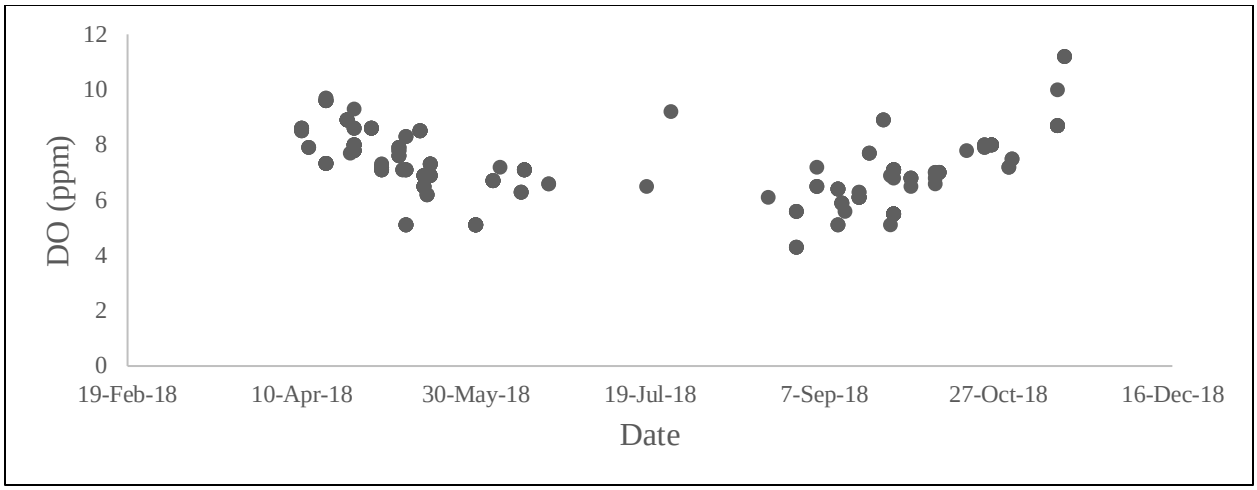

Figure 7. Dissolved oxygen (DO) at time of capture across sampling period.

Table 1. Summary of abiotic factors collected at time of capture.

Habitat	Factor	Min	Max	Mean
Backwater	Depth (m)	0.50	1.40	0.96
	Temperature (°C)	12.30	32.00	25.03
	Salinity (ppt)	1.70	28.40	9.05
	Dissolved Oxygen (ppm)	4.30	10.00	7.26
Upper	Depth (m)	0.30	2.10	1.07
	Temperature (°C)	16.70	31.50	24.68
	Salinity (ppt)	0.10	14.10	3.00
	Dissolved Oxygen (ppm)	5.10	8.60	7.39
Middle	Depth (m)	1.00	2.40	1.87
	Temperature (°C)	19.30	32.00	26.42
	Salinity (ppt)	0.20	11.30	4.83
	Dissolved Oxygen (ppm)	5.50	9.30	6.98
Lower	Depth (m)	0.40	12.50	4.40
	Temperature (°C)	8.90	31.00	26.53
	Salinity (ppt)	0.40	24.70	9.37
	Dissolved Oxygen (ppm)	5.10	11.20	7.15

Samples

A total of 380 individuals across all six species were captured. Ultimately, 335 individuals were retained for the analysis: 58 red drums, 33 black drums, 29 spotted seatrouts, 32 sand seatrouts, 115 Atlantic croakers, and 68 spots. The coefficient and y-intercept used in the linear regressions for estimating total length (TL) of individuals missing TL data are listed the Table 2 below – calculated from standard length (SL) and TL of sample data.

Table 2. Linear regressions between TL and SL, TL = m(SL) + b

Species	*m*	*b*	*r2*
Red Drum	1.1695	14.771	0.99
Black Drum	1.1578	24.83	0.99
Spotted Seatrout	1.1408	7.8701	0.99
Sand Seatrout	1.1907	5.1467	0.99
Atlantic Croaker	1.1861	6.3625	0.99
Spot	1.3085	-1.7779	0.99

Fish TL was significantly different across all species ($p = 2.2 \times 10^{-16}$), with red drum being the longest and spot being the shortest, on average (Figure 8, Table 3). The average wet weight (WW) of each species was significantly different between the species ($p = 2.2 \times 10^{-16}$), with red drum being the heaviest species on average and spot being the lightest (Figure 9, Table 3). Body condition for most of the specimens were near, or above expected, as assessed by Fulton's condition factor (*K*) (Figure 10, Table 3).

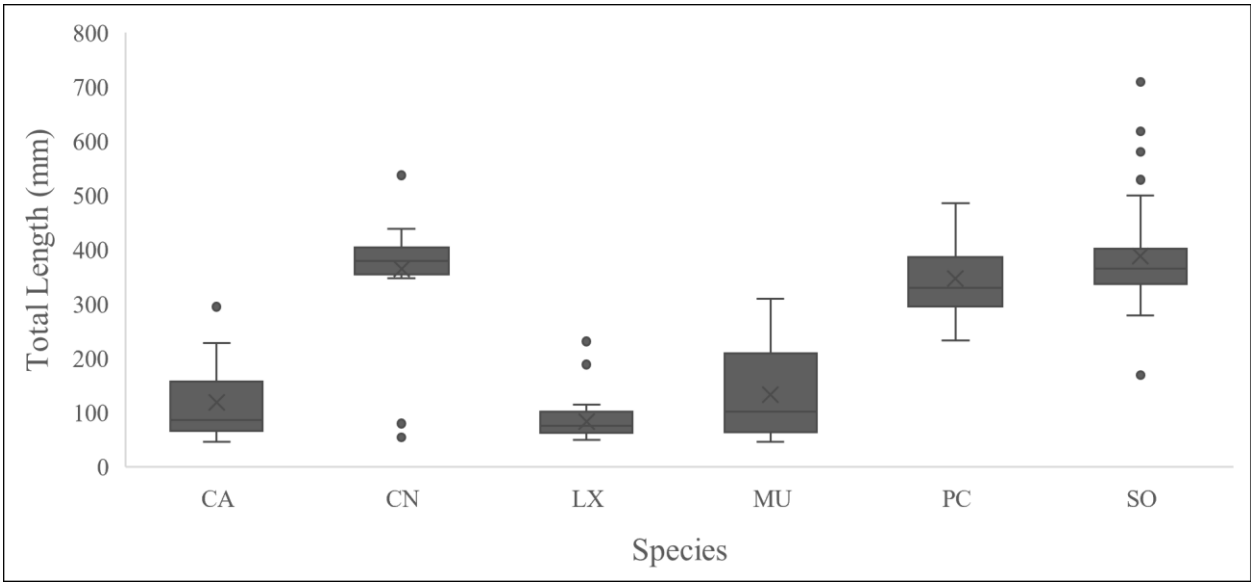

Figure 8. Box and whisker plot of fish length for all species. Red drum (SO), black drum (PC), Atlantic croaker (MU), spot (LX), spotted seatrout (CN), sand seatrout (CA).

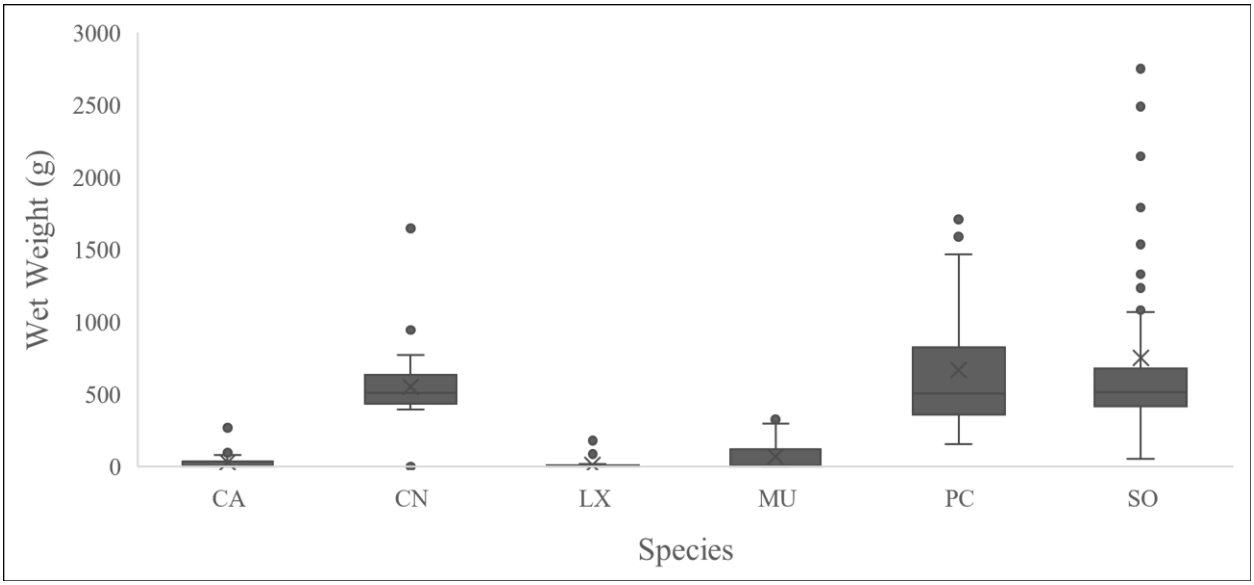

Figure 9. Box and whisker plot of fish mass for all species. Red drum (SO), black drum (PC), Atlantic croaker (MU), spot (LX), spotted seatrout (CN), sand seatrout (CA).

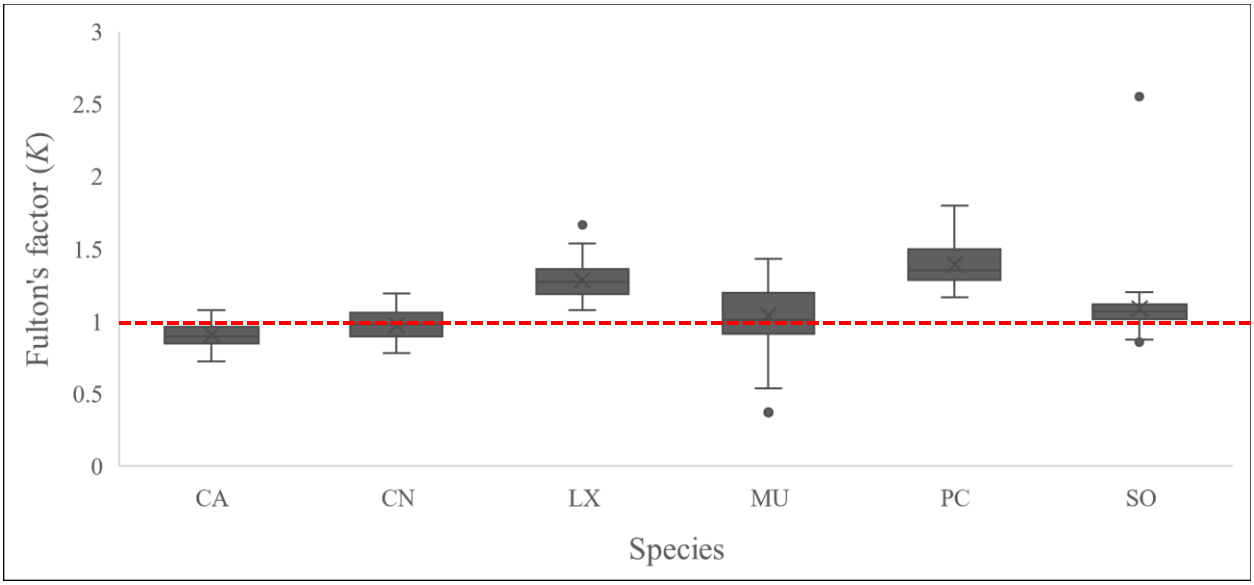

Figure 10. Box and whisker plot of fish body condition for all species. Red drum (SO), black drum (PC), Atlantic croaker (MU), spot (LX), spotted seatrout (CN), sand seatrout (CA). The red dashed line indicates expected body condition, a value of 1.

Table 3. Minimum, maximum, mean, and standard deviation (±SD) for fish total length (TL), wet weight (WW), and Fulton's condition (*K*) across all species.

Species	Parameter	Min	Max	Mean	(±SD)
Red Drum	TL (mm)	169.00	709.00	388.47	90.26
	WW (g)	53.70	4082.00	750.25	691.16
	K (kg m^{-3})	0.86	2.55	1.09	0.21
Black Drum	TL (mm)	233.00	486.00	346.88	68.36
	WW (g)	155.60	1716.10	667.18	450.26
	K (kg m^{-3})	1.17	1.80	1.39	0.16
Spotted Seatrout	TL (mm)	55.00	537.00	364.86	88.94
	WW (g)	1.40	1646.90	551.64	285.43
	K (kg m^{-3})	0.78	1.19	0.97	0.10
Sand Seatrout	TL (mm)	47.00	295.00	118.58	63.04
	WW (g)	0.93	270.10	30.78	52.62
	K (kg m^{-3})	0.72	1.08	0.91	0.08
Atlantic Croaker	TL (mm)	46.00	310.00	133.73	84.37
	WW (g)	0.41	364.30	70.54	106.94
	K (kg m^{-3})	0.37	1.43	1.04	0.20
Spot	TL (mm)	50.00	231.00	83.88	29.72
	WW (g)	1.56	180.00	11.33	23.53
	K (kg m^{-3})	1.08	1.67	1.28	0.12

Age

The mean estimated ages for each species, based on length at age from the literature, are listed in Table 4. The distribution of estimated ages across individuals is shown in Figures 11 and 12. All species, except black drum, had individuals under one year of age (Figure 11). Sand seatrout was the only species sampled to not have any individuals over two years of age (Figure 12).

Table 4. Mean age of each species based on general length-at-age from the literature.

Species	Avg. Age (yr.)	References
Red Drum	1-2	Pearson 1929, Miles 1950, Simmons and Breuer 1962
Black Drum	2	Simmons and Breuer 1962, Richards 1973, Weinstein 1981
Spotted Seatrout	1-2	Murphy and Taylor 1994
Sand Seatrout	<1	Ditty et al. 1991
Atlantic Croaker	<1	Barbieri 1994
Spot	<1	Welsh and Breder 1923, Townsend 1956, McRae et al. 1997

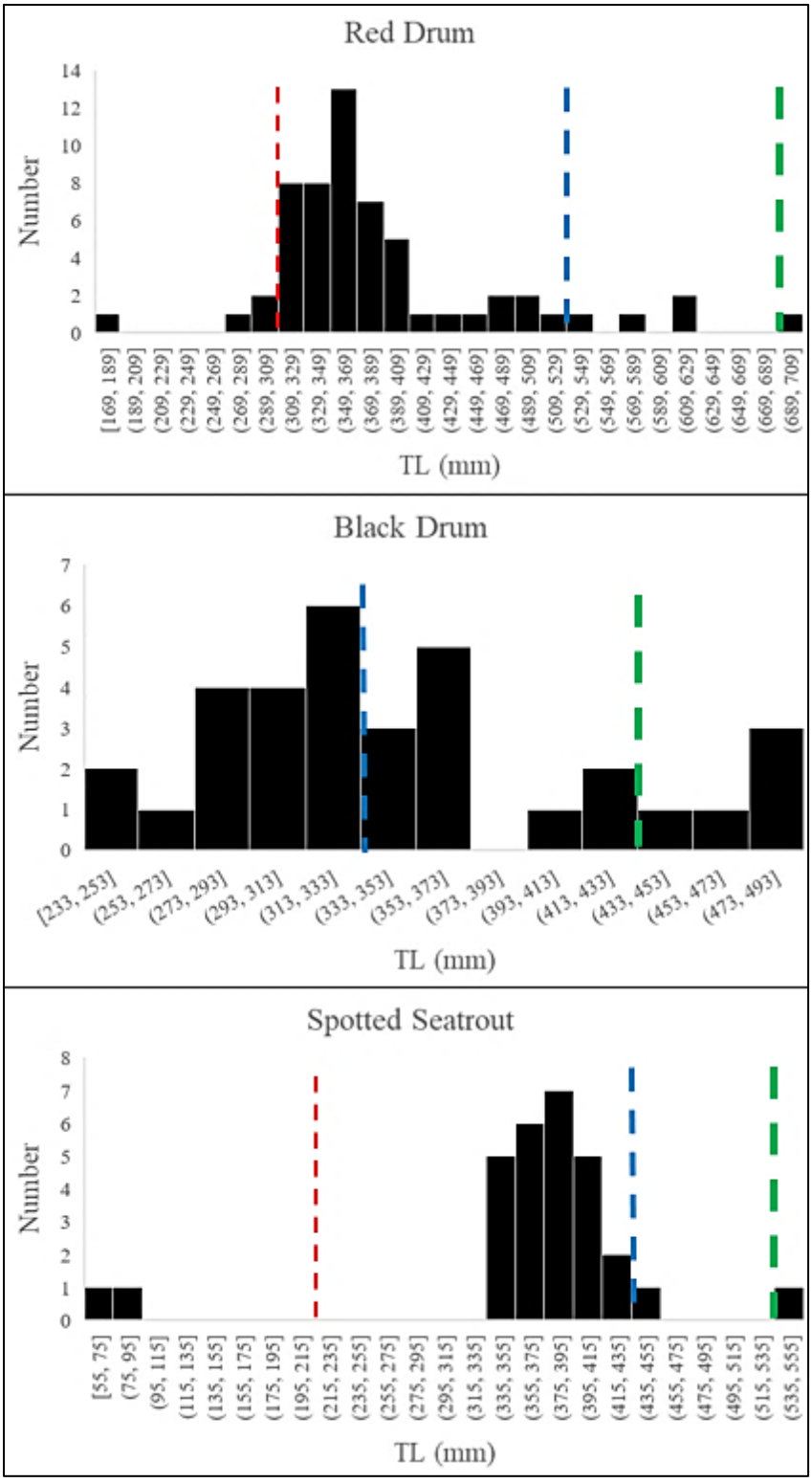

Figure 11. TL frequency distribution of red drum, black drum, and spotted seatrout with age lines (i.e., 1 year red, 2 years blue, 3 years green) overlaid on their corresponding size, where applicable, based on the length-at-age estimates from the literature.

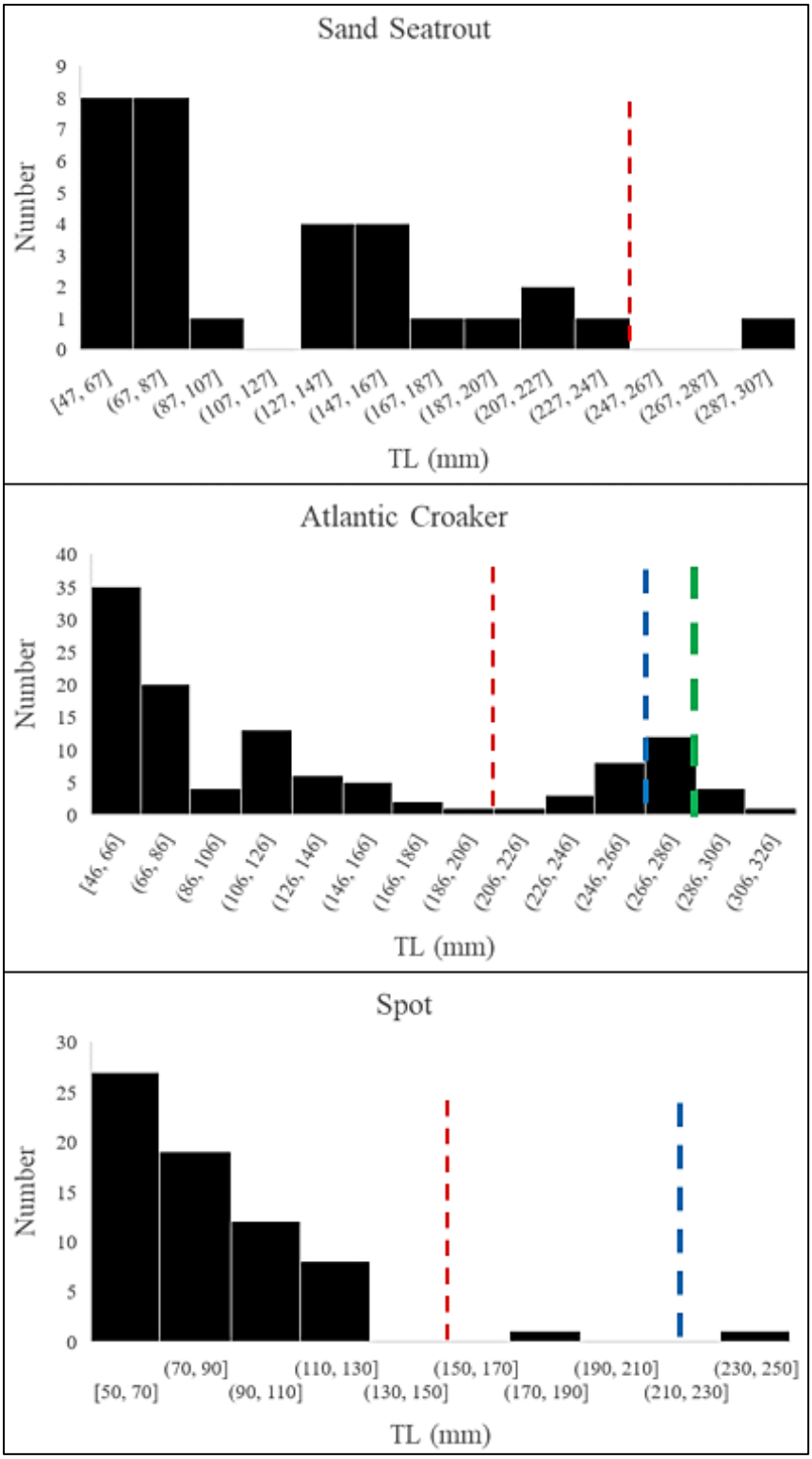

Figure 12. TL frequency distribution of sand seatrout, Atlantic croaker, and spot with age lines (i.e., 1 year red, 2 years blue, 3 years green) overlaid on their corresponding size, where applicable, based on the length-at-age estimates from the literature.

Otolith Metrics

Table 5 summarizes the standardized otolith metrics, specifically, otolith mass (OM), otolith length (OL), otolith width (OW), otolith perimeter (OP), and otolith area (OA). All metrics increased in value with increases in TL (Figures 13-18, Table 6). Correlations between TL and metrics varied between species. The smaller species of the study (i.e., Atlantic croaker, spot, and sand seatrout) showed the strongest relationships between TL and all metrics (Figures 13-18, Table 6). The larger species in the study (i.e., red drum, black drum, and spotted seatrout) did not have as strong relationships between TL and metrics (Figures 13-18, Table 6).

Table 5. Summary of the minimum, maximum, mean, and standard deviation (±SD) of standardized otolith metrics across all species.

Species	Metric	Min	Max	Mean	(±SD)
Red Drum	OM (g)	0.0004	0.0017	0.0009	0.0002
	OL (mm)	0.0278	0.0488	0.0330	0.0032
	OW (mm)	0.0155	0.0306	0.0204	0.0026
	OP (mm)	0.0835	0.1420	0.0986	0.0098
	OA (mm^2)	0.1626	0.3373	0.2058	0.0247
Black Drum	OM (g)	0.0006	0.0018	0.0012	0.0003
	OL (mm)	0.0277	0.0389	0.0339	0.0024
	OW (mm)	0.0226	0.0304	0.0272	0.0019
	OP (mm)	0.0979	0.1354	0.1181	0.0081
	OA (mm^2)	0.1837	0.2983	0.2436	0.0259
Spotted Seatrout	OM (g)	< 0.0001	0.0016	0.0012	0.0003
	OL (mm)	0.0364	0.0540	0.0457	0.0034
	OW (mm)	0.0164	0.0310	0.0193	0.0031
	OP (mm)	0.1067	0.1534	0.1300	0.0106
	OA (mm^2)	0.0672	0.2608	0.2167	0.0408
Sand Seatrout	OM (g)	0.0001	0.0008	0.0003	0.0002
	OL (mm)	0.0473	0.0610	0.0550	0.0031
	OW (mm)	0.0218	0.0368	0.0300	0.0050
	OP (mm)	0.1202	0.1708	0.1492	0.0114
	OA (mm^2)	0.0650	0.2182	0.1328	0.0442
Atlantic Croaker	OM (g)	0.0001	0.0025	0.0007	0.0006
	OL (mm)	0.0421	0.0662	0.0536	0.0048
	OW (mm)	0.0294	0.0509	0.0397	0.0033
	OP (mm)	0.1217	0.2056	0.1639	0.0128
	OA (mm^2)	0.0927	0.4159	0.1895	0.0936
Spot	OM (g)	0.0001	0.0002	0.0001	0.0000
	OL (mm)	0.0342	0.0533	0.0455	0.0039
	OW (mm)	0.0173	0.0412	0.0326	0.0048
	OP (mm)	0.0910	0.1630	0.1346	0.0135
	OA (mm^2)	0.0730	0.1150	0.0866	0.0077

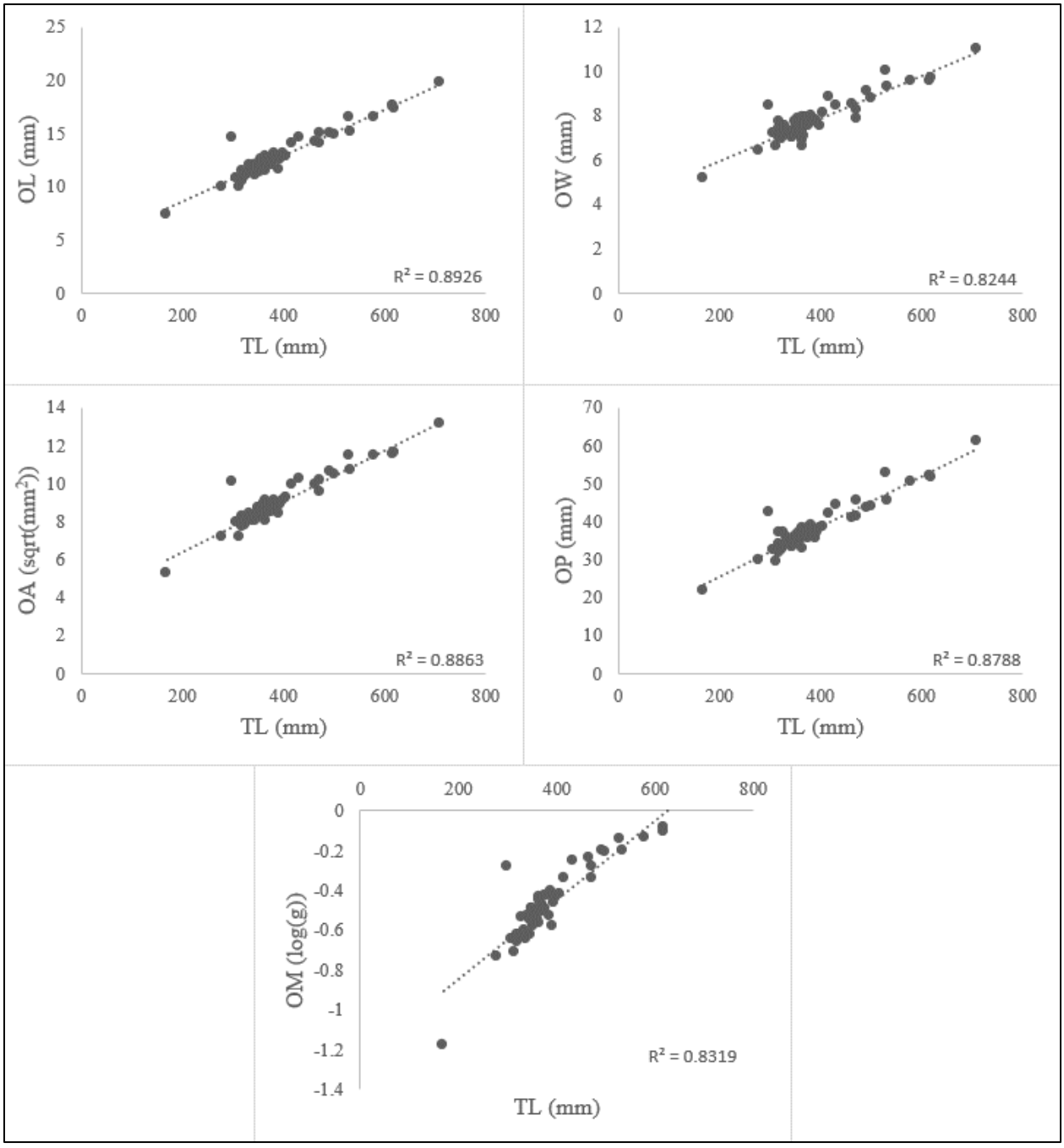

Figure 13. Linear regressions between TL and metrics in red drums.

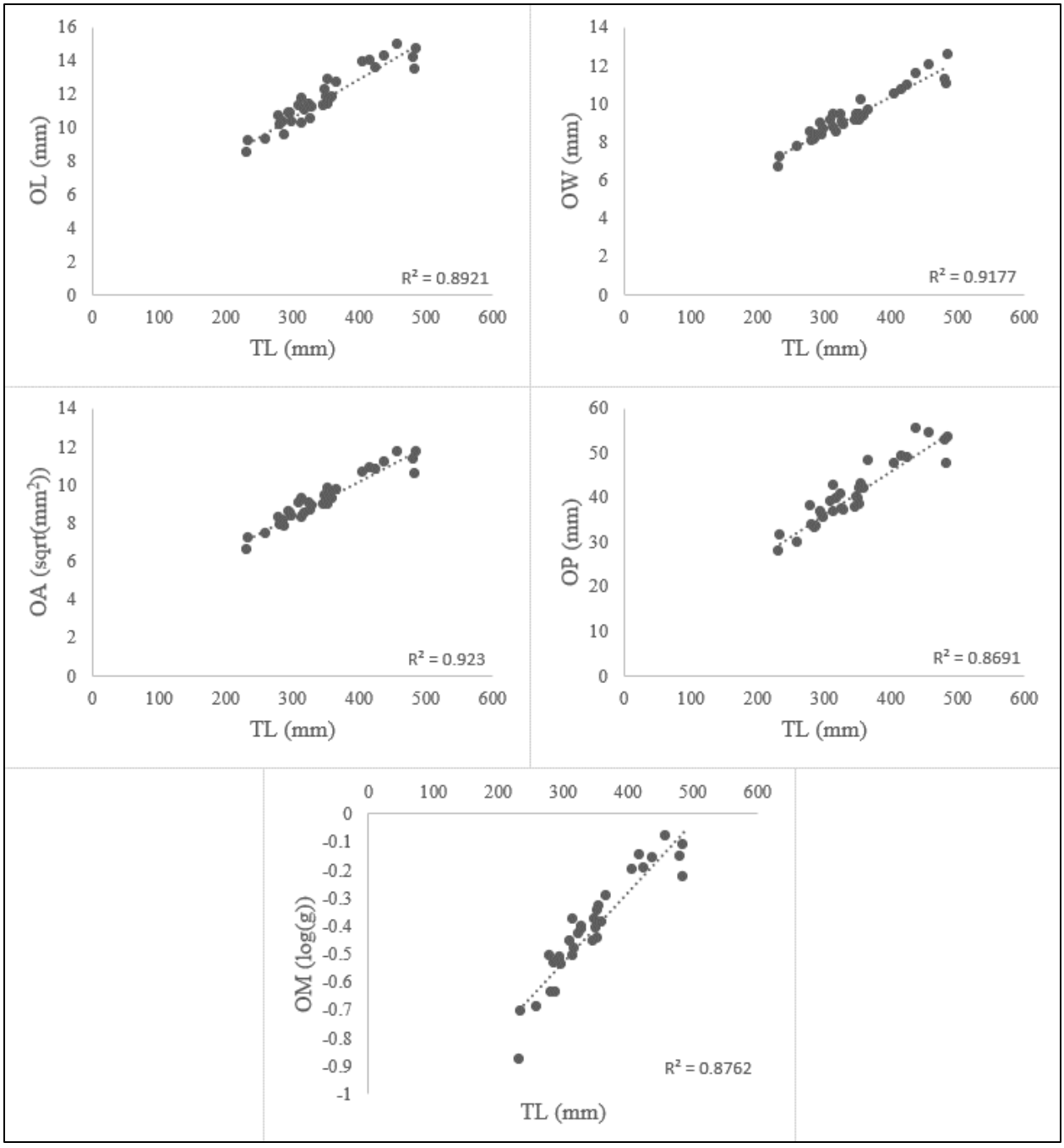

Figure 14. Linear regressions between TL and metrics in black drums.

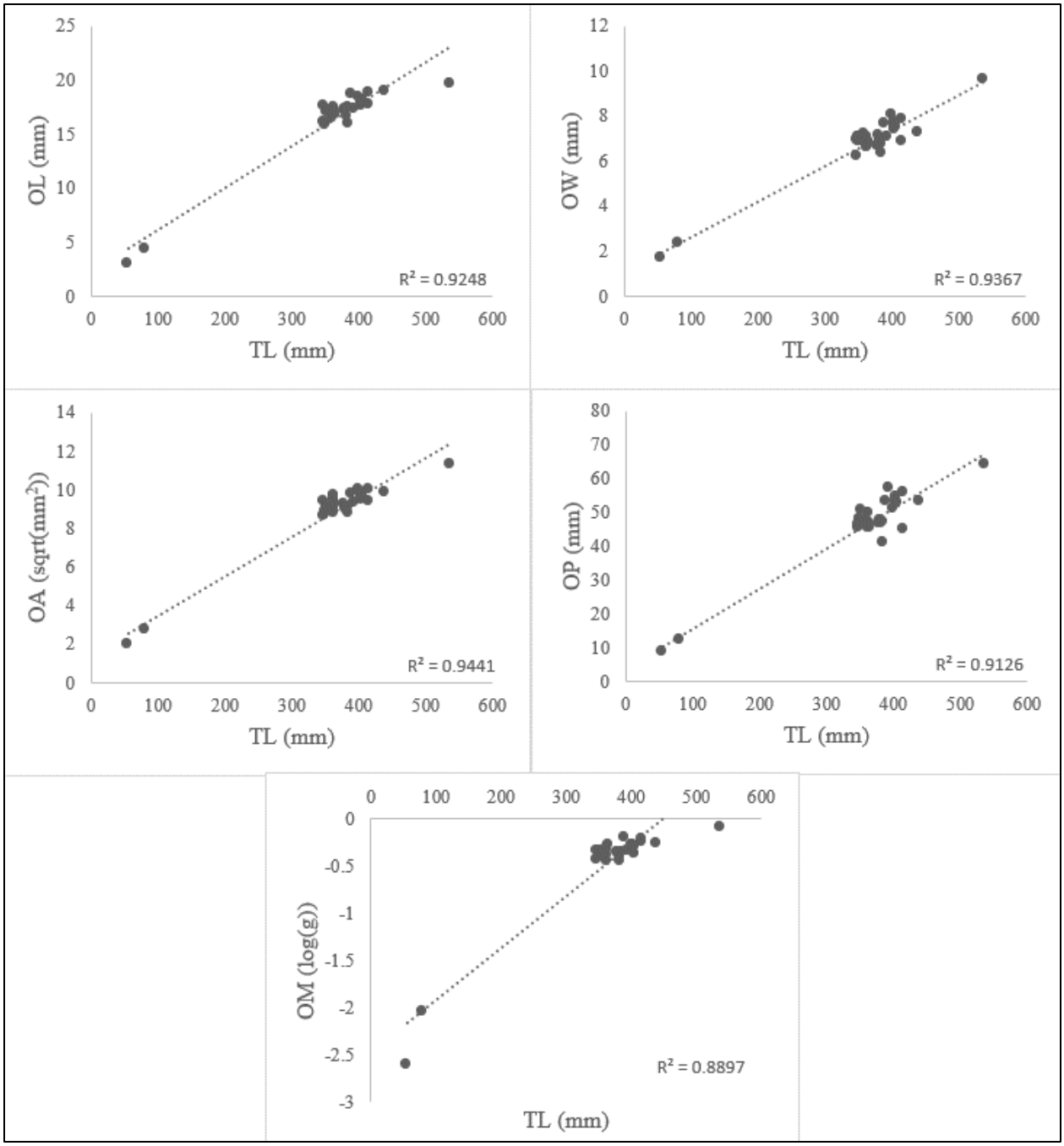

Figure 15. Linear regressions between TL and metrics in spotted seatrouts.

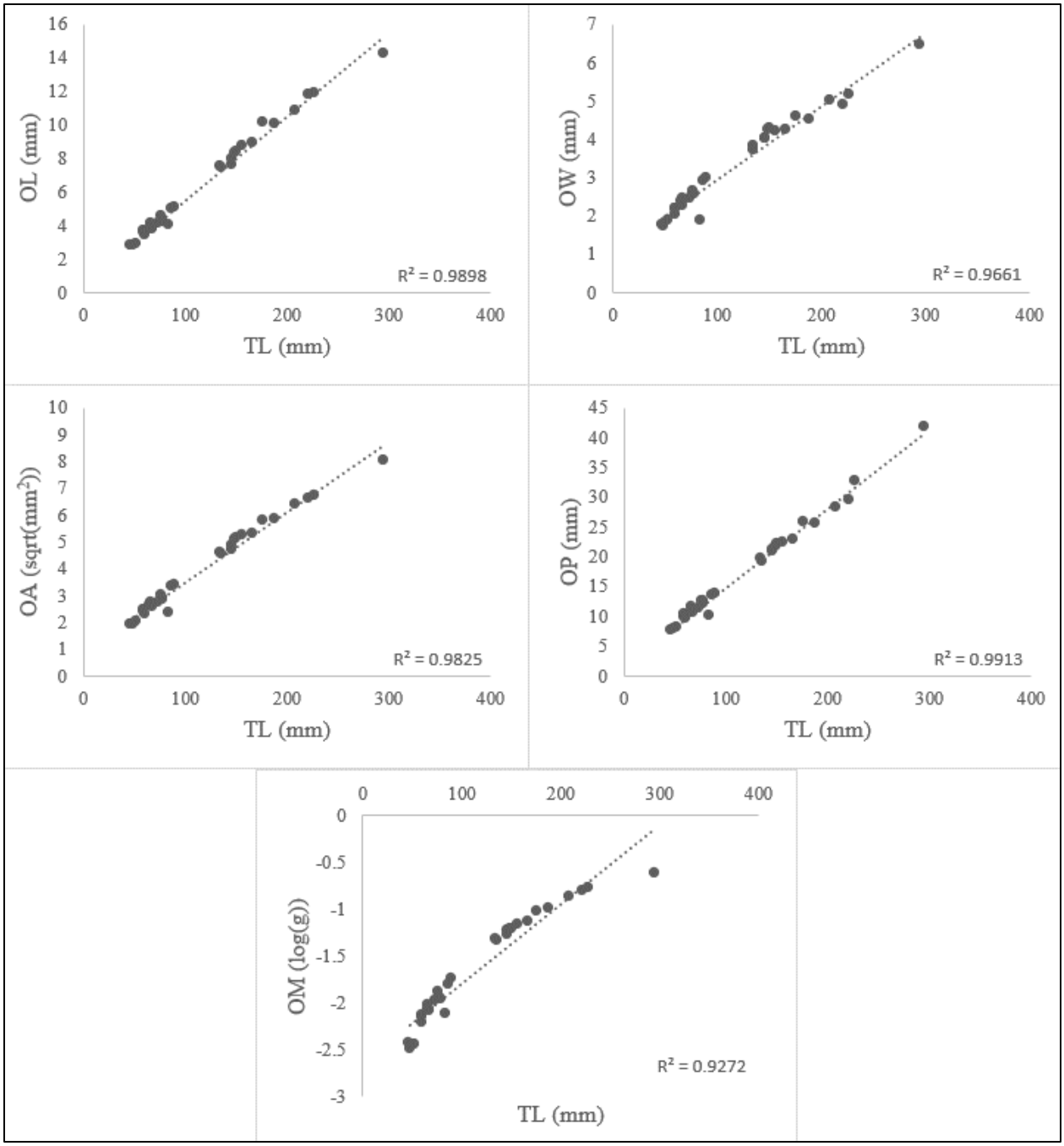

Figure 16. Linear regressions between TL and metrics in sand seatrouts.

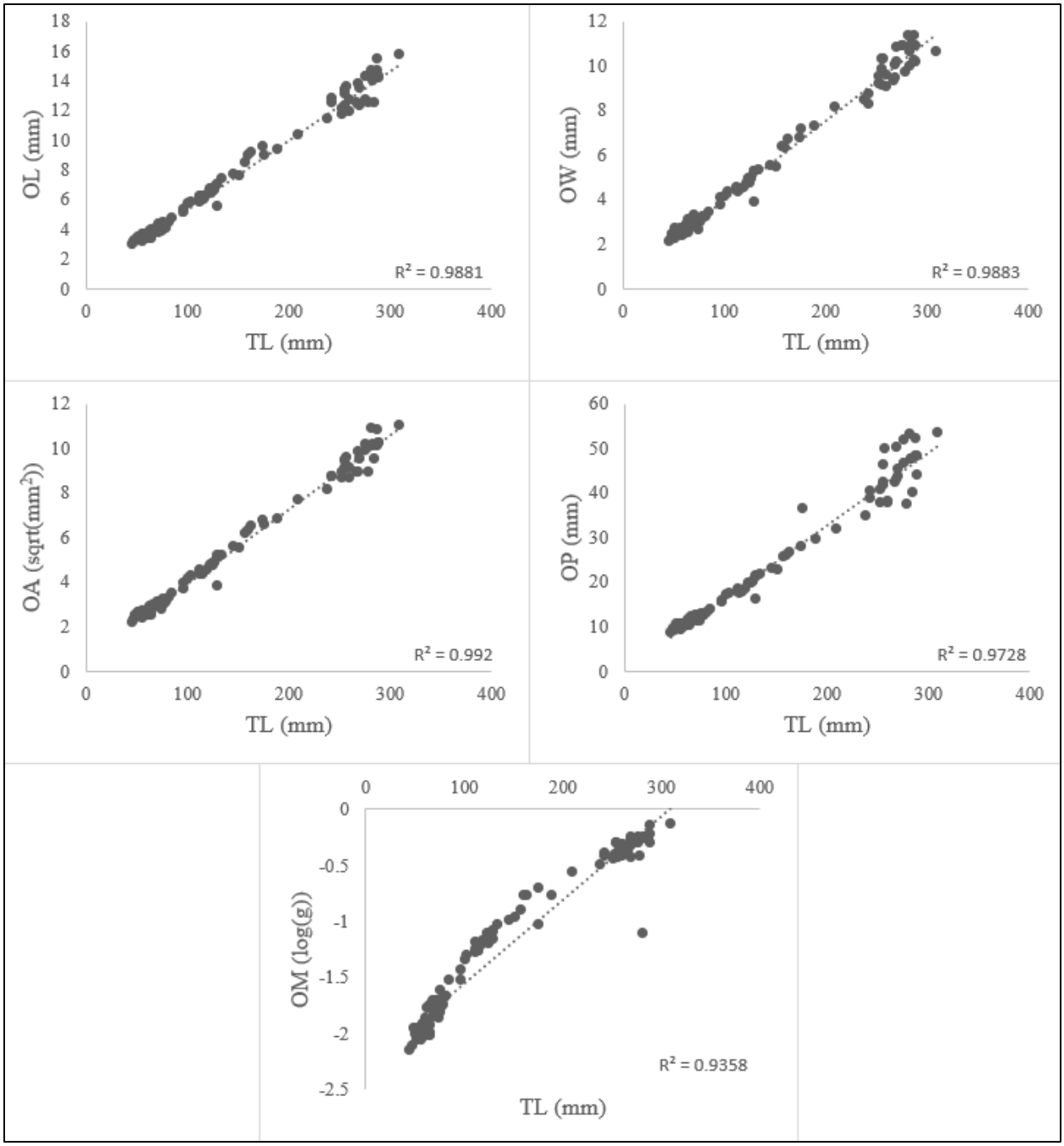

Figure 17. Linear regressions between TL and metrics in Atlantic croakers.

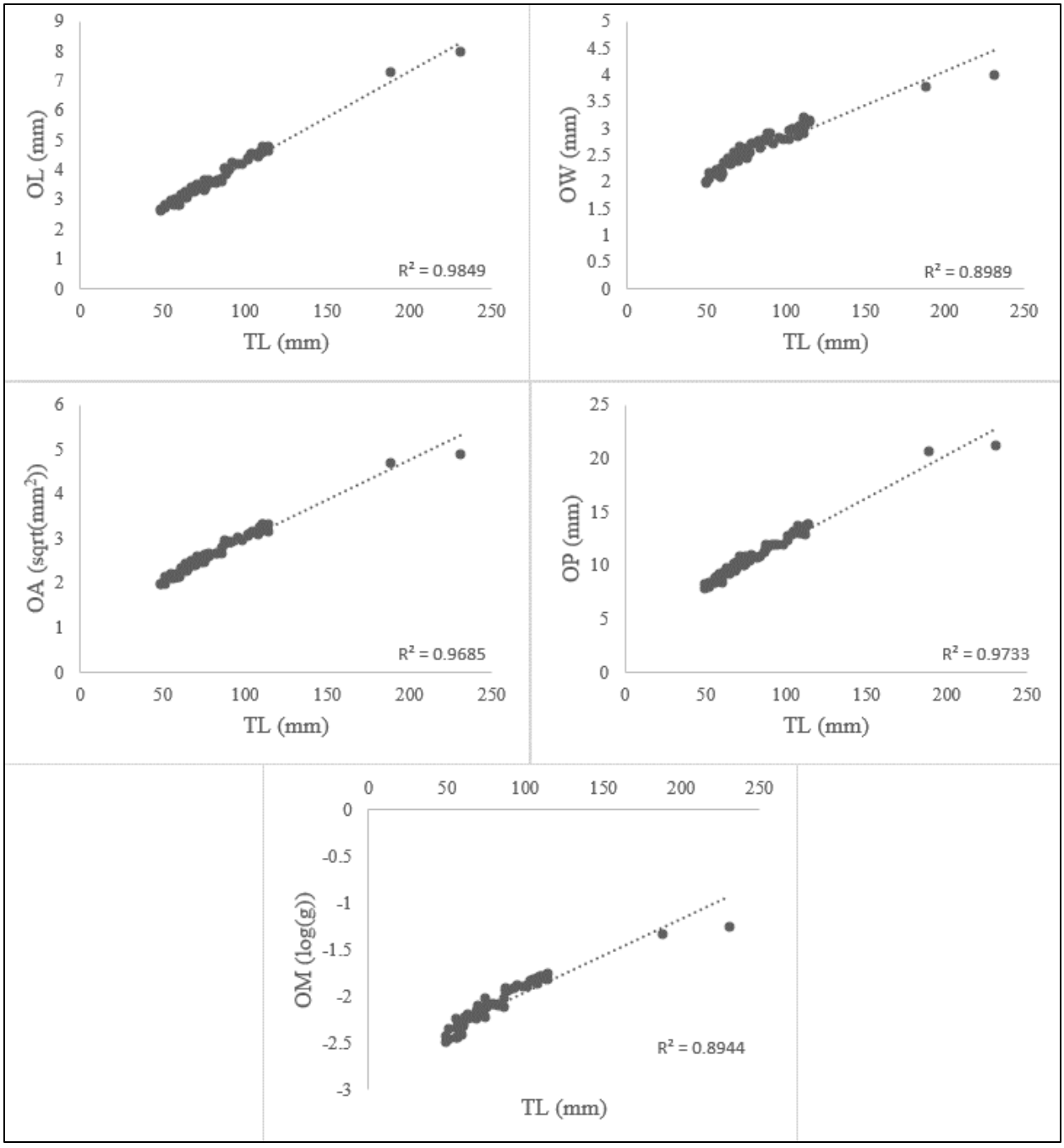

Figure 18. Linear regression between TL and metrics in spots.

Table 6. Summary of linear regression variables for all species, where metric = m*(TL) + b. Total length (TL), otolith length (OL), otolith width (OW), otolith area (OA), otolith perimeter (OP), and otolith mass (OM).

	Red Drum			**Black Drum**		
Relationship	*m*	*b*	R^2	*m*	*b*	R^2
TL/OL	0.0216	4.2405	0.89	0.0231	3.6198	0.89
TL/OW	0.0096	3.9947	0.82	0.0185	2.9259	0.92
TL/OA	0.0134	3.6923	0.89	0.018	2.9125	0.92
TL/OP	0.0662	12.014	0.88	0.097	7.0701	0.87
TL/OM	0.002	-1.2404	0.83	0.0025	-1.2866	0.88
	Spotted Seatrout			**Sand Seatrout**		
Relationship	*m*	*b*	R^2	*m*	*b*	R^2
TL/OL	0.039	2.1853	0.92	0.0498	0.5117	0.99
TL/OW	0.0157	1.0573	0.94	0.0191	1.0274	0.97
TL/OA	0.0203	1.4456	0.94	0.0263	0.8226	0.98
TL/OP	0.1179	3.8252	0.91	0.132	1.5537	0.99
TL/OM	0.0055	-2.4669	0.89	0.0084	-2.6312	0.93
	Atlantic Croaker			**Spot**		
Relationship	*m*	*b*	R^2	*m*	*b*	R^2
TL/OL	0.0465	0.6732	0.99	0.031	1.1165	0.98
TL/OW	0.0355	0.3912	0.99	0.0126	1.5432	0.90
TL/OA	0.0332	0.5768	0.99	0.018	1.1658	0.97
TL/OP	0.1629	-0.0274	0.97	0.0813	4.1163	0.97
TL/OM	0.0074	-2.3012	0.94	0.0079	-2.7373	0.89

Otolith Shape

Descriptors

Table 7 summarizes the otolith descriptors across all species, specifically form factor (FF), circularity (C), roundness (R), ellipticity (E), rectangularity (RC), aspect ratio (AR), and compactness (CP). Across all species, descriptors generally showed weak relationships with TL (Figures 19-24, Table 8). The descriptor with the strongest relationship to TL was CP – with otolith CP decreasing with increases in TL (Figures 19-24, Table 9). For all species, the descriptors that primarily dealt with how circular an otolith is (i.e., FF, C, R) all showed that the otoliths start out more circular then deviate from a circular shape over the life of the fishes (Figures 19-24, Table 6).

Table 7. Summary of descriptors across all species. Form factor (F), circularity (C), roundness (R), ellipticity (E), rectangularity (RC), aspect ratio (AR), and compactness (CP).

Species	Descriptor	Min	Max	Mean	(±SD)
Red Drum	FF	0.583	0.763	0.705	0.042
	C	16.460	21.561	17.901	1.159
	R	0.553	0.718	0.635	0.032
	E	0.174	0.302	0.237	0.029
	RC	0.720	0.858	0.809	0.024
	AR	1.423	1.865	1.626	0.100
	CP	0.354	0.792	0.484	0.065
Black Drum	FF	0.508	0.792	0.647	0.063
	C	15.868	24.719	19.607	1.982
	R	0.741	0.874	0.791	0.031
	E	0.065	0.153	0.109	0.021
	RC	0.740	0.802	0.773	0.015
	AR	1.139	1.361	1.247	0.053
	CP	0.393	0.645	0.490	0.059
Spotted Seatrout	FF	0.333	0.652	0.467	0.073
	C	19.266	37.725	27.510	4.001
	R	0.344	0.546	0.380	0.045
	E	0.265	0.449	0.408	0.041
	RC	0.656	0.767	0.709	0.033
	AR	1.720	2.628	2.394	0.210
	CP	0.503	2.283	0.663	0.370
Sand Seatrout	FF	0.463	0.777	0.692	0.069
	C	16.182	27.163	18.380	2.241
	R	0.397	0.612	0.516	0.072
	E	0.217	0.413	0.299	0.060
	RC	0.705	0.770	0.745	0.013
	AR	1.553	2.405	1.872	0.253
	CP	0.650	2.157	1.272	0.477
Atlantic Croaker	FF	0.401	0.834	0.729	0.097
	C	15.071	31.358	17.629	3.032
	R	0.590	0.809	0.685	0.039
	E	0.063	0.214	0.149	0.026
	RC	0.649	0.790	0.727	0.031
	AR	1.133	1.545	1.353	0.071
	CP	0.420	1.817	1.062	0.435
Spot	FF	0.643	0.809	0.757	0.037
	C	15.534	19.555	16.637	0.884
	R	0.484	0.732	0.669	0.047
	E	0.120	0.329	0.170	0.040
	RC	0.689	0.793	0.739	0.017
	AR	1.274	1.981	1.415	0.129
	CP	0.886	2.142	1.576	0.264

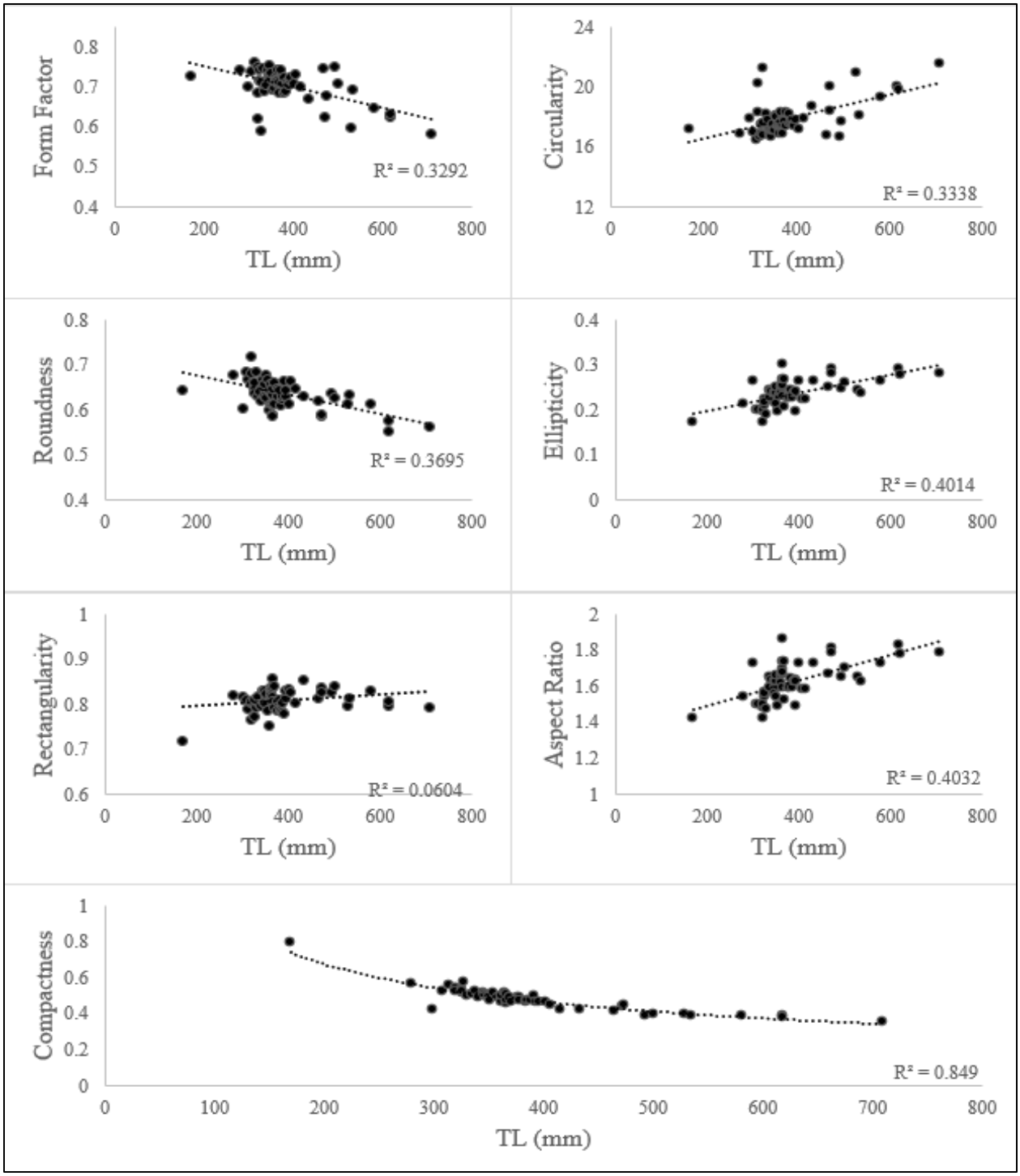

Figure 19. Linear and power regressions between TL and descriptors for red drums.

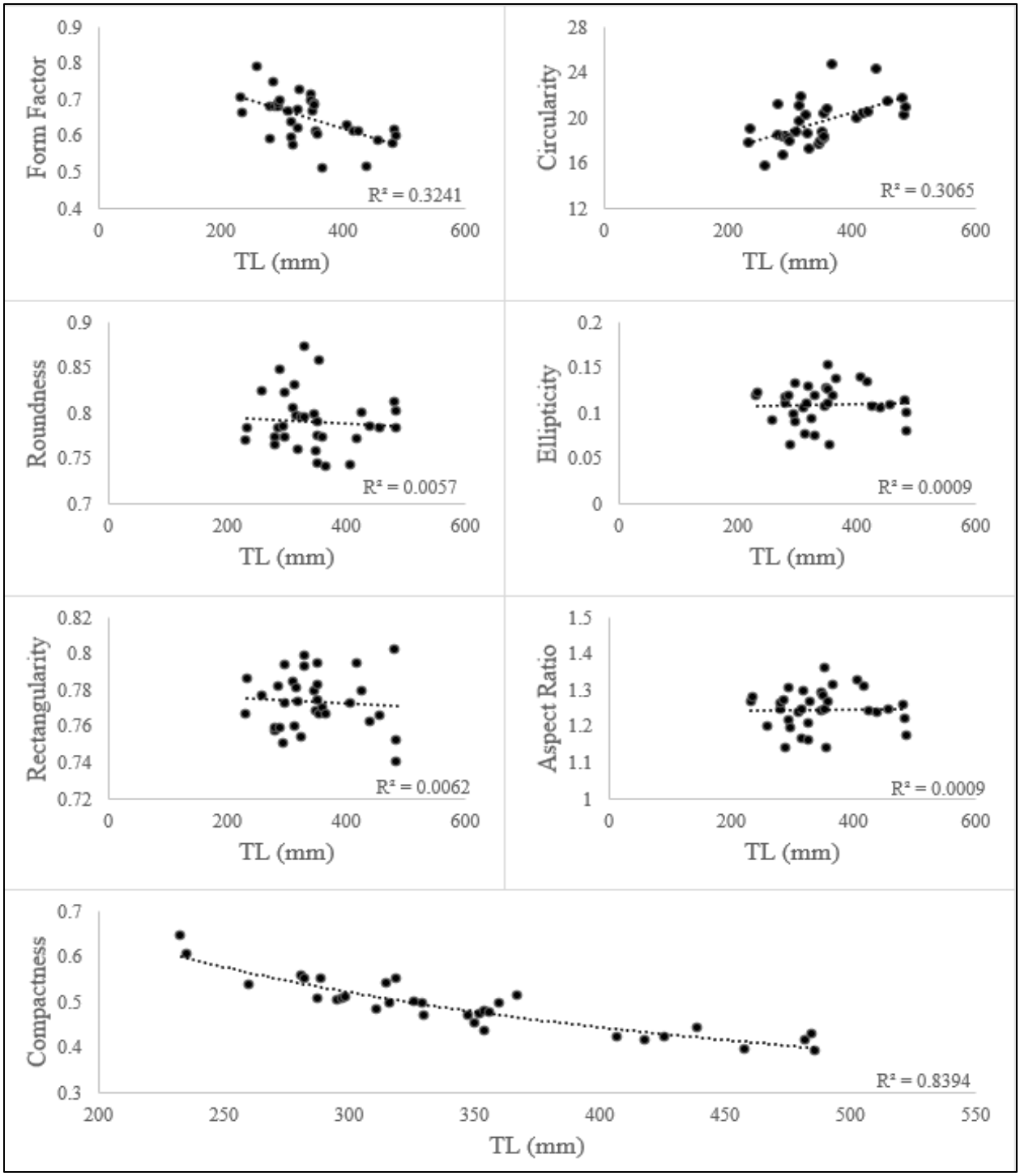

Figure 20. Linear and power regressions between TL and descriptors for black drums.

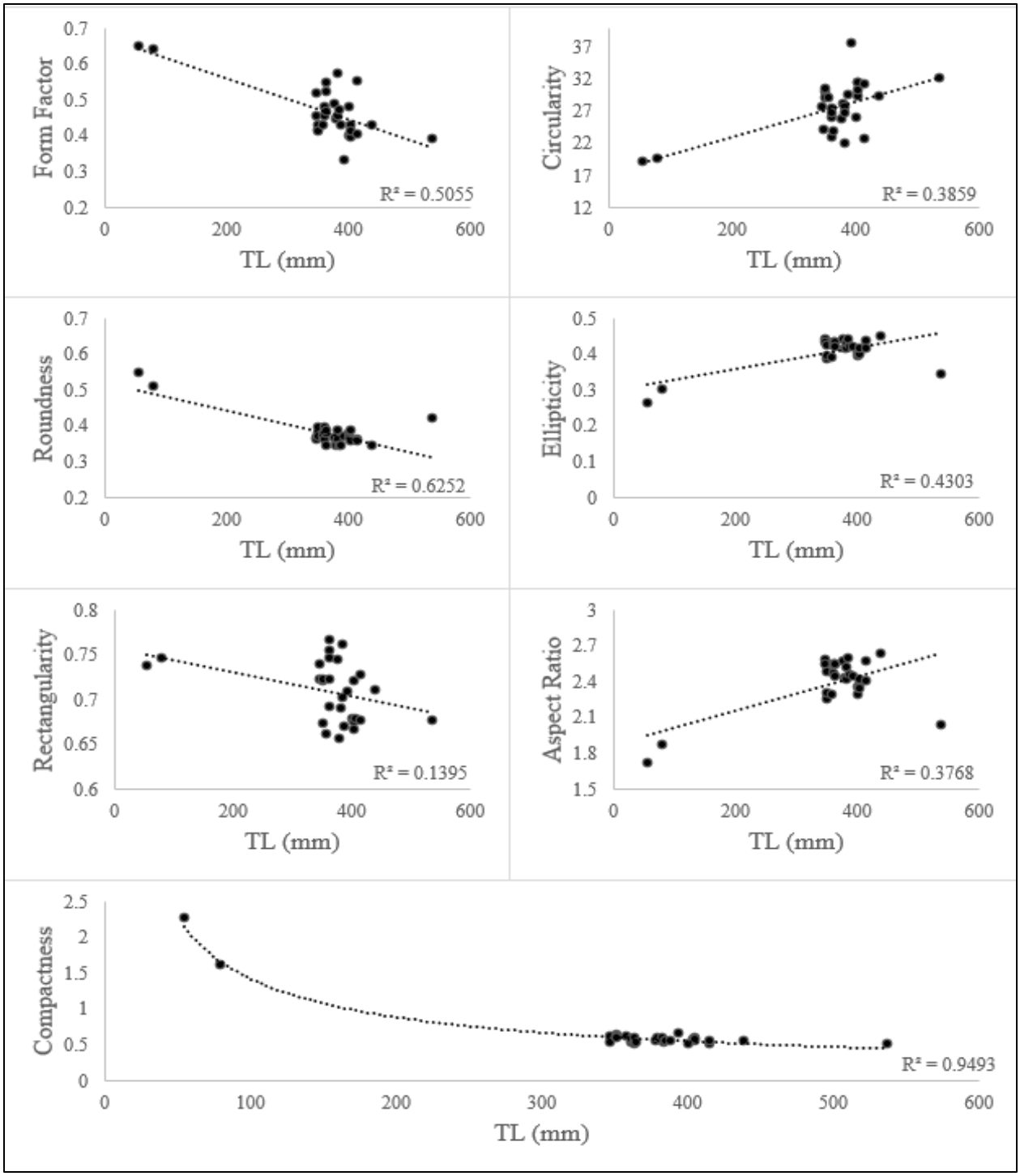

Figure 21. Linear and power regressions between TL and descriptors for spotted seatrouts.

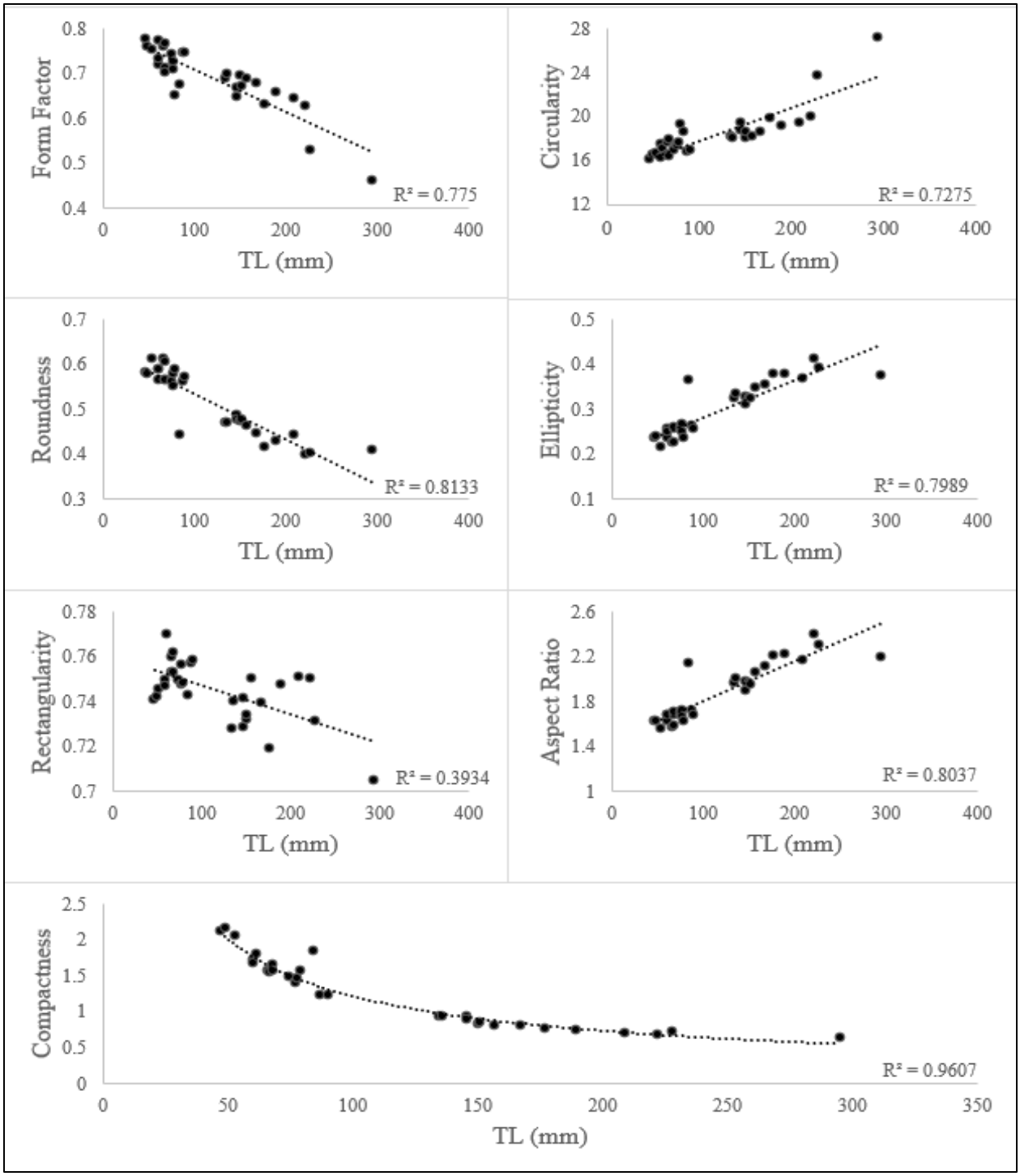

Figure 22. Linear and power regressions between TL and descriptors for sand seatrouts.

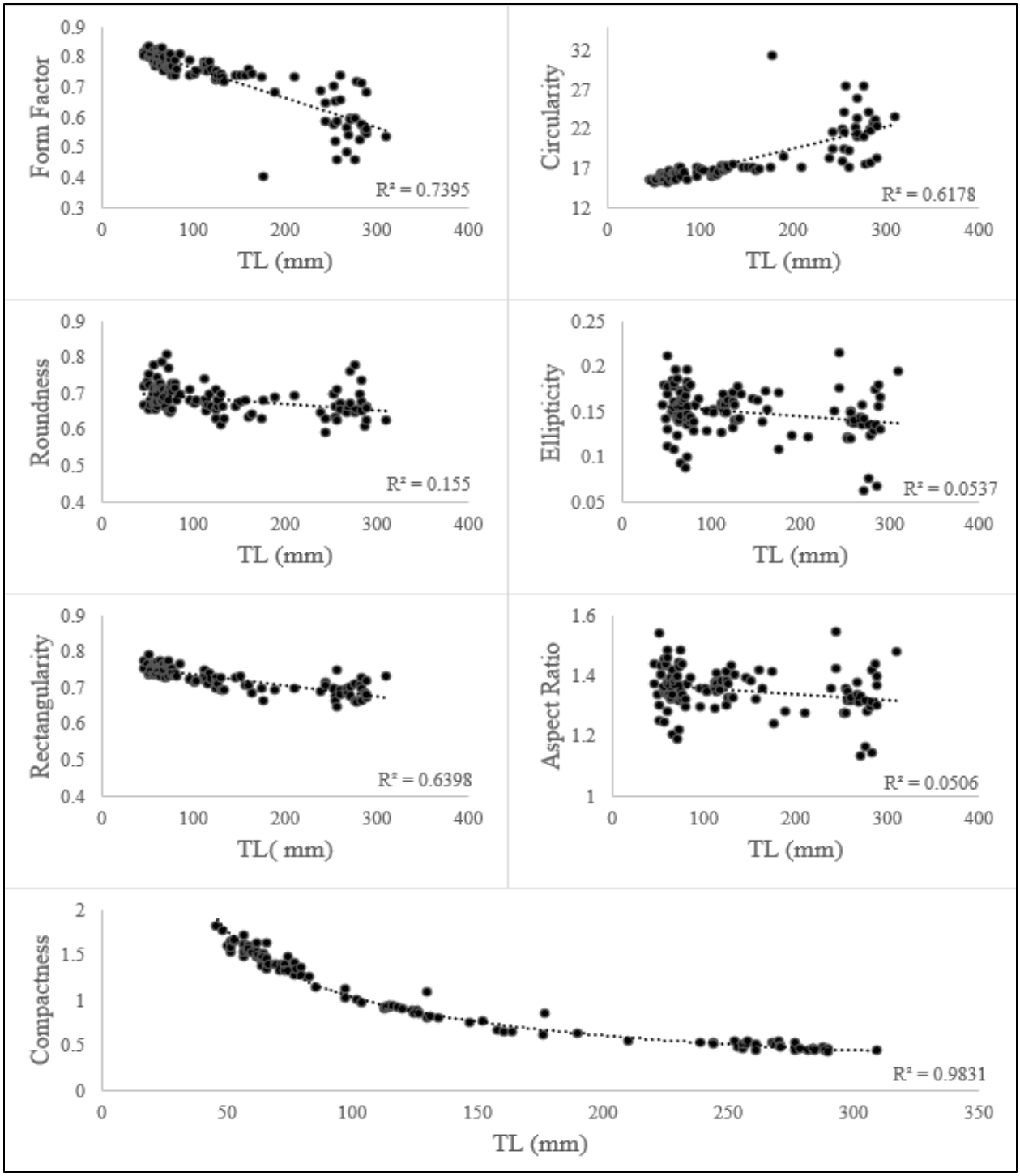

Figure 23. Linear and power regressions between TL and descriptors for Atlantic croakers.

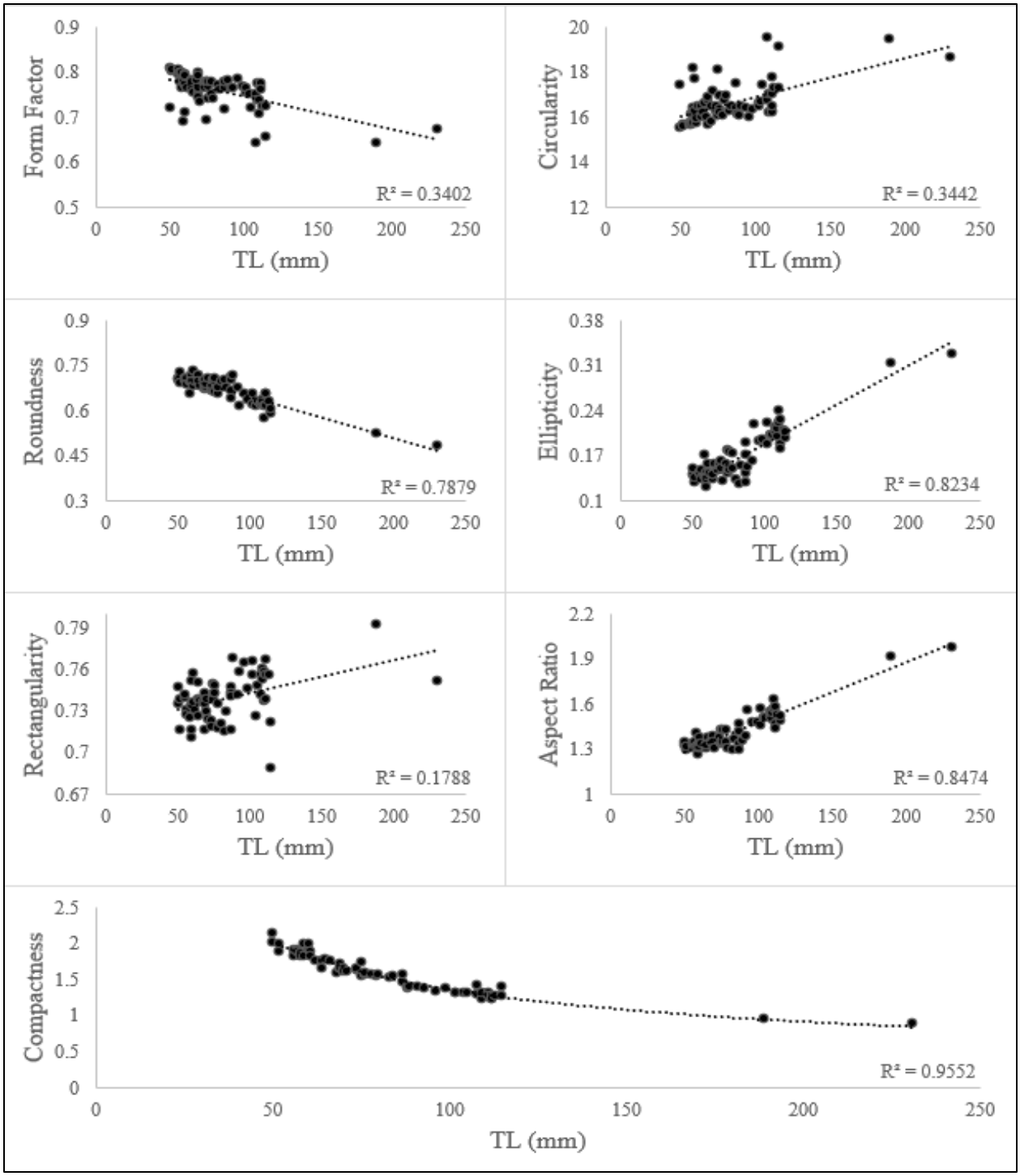

Figure 24. Linear and power regressions between TL and descriptors for spots.

Table 8. Summary of linear regression variables and significance for all species, where Descriptor = *m**(TL) + *b*.

	Red Drum				Black Drum			
Descriptor	*m*	*b*	R^2	*p*	*m*	*b*	R^2	*p*
Form Factor	-0.0003	0.8067	0.33	**<0.05**	-0.0005	0.8261	0.32	**<0.05**
Circularity	0.0074	15.045	0.33	**<0.05**	0.0158	14.124	0.31	**<0.05**
Roundness	-0.0002	0.7185	0.37	**<0.05**	-3.0×10^{-5}	0.8028	0.01	0.68
Ellipticity	0.0002	0.1589	0.4	**<0.05**	9.0×10^{-6}	0.1062	<0.01	0.87
Rectangularity	7.0×10^{-5}	0.784	0.06	0.06	-2.0×10^{-5}	0.7794	0.01	0.67
Aspect Ratio	0.0007	1.3541	0.4	**<0.05**	-2.0×10^{-5}	1.239	<0.01	0.87
	Spotted Seatrout				**Sand Seatrout**			
Descriptor	*m*	*b*	R^2	*p*	*m*	*b*	R^2	*p*
Form Factor	-0.0006	0.6769	0.51	**<0.05**	-0.0009	0.8305	0.78	**<0.05**
Circularity	0.0275	17.492	0.39	**<0.05**	0.0298	14.843	0.73	**<0.05**
Roundness	-0.0004	0.5228	0.63	**<0.05**	-0.001	0.6355	0.81	**<0.05**
Ellipticity	0.0003	0.2985	0.43	**<0.05**	0.0008	0.1996	0.8	**<0.05**
Rectangularity	-0.0001	0.7586	0.14	**<0.05**	-0.0001	0.76	0.39	**<0.05**
Aspect Ratio	0.0014	1.8745	0.38	**<0.05**	0.0035	1.4522	0.8	**<0.05**
	Atlantic Croaker				**Spot**			
Descriptor	*m*	*b*	R^2	*p*	*m*	*b*	R^2	*p*
Form Factor	-0.001	0.8609	0.74	**<0.05**	-0.0007	0.8184	0.34	**<0.05**
Circularity	0.0281	13.867	0.62	**<0.05**	0.0173	15.184	0.34	**<0.05**
Roundness	-0.0002	0.7093	0.16	**<0.05**	-0.0014	0.7856	0.79	**<0.05**
Ellipticity	-7.0×10^{-5}	0.1589	0.05	**<0.05**	0.0012	0.0677	0.82	**<0.05**
Rectangularity	-0.0003	0.7665	0.64	**<0.05**	0.0002	0.7195	0.18	**<0.05**
Aspect Ratio	-0.0002	1.3786	0.05	0.16	0.004	1.0822	0.85	**<0.05**

Table 9. Summary of power regression variables and significance for all species, where Descriptor = a*(TL^b).

	Compactness			
Species	*a*	*b*	R^2	*p*
Red Drum	11.584	-0.536	0.85	**<0.05**
Black Drum	12.477	-0.557	0.84	**<0.05**
Spotted Seatrout	33.27	-0.684	0.949	**<0.05**
Sand Seatrout	34.611	-0.727	0.96	**<0.05**
Atlantic Croaker	35.573	-0.767	0.98	**<0.05**
Spot	18.986	-0.572	0.96	**<0.05**

Elliptical Fourier Coefficients (EFC)

The R package ShapeR outputted 22 EFC after removal of significantly covarying coefficients. To reconstruct the outline of the otoliths, with 98.5% accuracy, 12 EFC were needed (Figure 25). The first 12 coefficients explained the most changes (e.g., distance of outlying perimeter point from center) in otolith shape (Figure 25). Using the EFC, average otolith shape for each species were plotted through ShapeR (Figure 26). Otolith shapes, as gauged by EFC, were significantly different between all species and between species (Table 10).

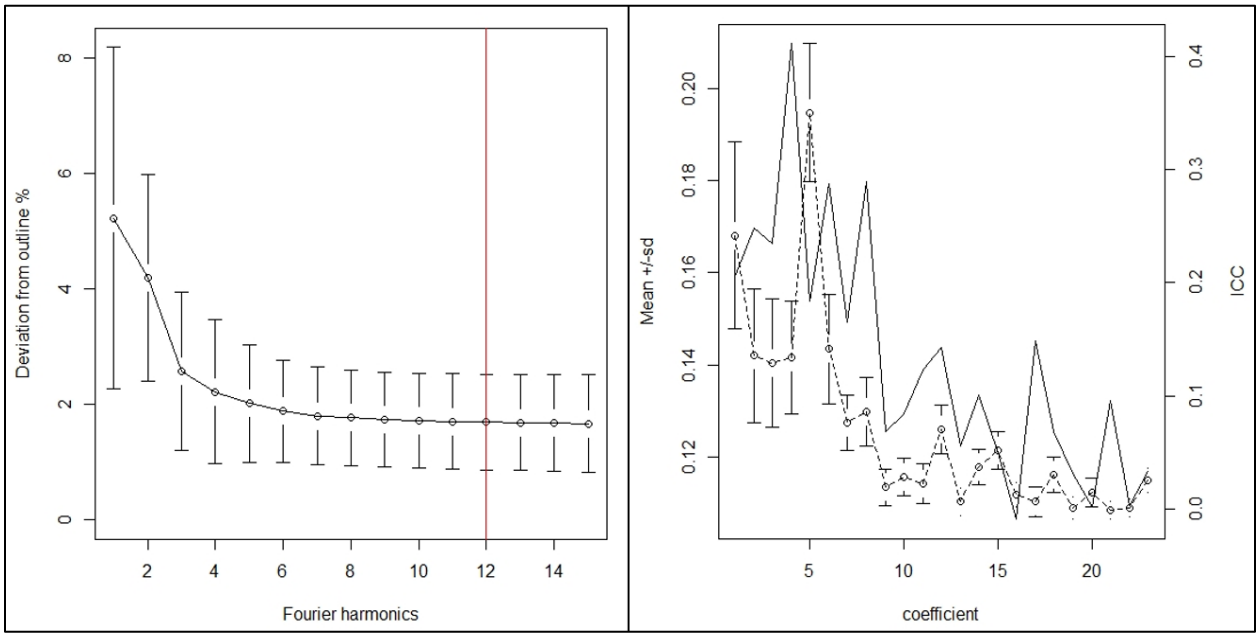

Figure 25. Number of EFC needed to recreate otolith shape with 98.5% accuracy (left panel), and degree of deviation from mean for each coefficient (right panel).

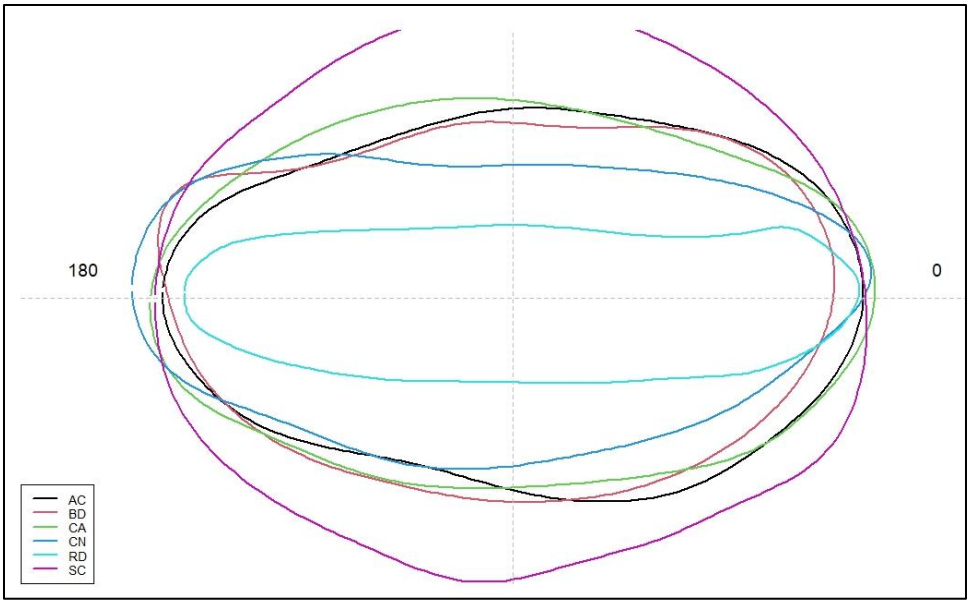

Figure 26. Average otolith shape for each species, across all sizes: Atlantic croaker (AC), black drum (BD), sand seatrout (CA), spotted seatrout (CN), red drum (RD), and spot (SC). The numbers (0 and180) represent angles in degrees (°) on a coordinate plane. The otolith shapes are aligned with the centroid of the otolith corresponding to the center point of the dashed cross (following Libungan and Pálsson 2015).

Table 10. One-way ANOSIM results examining the effect of species on EFC.

EFC			
Global Test	*R*	*P-Value*	*Permutations*
Species	0.437	**0.001**	999
Pairwise Tests	*R*	*P-Value*	*Possible Permutations*
MU, CA	0.223	**0.002**	Very Large
MU, LX	0.28	**0.001**	Very Large
MU, CN	0.343	**0.001**	Very Large
MU, SO	0.341	**0.001**	Very Large
MU, PC	0.463	**0.001**	Very Large
CA, LX	0.592	**0.001**	Very Large
CA, CN	0.469	**0.001**	Very Large
CA, SO	0.626	**0.001**	Very Large
CA, PC	0.707	**0.001**	94,884,480
LX, CN	0.483	**0.001**	Very Large
LX, SO	0.509	**0.001**	Very Large
LX, PC	0.634	**0.001**	Very Large
CN, SO	0.57	**0.001**	Very Large
CN, PC	0.487	**0.001**	Very Large
SO, PC	0.696	**0.001**	Very Large

EFC nMDS Plots

Red drum otolith shape, based EFC values, were not significantly different between size classes (ANOSIM: R = 0.119, p = 0.06, Table 11), except between three size classes (Table 11) (Figure 27). Additionally, EFC were not significantly different between season or habitat (Table 12). It appears that there is a binary split in red drum otolith shape (Figure 27).

Table 11. One-way ANOSIM results of size classes based on EFC of red drums.

Red Drum			
Global Test	*R*	*P-Value*	*Permutations*
Size Class	0.119	0.06	999
Pairwise Tests	*R*	*P-Value*	*Possible Permutations*
340-360, 400-420	0.269	**0.05**	220
360-380, 400-420	0.476	**0.02**	560
380-400, 400-420	0.451	**0.04**	84

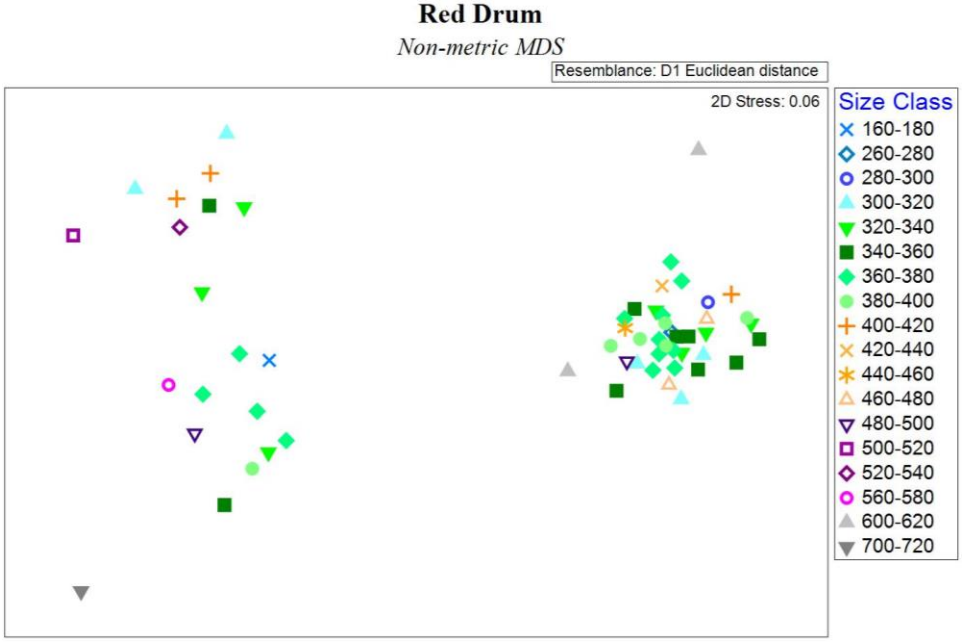

Figure 27. EFC of red drum otoliths, classified by size classes.

Table 12. Two-way ANOSIM results of season and habitat based on EFC of red drums.

Red Drum			
Global Test	*R*	*P-Value*	*Permutations*
Season	0.225	0.14	999
Habitat	0.152	0.06	999
Pairwise Tests	*R*	*P-Value*	*Possible Permutations*
Summer, Fall	0.376	0.07	2300
Summer, Spring	-0.333	1	4
Fall, Spring	-0.14	0.66	2898
Backwater, Middle	0.256	0.07	484380
Backwater, Upper	-0.17	0.60	15
Backwater, Lower	0.259	0.22	9
Middle, Upper	-0.167	0.98	11628
Middle, Lower	0.203	0.07	1287

Black drum otolith shape, based EFC values, were not significantly different between any size class (ANOSIM: R = 0.083, p = 0.21, Table 13) (Figure 28). Additionally, EFC were not significantly different between season or habitat (Table 14). It appears that there is a binary split in black drum otolith shape (Figure 28).

Table 13. One-way ANOSIM results of size classes based on EFC of black drums.

Black Drum			
Global Test	*R*	*P-Value*	*Permutations*
Size Class	0.083	0.21	999

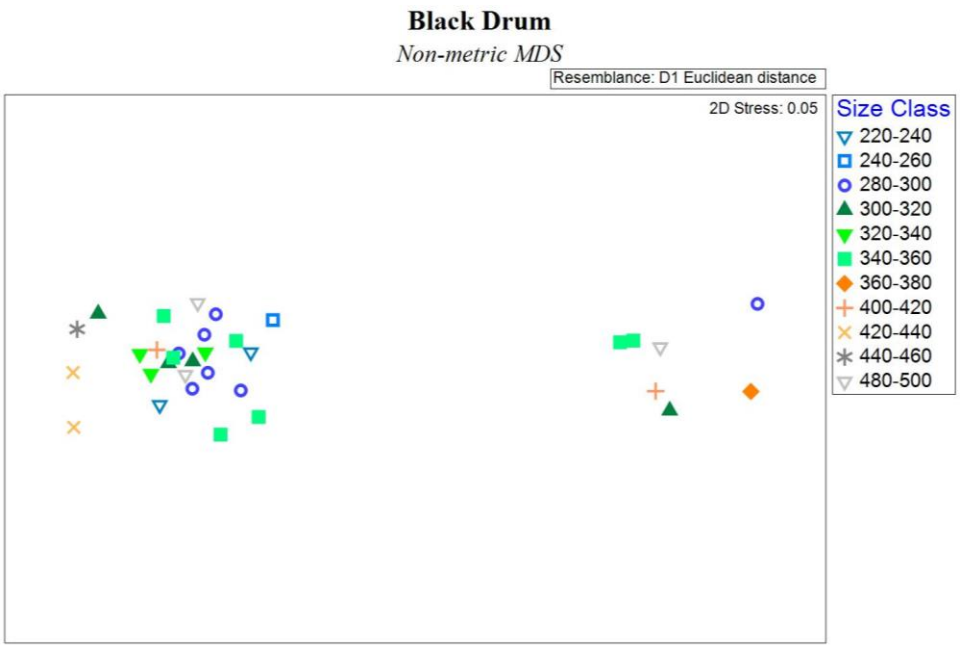

Figure 28. EFC of black drum otoliths, classified by size classes.

Table 14. Two-way ANOSIM results of season and habitat based on EFC of black drums.

Black Drum			
Global Test	*R*	*P-Value*	*Permutations*
Season	0	0.5	999
Habitat	-0.082	0.67	999
Pairwise Tests	*R*	*P-Value*	*Possible Permutations*
Backwater, Lower	-0.164	0.69	16
Lower, Middle	-0.163	0.98	126
Lower, Upper	-0.007	0.45	1287

Spotted seatrout otolith shape, based on EFC values, of were not significantly different between any size class (ANOSIM: R = 0.068, p = 0.18, Table 15) (Figure 29). EFC were not significantly different between seasons or habitats (Table 16).

Table 15. One-way ANOSIM results of size classes based on EFC of spotted seatrouts.

Spotted Seatrout			
Global Test	*R*	*P-Value*	*Permutations*
Size Class	0.068	0.18	999

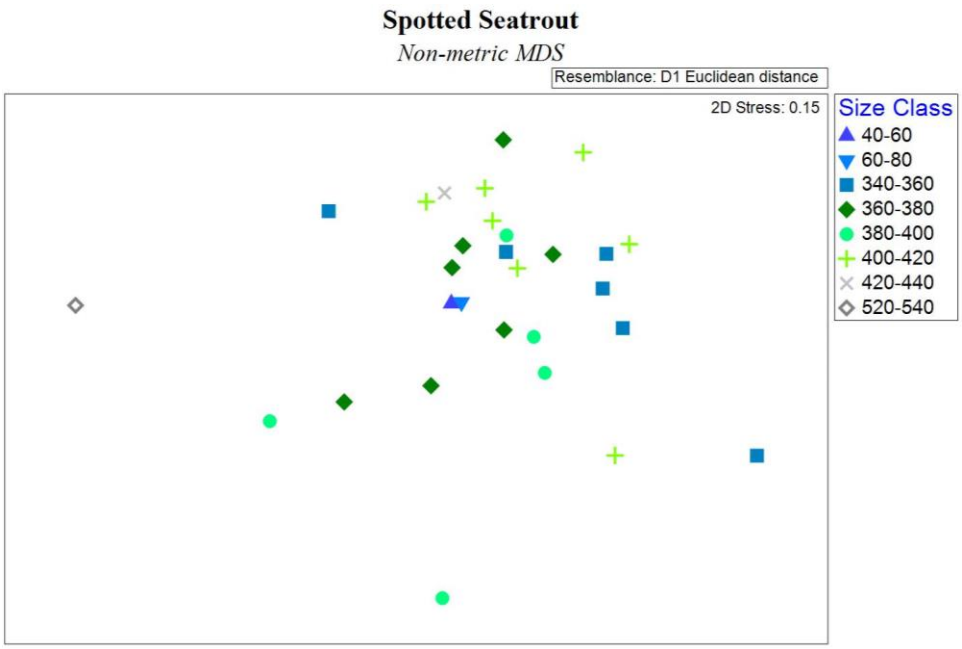

Figure 29. EFC of spotted seatrout otoliths, classified by size classes.

Table 16. Two-way ANOSIM results of season and habitat based on EFC of spotted seatrouts

Spotted Seatrout			
Global Test	*R*	*P-Value*	*Permutations*
Season	0.158	0.22	999
Habitat	0.104	0.22	999
Pairwise Tests	*R*	*P-Value*	*Possible Permutations*
Spring, Fall	0.284	0.12	455
Fall, Summer	-0.756	1	7
Upper, Lower	0.114	0.2	6188
Lower, Backwater	0.056	0.38	84

Sand seatrout otolith shape, based EFC values, were significantly different across size classes (ANOSIM: R = 0.426, p = 0.001, Table 17) (Figure 30). Multiple size classes showed significant differences in EFC (Table 17). EFC was significantly different between seasons (ANOSIM: R = 0.584, p = 0.04), but not between habitats (ANOSIM: R = 0.18, p = 0.15) (Table 18). There is a binary split in otolith shape in individuals below 80mm TL and individuals over 120mm TL (Table 17, Figure 30).

Table 17. One-way ANOSIM results of size classes based on EFC of sand seatrouts.

Sand Seatrout			
Global Test	*R*	*P-Value*	*Permutations*
Size Class	0.426	**0.001**	999
Pairwise Tests	*R*	*P-Value*	*Possible Permutations*
40-60, 120-140	0.727	**0.05**	21
40-60, 140-160	0.392	**0.02**	126
40-60, 160-180	0.745	**0.05**	21
40-60, 220-240	0.818	**0.05**	21
60-80, 120-140	0.793	**0.02**	55
60-80, 140-160	0.546	**0.001**	2,002
60-80, 160-180	0.808	**0.02**	55
60-80, 220-240	0.934	**0.02**	55

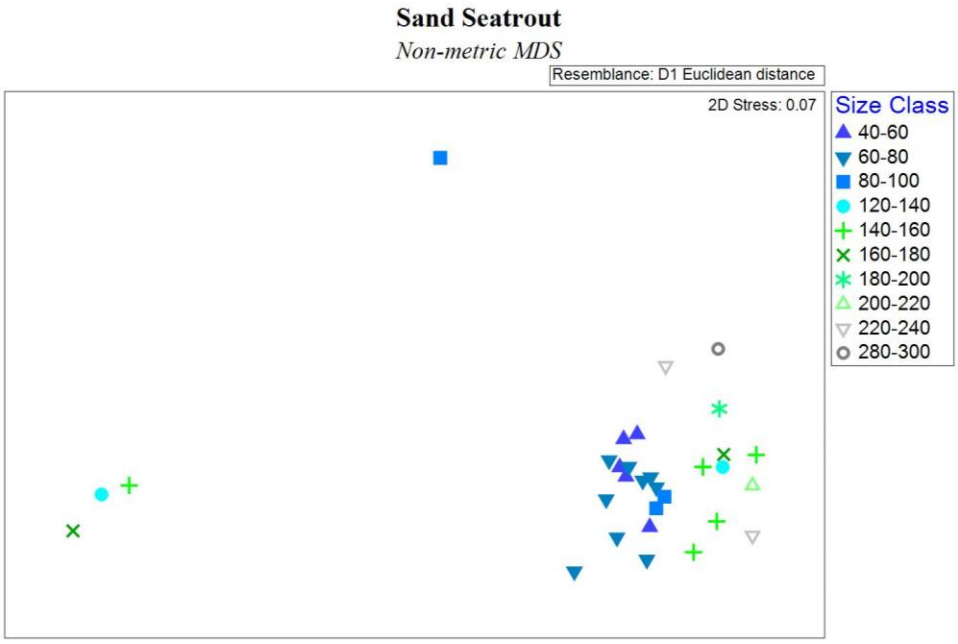

Figure 30. EFC of sand seatrout otoliths, classified by size classes.

Table 18. Two-way ANOSIM results of season and habitat based on EFC of sand seatrouts.

Sand Seatrout			
Global Test	*R*	*P-Value*	*Permutations*
Season	0.584	**0.04**	999
Habitat	0.18	0.15	999
Pairwise Tests	*R*	*P-Value*	*Possible Permutations*
Spring, Summer	0.138	0.33	15
Spring, Fall	1	0.07	15
Lower, Backwater	0.191	0.17	66
Lower, Middle	0.17	0.23	66
Backwater, Middle	0	1	3

Atlantic croaker otolith shape, based EFC values, were significantly different across size classes (ANOSIM: R = 0.338, p = 0.001, Table 19) (Figures 31 and 32). Multiple size classes showed significant differences in EFC (Table 19). EFC was significantly different between seasons (ANOSIM: R = 0.339, p = 0.001) and between habitats (ANOSIM: R = 0.149, p = 0.002)(Table 20). There appears to be a binary split in otolith shape in individuals under 200mm TL (Figure 32).

Table 19. One-way ANOSIM results of size classes based on EFC of Atlantic croaker.

Atlantic Croaker			
Global Test	*R*	*P-Value*	*Permutations*
Size Class	0.338	**0.001**	999
Pairwise Tests	*R*	*P-Value*	*Possible Permutations*
40-60, 120-140	0.185	**0.04**	4,686,825
40-60, 240-260	0.709	**0.001**	1,562,275
40-60, 260-280	0.533	**0.001**	13,123,110
40-60, 280-300	0.71	**0.001**	1,562,275
60-80, 180-200	0.514	**0.03**	36
60-80, 240-260	0.832	**0.001**	145,008,513
60-80, 260-280	0.732	**0.001**	Very Large
60-80, 280-300	0.838	**0.001**	145,008,513
60-80, 300-320	1	**0.03**	36
80-100, 120-140	0.339	**0.04**	715
100-120, 240-260	0.445	**0.001**	125,970
100-120, 260-280	0.262	**0.002**	646,646
100-120, 280-300	0.485	**0.001**	125,970
120-140, 240-260	0.36	**0.001**	24,310
120-140, 260-280	0.148	**0.01**	92,378
120-140, 280-300	0.341	**0.001**	24,310

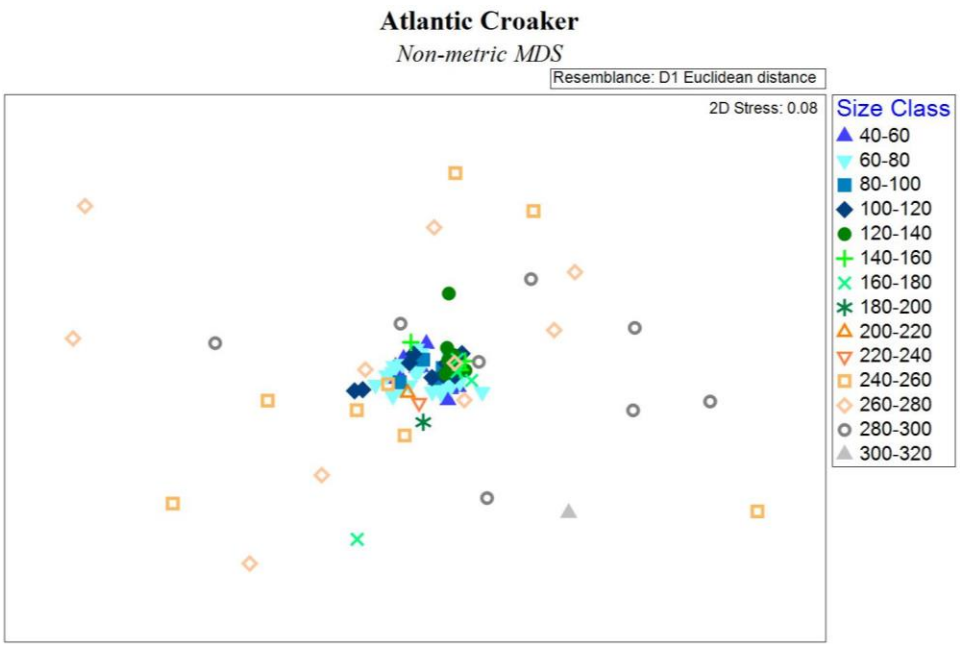

Figure 31. EFC of Atlantic croaker otoliths, classified by size classes.

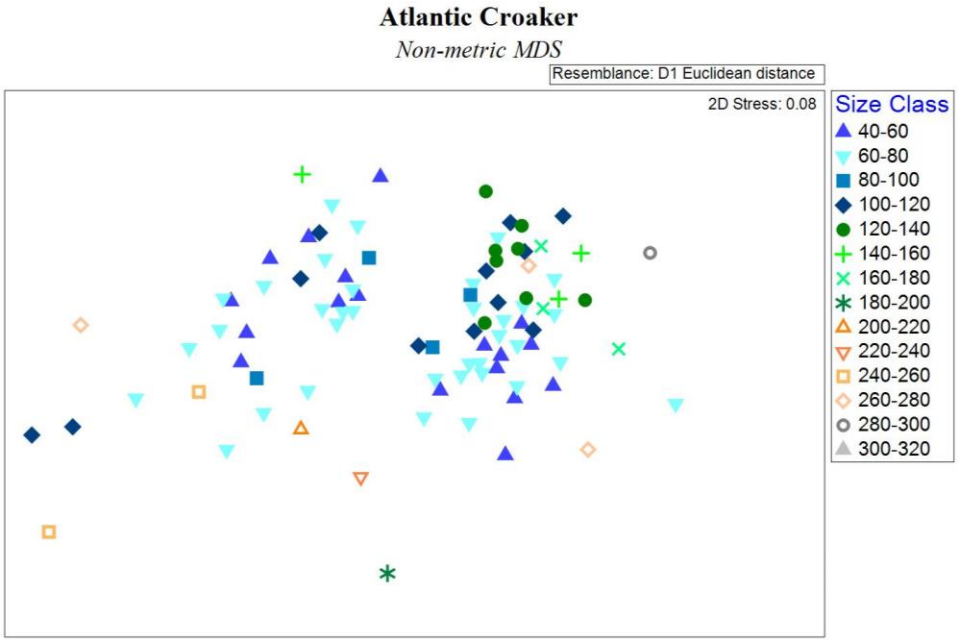

Figure 32. A zoomed-in plot of the center cluster in Figure 32 of the EFC of Atlantic croaker otoliths, classified by size classes.

Table 20. Two-way ANOSIM results of season and habitat based on EFC of Atlantic croakers.

Atlantic Croaker			
Global Test	*R*	*P-Value*	*Permutations*
Season	0.339	**0.001**	999
Habitat	0.149	**0.002**	999
Pairwise Tests	*R*	*P-Value*	*Possible Permutations*
Fall, Summer	-0.127	0.92	254592
Fall, Spring	0.516	**0.001**	310040640
Summer, Spring	0.389	0.08	120
Lower, Backwater	0.149	**0.001**	12345060
Lower, Middle	0.038	0.17	5290740
Lower, Upper	0.51	**0.001**	159120
Backwater, Middle	0.044	0.09	3527160
Backwater, Upper	0.084	0.24	1018368
Middle, Upper	0.29	**0.01**	95472

Spot otolith shape, based EFC values, were significantly different across size classes (ANOSIM: R = 0.076, p = 0.001, Table 21) (Figure 33). Three size classes had significantly different EFC (Table 21). Additionally, EFC was not significantly different between seasons or habitats (Table 22). There appears to be a binary split in otolith shape (Figure 33).

Table 21. One-way ANOSIM results of size classes based on EFC of spot.

Spot			
Global Test	*R*	*P-Value*	*Permutations*
Size Class	0.076	**0.04**	999
Pairwise Tests	*R*	*P-Value*	*Possible Permutations*
40-60, 60-80	0.115	**0.04**	Very Large
60-80, 100-120	0.13	**0.03**	Very Large

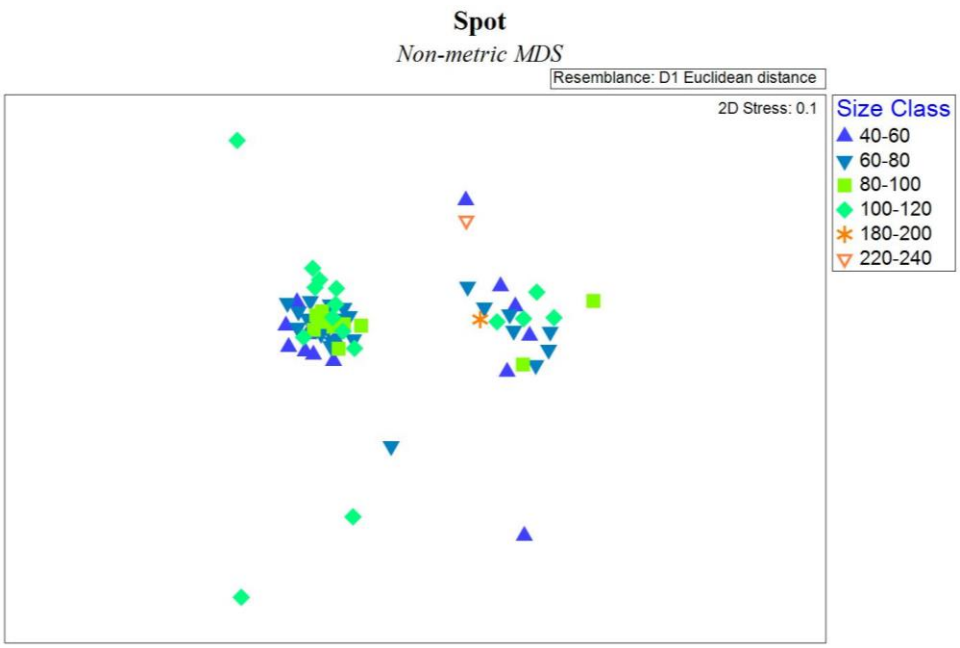

Figure 33. EFC of spot otoliths, classified by size classes.

Table 22. Two-way ANOSIM results of season and habitat based on EFC of spots.

Spot			
Global Test	*R*	*P-Value*	*Permutations*
Season	-0.167	0.59	999
Habitat	-0.168	0.89	999
Pairwise Tests	*R*	*P-Value*	*Possible Permutations*
Fall, Summer	-0.169	0.55	11
Fall, Spring	-0.16	0.67	6
Lower, Backwater	-0.4	1	6
Lower, Middle	-0.115	0.79	3003
Backwater, Middle	-0.307	0.82	11

CAP

Prediction of species identity through use of standardized metrics, descriptors, and EFC were evaluated by means of canonical analysis of principle coordinates (CAP). Of the three otolith morphology assessments, standardized metrics (i.e., where metrics were standardized by divided TL to remove the effect of fish size) showed the highest potential to correctly identify individuals to species. With metrics alone, individuals were correctly classified to species 95.2% of the time, with misclassification occurring 4.8% of the time (Figure 35). Correct identification was highest

in black drum (100%), followed by spot (97.1%), red drum (96.6%), Atlantic croaker (93.9%), spotted seatrout (93.1%), and sand seatrout (90.3%) (Figure 35). Descriptors (i.e., FF, C, R, E, RC, AR, CP) were the second best at correctly predicting species. Individuals were correctly identified to species 79.3% of the time using descriptors, with misclassification occurring 20.7% of the time (Figure 36). Correct classification was highest in black drum (100%), followed by red drum (98.3%), spotted seatrout (93.1%), sand seatrout (90.3%), Atlantic croaker (67%), and spot (63.2%) (Figure 36). The EFC were not as good predictors of species as standardized metrics or descriptors. With EFC individuals were correctly identified to species 73.1% of the time, misclassification occurred 26.9% of the time (Figure 37). Correct classification was highest in black drum (78.8%), followed by sand seatrout (77.4%), Atlantic croaker (75.7%), spotted seatrout (72.4%), spot (69.1%), and red drum (67.2%) (Figure 37).

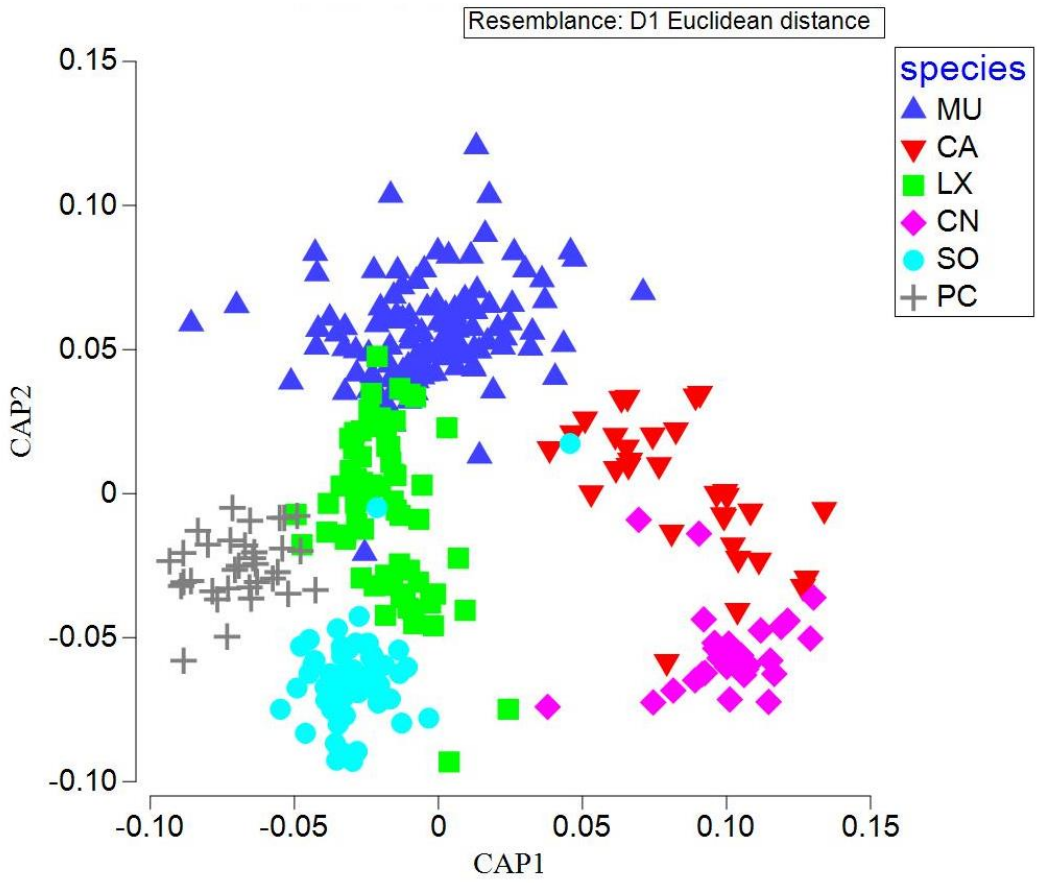

Figure 34. Standardized metric CAP of all individuals, grouped by species. Atlantic croaker (MU), spot (LX), red drum (SO), black drum (PC), spotted seatrout (CN), and sand seatrout (CA).

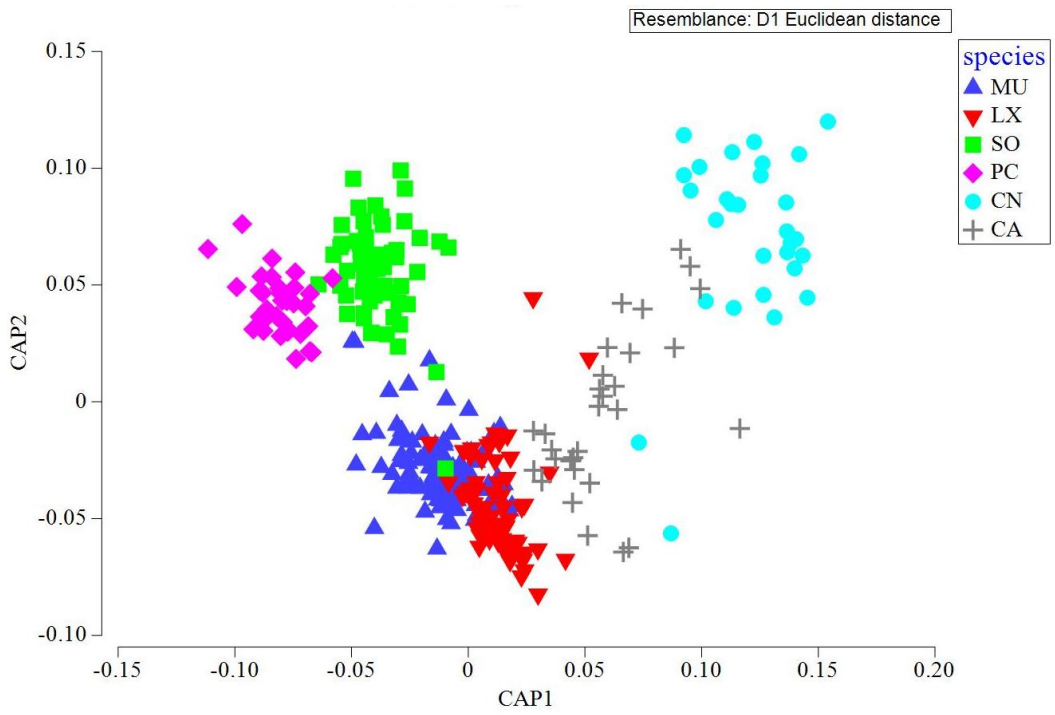

Figure 35. Descriptor CAP of all individuals, grouped by species. Atlantic croaker (MU), spot (LX), red drum (SO), black drum (PC), spotted seatrout (CN), and sand seatrout (CA).

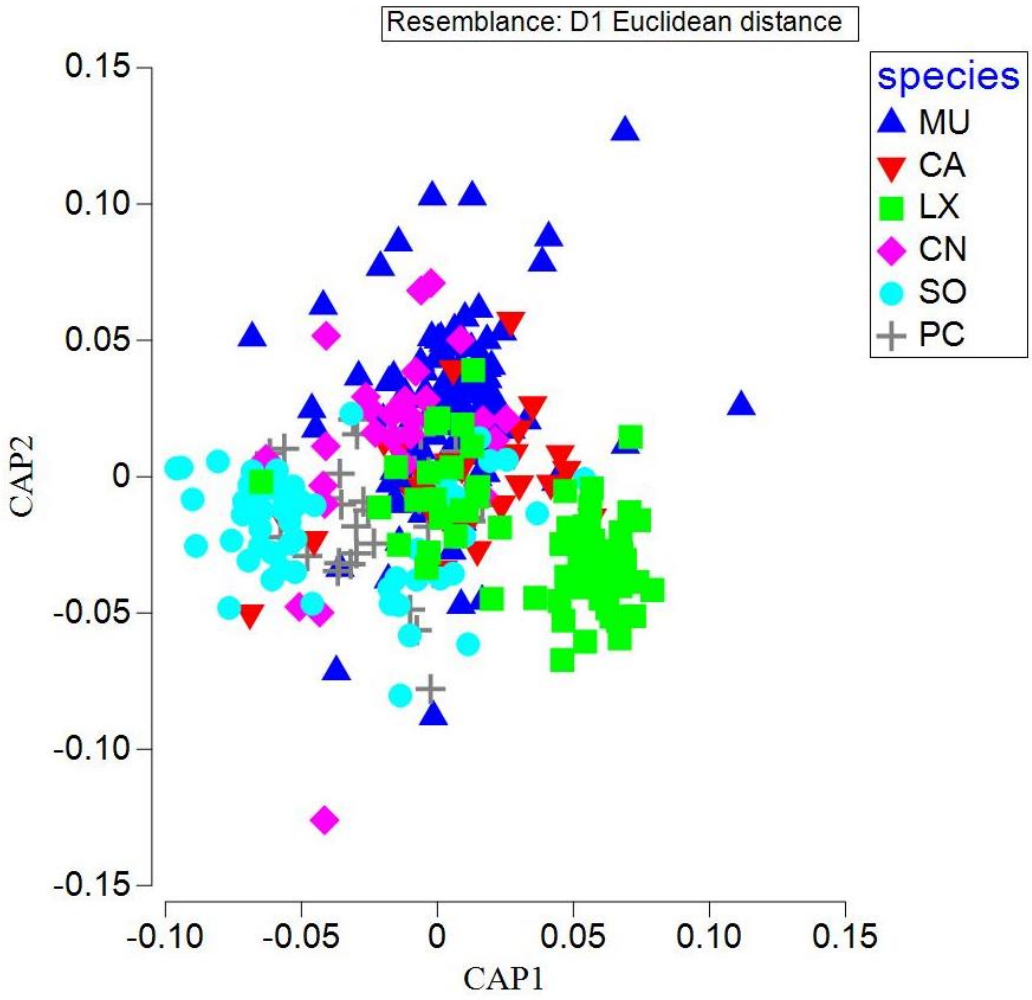

Figure 36. EFC CAP of all individuals, grouped by species. Atlantic croaker (MU), spot (LX), red drum (SO), black drum (PC), spotted seatrout (CN), and sand seatrout (CA).

DISCUSSION

Sagittal otoliths from red drums, black drums, spotted seatrouts, sand seatrouts, Atlantic croakers, and spots from the northern GOM, specifically Sabine Lake TX/LA, were analyzed for changes in morphology with increasing fish size. Environmental conditions at time of capture were normal for Sabine Lake (McFarlane 1996, Wooster 2010) over the eight month sampling period (Figures 5-7, Table 1). The environmental conditions (i.e., temperature, salinity, DO, and depth) at time of capture for the collected specimens were not abnormal conditions for these six species to reside in (Weinstein 1981, Odell et al. 2017). Over the course of the sampling period (April to

November of 2018) seasonal changes in environmental conditions occurred in Sabine Lake (Figures 5-7).

The environmental condition most relevant to otolith morphology in this study was water temperature (Fablet et al. 2011). Water temperature affects the morphogenesis of the otolith, with cooler temperatures slowing the development of the otolith and warmer temperatures accelerating the development of the otolith (Fablet et. al 2011). Over the sampling period, water temperature in Sabine Lake changed dramatically, with the temperature in the summer being over 20°C warmer than in spring or fall (Figure 5). The water temperatures in spring and fall (Figure 5) were cool enough to reduce the rate of accretion of calcium carbonate to the outer layers of the otolith (Fablet et al. 2011). However, the water temperature at time of capture is not necessarily indicative of the conditions the study specimens experienced over the course of their lives. Over the lives of the study specimens, the effects of season to season differences in environment on otolith morphology would have been smoothed out (Campana and Casselman 1993). With the data currently available, it is not possible at the moment to fully comprehend how the water temperature of Sabine Lake impacted the otolith development of the specimens used in this study. The reason for this is because the six study species will move within, and between, estuaries to avoid unfavorable environmental conditions, and it is not currently known the long term conditions these samples experienced. Additionally, the larger, and by extension older, a specimen is, the more its otolith morphology has been altered by environmental conditions (Campana and Casselman 1993).

The specimens collected of the six study species were predominantly smaller, younger, individuals (Figures 8, 11-12, Tables 3-4) of larger, longer lived species (Weinstein 1981). Sizes of collected drums were the furthest from their potential max sizes. Red and black drum, can grow to more than 1,500mm TL, for which the largest specimens found in this study were 709mm and 486mm TL, respectively. Spotted and sand seatrouts can grow up to 1,000mm and 630mm TL, respectively, for which the largest specimens studied in this study were 537mm and 295mm TL, respectively. The largest Atlantic croaker and spot specimens were closer to their potential max size (550mm and 360mm TL, respectively) than the other species. The largest Atlantic croaker and spot being 310mm and 231mm TL, respectively. The higher prevalence of smaller individuals captured during the sampling period could be expected as estuaries, like Sabine Lake, are predominantly nursery grounds for sciaenids. Of the six study species, red drum is the only species

where adults do not typically reside in estuaries after reaching sexual maturity (Weinstein 1981), which could explain why larger red drums were not captured during sampling.

Since smaller individuals were predominantly sampled of the study species, especially the drums and spotted seatrout, the morphological results presented in this research are more reflective of smaller individuals of the study species and may not fully reflect the otolith morphology of larger individuals across the six species. However, these results still could give a good reflection of study species in general. For instance, a recent meta-analysis found that the mean size of red drum, black drum, and spotted seatrout studied in the northern GOM from 1989-2015 was 503mm, 417mm, 396mm TL, respectively (Flinn 2018). The mean sizes of red drum, black drum, and spotted seatrout (Table 3), are more comparable to the mean sizes studied for these species in the GOM. To the best of the authors knowledge, there has been no meta-analysis to date for mean study size of Atlantic croaker, spot, and sand seatrout in the northern GOM over a similar time period. As of this time, it is not possible to see how reflective the morphometric results of Atlantic croaker, spot, and sand seatrout specimens studied here actually reflect the mean sizes studied in the northern GOM. In addition to consideration of overall specimen size and its impact on the morphometric results, general specimen health (e.g., starved or fat) was considered as a factor of driving otolith morphology and fish size relationships, as metabolic stress is known to impact otolith and fish growth (Fablet et al. 2011).

Overall, specimens of all six species could be considered generally healthy, with mean body conditions near or above expected (Figure 10, Table 3). Body condition can be indictive of metabolic stress (Stevenson and Woods 2006), for which metabolic stress can limit otolith development and the relationship between otolith size and fish size (Fablet et al. 2011). As it relates to this study, the specimens with body conditions near, or above, expected (a value of 1 for Fulton's condition factor *K*) indicates that the samples were not likely under metabolic stress. However, the results for body condition could be misleading based on how body condition was calculated. If the specimens had eaten right before capture, and that mass had not been expelled, then the specimen would have an inflated mass, giving it a higher *K* value. For example, the outlying red drum individual in Figure 10 may have just eaten, increasing its overall mass, which could explain why it has a body condition value over twice of the mean for the species (Table 3). While it is harder to say how the acute diet of the six study species impacted their body condition, and ultimately the

morphology of their otoliths, the longer term diet of these species will have impacted their body condition, and by extension otolith morphology. In context of their ecology, it could be expected that the study species will generally have body conditions near expected. The six study species are opportunistic omnivores, usually feeding on crustaceans, bivalves, worms, and fishes (Weinstein 1981). All six species are known to actively travel within and between estuaries when prey availability is low (Weinstein 1981, Odell et al. 2017), inferring these species may not necessarily experience large periods of metabolic stress due to their ability to move. However, it is still entirely possible that these species may experience longer periods of metabolic stress when rapid environmental changes (e.g., cold snaps, anoxic events) kill off prey populations (Weinstein 1981). Depending on prey availability, the species metabolism, and ultimately body condition, could be affected. Changes to fish metabolism (e.g., a decrease in metabolism during limited prey availability) will alter the development of the otolith. Fablet et al. (2011) noted that fish body growth slows more than otolith growth during periods of metabolic, which could affect the strength of relationships between otolith morphology and TL.

Across all study species, all otolith metrics (i.e., OL, OW, OP, OA, and OM) were strongly correlated with fish TL (Figures 13-18, Table 6). Some previous studies of tropical and temperate fishes noted that otolith size (specifically OL and OW) follows a strong linear relationship with TL until reaching an asymptote at a certain size (Boehlert 1985, Pilling et al. 2003, Bermejo 2014). An asymptote was not observed in the present study. Two possible explanations for the strong linear correlations between all metrics and TL found in this study may relate to the ecology and biology of these species, and the body size and condition of the samples. In the studies that noted weaker correlations between metrics and fish size (e.g., Boehlert 1985, Pilling et al. 2003, Bermejo 2014), the species of interest in those studies were not sciaenids, and not as dependent on auditory cues for mating, feeding, and signaling arrival of predators as sciaenids are (Ramcharitar 2006). The higher dependency on sound transduction in sciaenids could explain the strong positive correlations between metrics and TL, where the size of the otolith is vital for individual survival and population growth. A similar morphometric study of sagittal otoliths of sciaenids also found linear relationships with otolith size and fish size (Kumar 2012), supporting the results found in this study.

The second, and possibly covarying, explanation is that the results are more of a reflection of the samples studied (i.e., predominantly shorter, younger, individuals of larger older lived species) than of the species themselves. In teleost fishes the relative growth of the otolith is usually negatively allometric, meaning that smaller, younger individuals will initially have a more linear relationship with fish size until reaching an asymptote (Lombarte and Lleonart 1993, Shingleton 2010). In this study, the strongest linear relationships between metrics and TL were found to be in Atlantic croaker, spot, and sand seatrout, which were the species that had the highest percentage of smaller individuals (Figures 11-12, 16-18 , Tables 3 and 6). This result though may again reflect the specimens studied. In a study of sciaenids from northern Rio de Janeiro, some size metrics (e.g., OW) were found to have a negatively allometric relationship with fish size (Monteiro et al. 2005), so it is possible that six species of sciaenids study here could follow this pattern after a certain size is reached. Further work studying the relationship of otolith size and TL in larger individuals of all study species would be needed to say with more certainty about this matter.

Congruent with the specimen size, was the general health of the specimens. As previously noted, metabolic stress will impact the relationship between otolith size and fish size. Over time individuals may experience more episodes of metabolic stress, and similar to the long term impacts of environment on otolith morphology, those periods of metabolic stress could continually reduce the strength of the relationship of otolith size with fish size (Fablet et al. 2011) The species with the highest percentage of larger individuals (i.e., red drum, black drum, spotted seatrout), had weaker relationships between otolith metrics and TL (Figures 11-12, 13-15 , Tables 3 and 6). Which could be indicative that they experienced more periods of metabolic stress, weaking the correlation between otolith size and TL. However, for the most part, all study specimens were in generally good health at time of capture, so it only could be inferred that some specimens of red drum, black drum, and spotted may have experienced more periods of metabolic stress. Overall, the strong linear relationships with metrics and TL in the study species could be a resultant property of their biology, or a reflection of the smaller, generally healthy, collected specimens, or a combination of both. To fully understand the correlations between metrics and TL in the six sciaenid species studied here more work is required, specifically looking at larger older individuals across all species.

In addition to otolith size changes, the shape of the otoliths changed with increasing fish size. The intra-specific changes in otolith shape with TL was evaluated using both shape descriptors and EFC. Both shape evaluation methods helped describe the changes in otolith shape in different ways for the study species. The descriptors (i.e., form factor (FF), circularity (C), roundness (R), ellipticity (E), rectangularity (RC), aspect ratio (AR), and compactness (CP)) highlighted more overall changes in shape, while the EFC were able to show the finer changes in shape. As assessed by most descriptors, otolith shape changed significantly, $p < 0.05$, with increasing TL (Figures 19-24, Tables 8-9). In the six species studied, otolith shape started more circular and deviated towards elongated elliptical shapes, with smaller individuals having more similar otolith shapes compared to larger individuals (Figures 19-24). This follows with the general pattern of otolith development as otoliths start out as more spherical or oblate structures before they develop into species-specific shapes (Campana 1989, 2004). Another shape development pattern that has been noted in past sciaenid otolith morphology studies (e.g., Kumar 2012, Taylor 2020) that was also found in this study was the development of calcareous protuberances and concrescence. Which was evaluated by the CP shape descriptor.

Compactness showed a strong negative curvilinear relationship with TL across all species (Figures 19-24, bottom panels). CP in all species likely changed with TL because of the development of calcareous protuberances on distal, dorsal, and ventral sides of the otoliths. During otolith morphogenesis accretion of calcium carbonate is not always evenly deposited across the surface of the otolith (Wu et al. 2011), leading to the formation of protuberances. The growth of these features' changes throughout an individual's life and varies with species, age, and environmental factors (e.g., habitat, temperature, and diet) (Taylor 2020). Over time the spaces between the protuberances are filled in with new material (Taylor 2020), which causes CP to level off in larger individuals. This was seen across all study species (Figures 19-24, bottom panels). Unique amongst the study species, however, was Atlantic croaker that actually developed a very specific protuberance, called an accessory growth center, in larger individuals (around 200mm TL) (Appendix E, Figure 41). It was found though, that even with the development of the accessory growth center, CP in Atlantic croaker otoliths did level off in larger individuals, suggesting that after the accessory growth center formed and a certain CP level is reached, the value does not deviate much with continual increases in TL (Appendix E, Figure 41).

The more subtle change in otolith shape were found using the EFC. Atlantic croaker, spot, and sand seatrout were the only species in the study to show significant differences in otolith shape, based on EFC, with changes in fish size (Tables 17, 19, and 21). As expected with the ANOSIM results, where otolith shape was significantly different across size classes, the otolith shape groupings in Atlantic croaker, spot, and sand seatrout showed more relation to fish size than in the other three species (Figures 30-33). However, across all species, shape groupings were not fully explained by fish size, if at all (Figures 27-33), suggesting that other external factors are affecting otolith shape. In most of the study species, there appears to be binary groupings of individuals based on otolith shape (Figures 27-33). Prominent factors in all of the study species that could cause a binary grouping are sex (e.g., male or female) and or sexual maturity (e.g., mature or immature). As estimated from the literature, all species in this study except for red drum, had some specimens collected that were near, or larger, than the lengths typically reached at sexual maturity (red and black drum: Pearson 1929, Simmons and Breuer 1962; spotted seatrout: Miles 1950, Nieland 2002; sand seatrout: Sutter and McIlwain 1987; Atlantic croaker: Weinstein 1981; spot: Hildebrand and Cable 1930, Gunter 1945, Townsend 1956, Dawson 1958, Hales and Van Den Avyle 1989). An individual's sex and the onset of sexual maturity are typically associated with shifts in habitat, metabolism, and body growth rates, all of which may alter otolith morphogenesis in sciaenids. This could explain the shape groupings in the nMDS plots that were not explained by fish size. Because specimen sex and gonadal development were not evaluated in this present study, it is just speculative that these factors caused the binary shape groupings seen in most of the nMDS plots of the study species (Figures 27-33). Until complementary maturity studies are conducted for the study species, any impact of sex and maturity on otolith morphology is still speculative.

An important finding of this study came from the EFC analysis on Atlantic croakers. Amongst all of the EFC analyzed visually using nMDS plots, Atlantic croakers were notable in that the larger individuals appeared to have drastically different shapes from one another, as inferred from the high variance in the nMDS plots (Figures 31-32). When investigated further it was found that shape of Atlantic croaker otoliths become non-holomorphic (i.e., the shape overlaps on itself) when they develop the accessory growth center. The problem with this is EFC cannot correctly identify the perimeter of non-holomorphic shapes because the vectors radiating from the center of the otolith come into contact with the perimeter multiple times making it impossible to assess which point marks the edge of the otolith. The effect of this is that non-holomorphic shapes

analyzed using EFC become distorted and stretched in multiple directions (Sanchez-Corrales et al. 2017). This explains the scattering pattern in Atlantic croaker otoliths of individuals over ~200mm TL (Figures 31-32). As a shape evaluation technique, EFC is appropriate for Atlantic croakers under 200mm TL (before the formation of the accessory growth center), and for all other study species regardless of TL. For future studies of Atlantic croaker otolith shape, a different method of shape evaluation should be used if the desire is to study the shape in individuals over ~200mm TL. One potential method is wavelet analysis, as suggested by Libungan and Pálsson (2015), which is not impacted so severely by complex shapes.

The inter- and intra-specific differences in otolith morphology allowed for discrimination of species and for individuals to be correctly identified to species. Correct species identification by canonical analysis of principal coordinates (CAP) was highest using standardized metrics (~95%, Figure 34), followed by descriptors (~79%, Figure 35) and EFC (~73%, Figure 36). It was not expected that the most accurate morphometric assessment method, EFC, would be the least accurate tool in identifying the study specimens to their correct species. A possible explanation is that the finer resolution in shape differences using EFC could have resulted in the lower accuracy, because in each species there were more possibilities of what the otolith shape could be, that when shape was compared between species there was more overlap in EFC values. Further investigation would be needed to confirm this, and to see if various methods of sorting individuals (e.g., sub dividing species into different size classes), improves the accuracy of EFC in discriminating between species. The results of CAP further demonstrate the utility of morphometric assessment by means of image analysis. With one photograph of an individual's otolith, a specimen can be correctly identified to species and the general size of the fish it came from. With future work expanding on the impacts of environment, body condition, and sex, it is possible that these factors could potentially be analyzed through morphometric assessment too. This is not unrealistic as morphometric analysis has already been widely used to separate stocks based on changes in otolith morphology due to environmental differences (Campana and Casselman 1993, Libungan and Pálsson 2015, Hüssy et al. 2016).

As management of fisheries incorporates more holistic approaches external analysis of otolith morphology will increase in importance to fisheries scientists , as it can further explain inter- and intra-specific variability and ecological changes at a much faster rate than traditional

evaluation methods (e.g., annuli analysis) (Qamar 2019). Another benefit of using otolith morphology to assess the life history (e.g., fish size, age, maturity, stock) of individuals is that it can be measured without significant measurement error nor is it subjected to size or shape distortion from shrinkage or preservation (Campana and Casselman 1993). An important focus of fisheries is studying stocks and the differences (e.g., fish growth, age, fecundity) between stocks (Campana 2004). As all study species are known to travel between estuaries in search of prey and to avoid unfavorable environmental conditions (Weinstein 1981), work is first needed to identify whether stocks of each species exist in the northern GOM, before morphometric assessments can be done to evaluate differences between the stocks. Past studies have found strong connections between age and otolith morphology (e.g., Bermejo 2007, 2014, Doering-Arjes 2008, Steward 2009). As the study species are a part of commercially and recreationally important fisheries in the northern GOM, being able to estimate age from otolith morphology, beyond that of age proxies from fish TL, would be a further asset to fisheries managers. Overall, the gathering all of this life history information through evaluation of a photograph of the otolith could be a promising avenue of interest for fishery agencies looking to reduce time and money spent on traditional otolith evaluation methods (Campana 2004, Steward 2009, Qamar 2019).

CONCLUSION

In conclusion the results of this study show that otolith morphology of red drum, black drum, spotted seatrout, sand seatrout, Atlantic croaker, and spot changes with increases in fish total length (TL). Otolith metrics (i.e., length, width, perimeter, area, and mass) increase linearly with increasing TL. Otolith shape in these species of sciaenids changes from a more circular shape to elliptical with increases in TL. As the samples in this study consisted of smaller, younger, individuals of large, long-lived species, patterns of shape change may not fully reflect the continual changes in otolith morphology over the life of these fishes. The results of this study inform us that otolith morphology of sciaenid's in the northern GOM correlate with ontogenetic changes in the fishes. To the best of the authors knowledge, this work is the first of its kind on sciaenid species in the northern GOM.

REFERENCES

Able K.W., Fahay M.P. (2010) Ecology of Estuarine Fishes: Temperate Waters of the Western North Atlantic. Johns Hopkins University Press. Baltimore, MD.

Afanasyev P., Orlov A.M. (2017) Otolith Shape Analysis as a Tool for Species Identification and Studying the Population Structure of Different Fish Species. *Bio. Bull.* 44:8, 952-959.

Armstrong, N.E. (1987) The ecology of open-bay bottoms of Texas: a community profile. *USDI Fish & Wildl. Serv. Biol. Report* 85, 104.

Bal H., Türker D., Zengin K. (2018) Morphological characteristics of otolith for four fish species in the Edremit Gulf, Aegean Sea, Turkey. *Iran. J. Ichthyol*. 5:4, 303-311.

Barbieri L.R., Chittenden M.E., Jones C.M. (1994). Age, growth, and mortality of Atlantic croaker, *Micropogonias undulatus*, in the Chesapeake Bay-region, with a discussion of apparent geographic changes in population-dynamics. *Fish. Bull*. 92:1, 1-12.

Barger L.E. (1985) Age and Growth of Atlantic Croakers in the Northern Gulf of Mexico, Based on Otolith Sections. *Trans. Amer. Fish. Soc*. 114:6, 847-850.

Beckman D.W., Stanley A.L., Render J.H., Wilson C.A. (1990). Age and growth of black drum in Louisiana waters of the Gulf of Mexico. *Trans. Am. Fish. Soc.* 119:3, 537-544.

Bermejo S. (2007) Fish age classification based on length, weight, sex and otolith morphological features. *Fish. Res.* 84, 270-274.

Bermejo S. (2014) The benefits of using otolith weight in statistical fish age classification: A case study of Atlantic cod species. *Computers and Electronics in Agriculture*. 107, 1-7.

Boehlert G.W. (1985) Using Objective Criteria and Multiple Regression Models for Age Determination in Fishes. *Fish. Bull.* 83:2, 103-117.

Boyd, N. (2019) "All in the Family". Texas Parks and Wildlife Department. url: https://tpwd.texas.gov/fishboat/fish/didyouknow/coastal/allinthefamily.phtml (Accessed on: 03/14/19)

Britton J.R., Blackburn R. (2014) Application and utility of using otolith weights in the ageing of three flatfish species. *Fish Res*. 154, 147-151.

Burke, N., Brophy, D., King, P.A. (2008) Shape analysis of otolith annuli in Atlantic herring (*Clupea harengus*); a new method for tracking fish populations. *Fish. Res*. 91, 133-143.

Byrd B.L., Hohn A.A., Krause J.R. (2020) Using the otolith sulcus to aid in prey identification and improve estimates of prey size in diet studies of a piscivorous predator. *Ecol. Evol.* 10, 3584-3604.

Caillon F., Bonhomme V., et al. (2018). A morphometric dive into fish diversity. *Ecosphere* 9:5, 1-10.

Campana, S.E. 1999. Chemistry and composition of fish otoliths: pathways, mechanisms and applications. Mar. Ecol. Prog. Ser. 188: 263-297

Campana S.E., Casselman J.M. (1993) Stock discrimination using otolith shape analysis. Can. J. Fish. Aquat. Sci. 50, 1062-1083

Campana S.E. (1989) Otolith microstructure of three larval gadids in the Gulf of Maine, with reference on early life history. Can. J. Zool. 67, 1401-1410.

Campana S.E., Thorrold S.R. (2001) Otoliths, increments, and elements: keys to comprehensive understanding of fish populations? Can. J. Fish. Aquat. Sci. 58, 30-38.

Campana S.E. (2004) Photographic atlas of fish otoliths of the Northwest Atlantic Ocean. NRC Research Press, Ottawa, Ontario.

Carlström D. (1963). A Crystallographic Study of Vertebrate Otoliths. *Biol. Bull.* 125:3, 441-463.

Chao L.N. (1978). Sciaenidae. In W. Fischer (ed.) FAO species identification sheets for fishery purposes. West Atlantic (Fishing Area 31). Volume 4. FAO, Rome.

Chao L.N., Musick J.A. (1977) Life history, feeding habits, and functional morphology of juvenile sciaenid fishes in the York River estuary, Virginia. Fish. Bull. U.S. 75, 657-702.

Dawson C.E. (1958). A study of the biology and life history of the spot, *Leiostomus xanthurus* Lacepede, with special reference to South Carolina. S.C. Wildl. Mar. Res. Dep. Contrib. Bears Bluff Lab. No. 28, 48.

DeVries, D.A. (1982) Age and growth of spot in North Carolina. Northeast Fish Widl. Conf., April 13-15, 1982 Cherry Hill, NJ (Abstract).

Ditty J.G., Bourgeois M., Kasprzak R., Konikoff M. (1991) Life History and Ecology of Sand Seatrout *Cynoscion arenarius* Ginsburg, in the Northern Gulf of Mexico: A Review. Northeast Gulf Science 12:1, 35-47

Doering-Arjes P., Cardinale M., Mosegaard H. (2008) Estimating population age structure using otolith morphometrics: a test with known-age Atlantic cod (*Gadus morhua*) individuals. Can. J. Fish. Aqut. Sci. 65:11, 2342-2350

Fablet R., Pecquerie L., et al. (2011) Shedding Light on Fish Otolith Biomineralization Using a Bioenergetic Approach. *PLoS ONE.* 6:11, e27055.

Flinn S. (2018) An Evaluation of Sciaenid Growth in the Gulf of Mexico. *LSU Master's Theses*. 4805

Fisher, M., Hunter, E. (2018) Digital imaging techniques in otolith data capture, analysis and interpretation. *Mar. Ecol. Prog. Ser.* 598, 213-231

Frimodt C. (1995) Multilingual illustrated guide to the world's commercial coldwater fish. Fishing News Books, Osney Mead, Oxford, England. p.215

Gunter G. (1945) Studies on marine fishes of Texas. Publ. Instit. Mar. Sci. Univ. Tex. 1, 1-90

Gunter G., Hildebrand H.H. (1951) Destruction of fishes and other organisms on the south Texas coast by the cold wave of January 28 – February 3, 1951. Ecology. 32, 731-735.

Hales L.S., Van Den Avyle M.J. (1989) Species profiles: life histories and environmental requirements of coastal fishes and invertebrates (South Atlantic) Spot. U.S. Fish and Wildlife Service Biological Report 82(11). U.S. Army Corps of Engineers TR EL-82-4.

He T., Cheng J., et al. (2018) Comparative analysis of otolith morphology in three species of Scomber. *Ichthyol. Res.* 65, 192-201

Hendrickson D.A., Cohen A. E. (2015). Fishes of Texas Project Database (version 2.0). Texas Advanced Computing Center, University of Texas at Austin. Accessed 14 July 2019.

Hildebrand S.F., Cable L. (1930) Development and life history of fourteen teleostean fishes at Beaufort, North Carolina. Bull. U.S. Bur. Fish. 46, 383-488.

Hugg D.O., (1996) MAPFISH georeferenced mapping database. Freshwater and estuarine fishes of North America. Life Science Software 1278 Turkey Point Road, Edgewater, Maryland, USA.

Hunt J.J. (1992) Morphological characteristics of Otoliths for selected fish in the Northwest Atlantic. *J. Northw. Atl. Fish. Sci.* 13, 63-75.

Hüssy K., Mosegaard H., et al. (2016) Evaluation of otolith shape as a tool for stock discrimination in marine fishes using Baltic Sea cod as a case study. *Fish. Res*. 174, 210-218.

International Game Fish Association (1991) World record game fishes. International Game Fish Association, Fort Lauderdale, Florida.

International Game Fish Association (2001) Database of IGFA angling records until 2001. IGFA, Fort Lauderdale, Florida.

Jaramillo A.M., Tombari A.D., et al. (2014) Otolith Eco-Morphological Patterns of Benthic Fishes from the Coast of Valencia (Spain). *Thalassas.* 30:1, 57-66.

Johnson G.D. (1978) Development of Fishes of the Mid-Atlantic Bight. Volume IV, Carangidae through Ephippidae. *U.S. Fish. Wildl. Serv. Biol. Serv*. Program FWS/OBS. 78:12, 416

Jordan D.S., Evermann B.E. (1898) The fishes of north and middle America. Bull. *U.S. Nat. Mus. No*. 47:2, 1392-1490.

Kumar, P., Chakraborty, S.K., Jaiswar, A.K. (2012) Comparative otolith morphology of sciaenids occurring along the north-west coast of India. Ind. J. Fish. 59:4, 19-27

Lepak J.M., Cathcart C.N., Hooten M.B. (2012) Otolith mass as a predictor of age in kokanee salmon (*Oncorhynchus nerka*) from four Colorado reservoirs. *Can. J. Fish. Aquat. Sci*. 69, 1569-1575

Libungan, L.A., Pálsson, S. (2015) ShapeR: An R Package to Study Otolith Shape Variation among Fish Populations. PLoS ONE. 10:3.

Lombarte A., Lleonart J. (1993) Otolith size changes related with body growth, habitat depth, and temperature. *Environ. Biol. Fishes.* 37, 297-306.

Lou, D.C., Mapstone, B.D., Russ, G.R., Davies, C.R., Begg, G.A.(2005) Using otolith weight-age relationships to predict age-based metrics of coral reef fish populations at different spatial scales. Fish. J. 71:3, 279-294

Maceina M.J., Hata D.N., Linton T.L., Landry A.M. Jr. (1987) Age and Growth Analysis of Spotted Seatrout from Galveston Bay, Texas. Tran. Americ. Fish. Soc. 116:1, 54-59.

McFarlane R.W. (1996) A Conceptual Ecosystem Model for Sabine Lake. Sabine Lake Conference. 27-31.

McRae G., Muller R.G., Paperno R. (1997). 1997 Update on Florida's Spot Fishery: Report to the Marine Fisheries Commission. Department of Environmental Protection Florida Marine Research Institute, St. Petersburg, Florida.

Mendoza R.P.R (2006) Otoliths and Their Application in Fishery Science. *Ribarstvo.* 64:3, 89-102.

Miles D.W. (1950) The life histories of the spotted seatrout, Cynoscion nebulosus, and the redfish, Sciaenops ocellatus. Texas Game, Fish and Oyster Comm., Mar. Lab. Ann. Rept.

Milton D.A., Chenery S.R. (1998) The effect of otolith storage methods on the concentrations of elements detected by laser-ablation ICPMS. *J. Fish. Bio*. 53:4, 785-794.

Monteiro, L.R., Di Beneditto A.P.M., Guillermo, L.H., Rivera, L.A. (2005) Allometric changes and shape differentiation of sagitta otoliths in sciaenid fishes. *Fish. Res*. 74:1-3, 288-299.

Mosegaard H., Morales-Nin B. (2000) Section 1: Otolith physiology and morphology. *Fish. Res.* 46, 3-4.

Mugiya Y., Watabe N. (1977) Studies on fish scale formation and resorption -II. Effect of estradiol on calcium homeostasis and skeletal tissue resorption in the goldfish, *Carassius auratus*, and the killifish, *Fundulus heteroclitus*. *Comp. Biochem. Physio. Part A: Physio*. 57:2, 197-202.

Murphy M.D, Taylor R.G. (1994) Age, Growth, and Mortality of Spotted Seatrout in Florida Waters. *Trans. Am. Fish. Soc.* 123:4, 482-497.

National Marine Fisheries Service (2018a) Fisheries of the United States, 2017 Report. U.S. Department of Commerce, NOAA Current Fishery Statistics No. 2017 Available at: https://www.fisheries.noaa.gov/feature-story/ fisheries-united-states-2017

National Marine Fisheries Service (2018b) Fisheries Economics of the United States, 2016. U.S. Dept. of Commerce, NOAA Tech. Memo. NMFS-F/SPO-187. p. 243

Nelson,W.R. (1969) Studies on the Croaker, *Micropogon undulatus* Linnaeus, and the spot, *Leiostomus xanthurus* Lacepede, in Mobile Bay, Alabama. J. Mar. Sci. Alabama 1, 4-92.

Nemeth D.J., Jackson J.B., Knapp A.R., Purtlebaugh C.H. (2006) Age and growth of sand seatrout (*Cynoscion arenarius*) in the estuarine waters of the Eastern Gulf of Mexico. Gulf of Mexico Sci. 1/2, 45-60.

Newman S.J., Williams D.M., Russ G.R. (1996) Age validation, growth and mortality rates of the tropical snappers (Pisces: Lutjanidae) Lutjanus adetii (Castelnau, 1873) and L. quinquelineatus (Bloch, 1790) from the central Great Barrier Reef, Australia. *Mar. Fresh. Res.* 47:4, 575-584.

Nieland D.L., Thomas R.G., Wilson C.A. (2002) Age, Growth, and Reproduction of Spotted Seatrout in Barataria Bay, Louisiana. *Trans. Americ. Fish. Soc*. 131-245-259.

Nolf D. (1985) Otolithi Piscium. In Handbook of Paleoichthyology, Vol. 10. Edited by H.P. Schultze. Gustav Fischer Verlag, New York. p. 145

Odell J., Adams D. H., et al. (2017) Atlantic Sciaenid Habitats: A Review of Utilization, Threats, and Recommendations for Conservation, Management, and Research. Atlantic States Marine Fisheries Commission Habitat Management Series No. 14, Arlington, VA.

Oliveira A.M., Farina M., Ludka I.P., Kachar B. (1996) Vaterite, calcite and aragonite in the otoliths of three species of piranha. *Naturwissenschaften*. 83, 133-135.

Omar, A.M., AMohamed, S.K.H. (2016) Comparative morphological studies on the otoliths (ear stones or crystals) in some marine and fresh water fishes. *Inter. J. Fish. Aqu. Stu*. 4, 512-517.

Qamar N., Panhwar S.K., et al. (2019) Numerical expressions of otolith shape and morphometric relationships for five fish species in tidal-linked lagoons in the northern Arabian Sea. *Lakes & Reserv.* 24, 354-361.

Pannella G. (1971) Fish Otoliths: Daily Growth Layers and Periodical Patterns. *Sci.* 173:4002, 1124-1127.

Patterson W.P., Smith G.R., Lohmann K.C. (1993) Continental paleothermometry and seasonality using the isotopic composition of aragonitic otoliths of freshwater fishes. *Geophys. Monogr. Ser.* 78, 191-202.

Patterson W.P. (1999) Oldest isotopically characterized fish otoliths provide insight to Jurassic continental climate of Europe. *Geo.* 27:3, 199-202.

Pearson J.C. (1929) Natural history and conservation of redfish and other commercial sciaenids of the Texas Coast. *Bull. Bur. Fish*. 44, 129-214.

Peters K.M., McMichael R.H. (1987) Early life history of red drum, *Sciaenops ocellatus* (Pisces: Sciaenidae), in Tampa Bay, Florida. *Estuaries* 10, 92-107.

Pilling, G.M., Grandcourt, E.M., Kirkwood, G.P. (2003) The utility of otolith weight as a predictor of age in the emperor *Lethrinus mahsena* and other tropical species. *Fish. Res*. 60:2-3, 493-506.

Popper A.N., Lu Z. (2000) Structure-function relationships in fish otolith organs. *Fish. Res*. 46, 15-25.

Popper A.N., Platt C. (1993) Inner ear and lateral line. In Physiology of Fishes, Edited by D.H. Evans, CRC Press, London, UK. 99-136

R Core Team (2020). R: A Language and Environment for Statistical Computing. R Foundation for Statistical Computing, Vienna, Austria.

Ramcharitar J., Gannon D.P., Popper A.N. (2006) Bioacoustics of Fishes of the Family Sciaenidae (Croakers and Drums) *Trans. Am. Fish. Soc*. 135, 1409-1431.

Ramírez-Pérez J.S., et al. (2010) Using the Shape of Sagitta Otoliths in the Discrimination of Phenotypic Stocks in *Scomberomorus sierra* (Jordan and Starks, 1895). *J. Fish. Aquat. Sci.* 5:2, 82-93.

Richards C.E. (1973) Age, growth and distribution of the black drum (*Pogonias cromis*) in Virginia. *Trans. Amer. Fish. Soc.* 102, 584-590.

Robins C.R., Ray G.C (1986) A field guide to Atlantic coast fishes of North America. Houghton Mifflin Company, Boston, Massachusetts.

Rohlf J.F. (1988). Chapter 3 An overview of Image Processing and Analysis Techniques for Morphometrics. In Proceedings of the Michigan Morphometrics Workshop. Special Publication No 2, Univ. of Michigan Museum of Zoology. 37-60

Rooker J.R., Holt S.A. (1997) Utilization of subtropical seagrass meadows by newly settled red drum *Sciaenops ocellatus*: patterns of distribution and growth. *Mar. Ecol. Prog. Ser.* 158, 139-149.

Ross J.L., Stevens T.M., Vaughan D.S. (1995) Age, growth, mortality, and reproductive biology of red drums in North Carolina waters. *Trans. Am. Fish. Soc*. 124:1, 37-54.

Sadighzadeh Z., Otero-Ferrer J.L., et al. (2014) An approach to unraveling the coexistence of snappers (Lutjanidae) using otolith morphology. *Scientia Marina.* 78:3, 353-362.

Sanchez-Corrales Y.E., Hartley M., et al. (2017) Morphometrics of complex cell shapes: Lobe Contribution Elliptic Fourier Analysis (LOCO-EFA). *Grieneisen*. 1:4

Schade F.M., Weist P., Krumme U. (2019) Evaluation of four stock discrimination methods to assign individuals from mixed-stock fisheries using genetically validated baseline samples. *Mar. Ecol. Prog. Ser.*627, 125-139.

Schulz-Mirbach T., Stransky C., Schlickeisen J., Reichenbacher B. (2008) Differences in otolith morphologies between surface- and cave-dwelling populations of *Poecilia mexicana* (Teleostei, Poeciliidae) reflect adaptations to life in an extreme habitat, *Evol. Ecol. Res*. 10, 537-558

Shingleton, A. (2010) Allometry: The Study of Biological Scaling. *Nature Education Knowledge*. 3:10, 2.

Shlossman P.A., Chittenden Jr. M.E. (1981) Reproduction, Movements, and Population Dynamics of the Sand Seatrout, *Cynoscion arenarius*. *Fish. Bull.* 79:4, 649-669.

Simmons E.G., Breuer J.P. (1962) A study of Redfish, *Sciaenops ocellate* Linnaeus and Black Drum, *Pogonias cromis* Linnaeus. *Publ. Instit. Mar. Sci. Univ. Tex*. 8, 184-211.

Smale M.J., Watson G., Hecht T. (1995) Otolith atlas of southern African marine fishes. Ichthylological monographs of the J.L.B. Smith Institute of Ichthylology. 1, xiv, 253.

Song J., Dou S., et al. (2020) Sulcus and otolith outline analyses: complementary tools for stock discrimination in white croaker *Pennahia argentata* in northern Chinese coastal waters*. *J. Oceanol. Limnol.*

Steward, C.A., DeMaria, K.D., Shenker, J.M. (2009) Using otolith morphometrics to quickly and inexpensively predict age in the gray angelfish (*Pomacanthus arcuatus*). *Fish. Res.* 99:2, 123-129.

Stransky C., Murta A.G., et al. (2008) Otolith shape analysis as a tool for stock separation of horse mackerel (*Trachurus trachurus*) in the Northeast Atlantic and Mediterranean. *Fish. Res.* 89, 159-166.

Sutter F.C., McIlwain T.D. (1987) Sand Seatrout and Silver Seatrout (Species profiles: Life Histories and Environmental Requirements of Coastal Fishes and Invertebrates (Gulf of Mexico)). Fish and Wildlife Service, U.S. Department of Interior, Coastal Ecology Group.

Tabb D.C. (1961) A contribution to the biology of the spotted seatrout, *Cynoscion nebulosus*, (Cuvier), of the east-central Florida. *Fla. State Bd. Cons. Univ. Miami Mar. Lab. Tech. Ser*. 35, 1-23.

Tatsuta H., Takahashi K.H., Sakamaki Y. (2018) Geometric morphometrics in entomology: Basics and applications. *Entomol. Sci.*21, 164-184.

Taylor M.D., Fowler A.M., Suthers I.M. (2020) Insights into fish auditory structure–function relationships from morphological and behavioral ontogeny in a maturing sciaenid. *Mar. Bio.* 167:21, 1-11.

Towne, I.A. (2018) Age and Growth of Hogfish (*Lahnolaimus maximus*) in Southeast Florida. Master's thesis, Nova Southeastern University.

Townsend, B.C. Jr. (1956) A study of the spot, *Leiostomus xanthurus* Lacepede, in Alligator Harbor, Florida. M.S. Thesis, Florida State University.

Tuset V.M., Lombarte A., et al. (2003) Comparative morphology of the sagittal otolith in *Serranus* spp. *J. Fish. Bio.* 63, 1491-1504

Tuset V.M., Farré M., et al. (2016) Testing otolith morphology for measuring marine fish biodiversity. *Mar. Freshw.* 67, 1037-1048.

Vanderkoov S. (2009) A Practical Handbook for Determining the Age of Gulf of Mexico Fishes – Second Edition. Gulf States Marine Fisheries Commission, 167.

Waessle J.A., Lasta C.A., Favero M. (2003) Otolith morphology and body size relationships for juvenile Sciaenidae in the Rio de la Plata estuary (35-36°S)*. *Sci. Mar*. 67:2, 233-240.

Weinstein M.P. (1981) Biology of Adult Sciaenids. *Proc. Sixth. Ann. Mar. Rec. Fish*. 125-138.

Weinstein M.P., Walters M.F. (1981) Growth, survival, and production in young-of-year spot *Leiostomus xanthurus* Lacepede residing in tidal creeks. *Estuaries*. 4, 185-197.

Welsh W.W., Breder C.M. Jr. (1923) Contributions to the life histories of Sciaenidae of the eastern United States coast. *Bull. U.S. Bur. Fish*. 39, 141-201.

White M.L., Chittenden M.E. (1977) Age determination, reproduction and population dynamics of the Atlantic croaker *Micropogonias undulatus*. *Fish. Bull*. 75:1, 109-124.

Wooster R. (2010) "Sabine Lake". Handbook of Texas Online. Accessed June 01, 2019.

Wu D., Freund J.B., et al. (2011) Mechanistic basis of otolith formation during teleost inner ear development. *Dev. Cell.* 20:2, 271-278.

Zengin M., Saygin S., Polat N. (2015) Otolith Shape Analyses and Dimensions of the Anchovy *Engraulis encrasicolus* L. in the Black and Marmara Seas. *Sains Malaysiana*. 44:5, 657-662.

Zorica B, Sinovčić G., Čikeš Keč V. (2010) Preliminary data on the study of otolith morphology of five pelagic fish species from the Adriatic Sea (Croatia). *Acta Adriatica*. 51:1, 89-96.

APPENDIX A

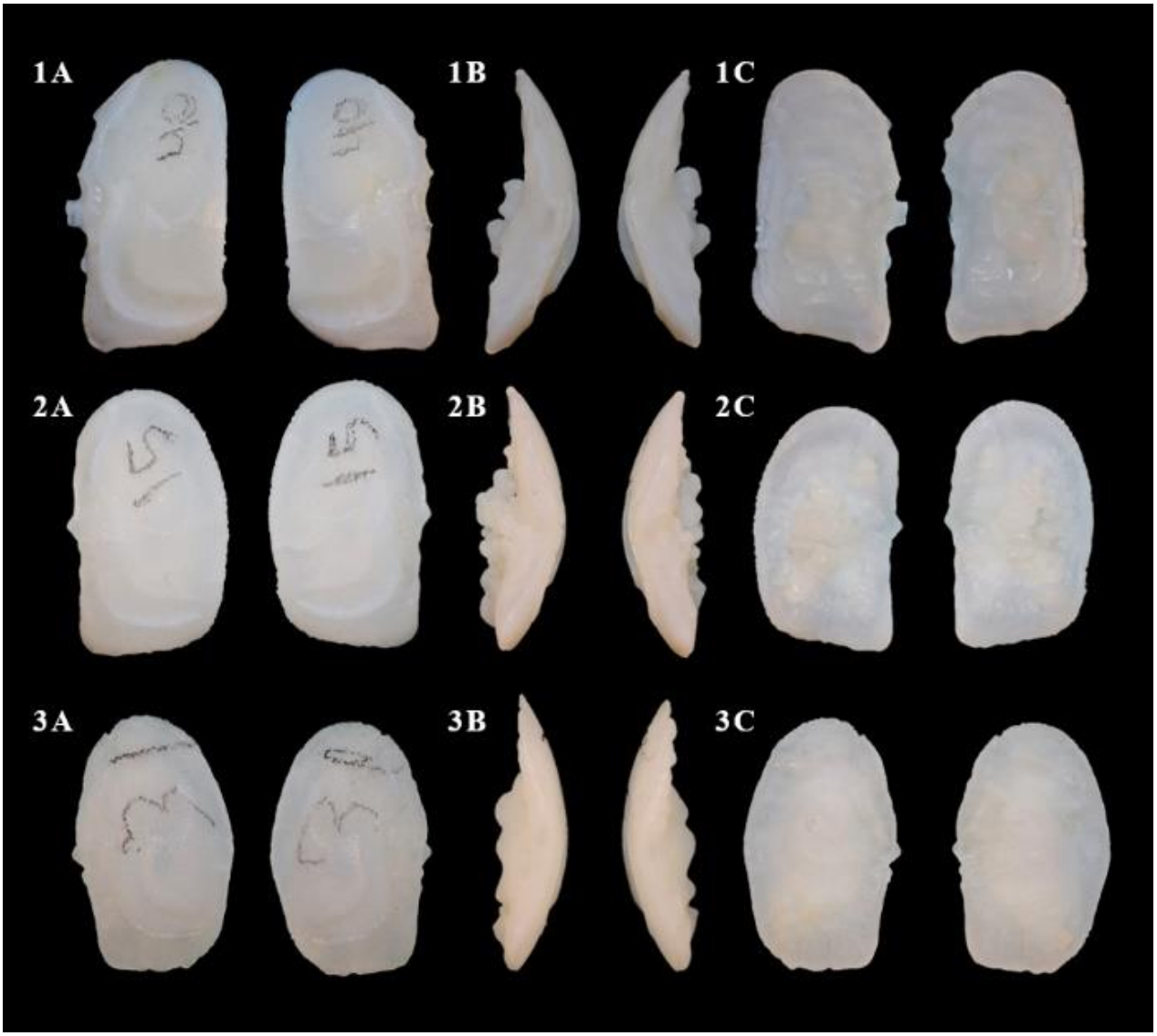

Figure 37. Red drum sagittal otoliths. Highlighting variance in otolith shape, structure, and development of protuberances. Side (A) is the proximal side of the otolith. Side (B) is the dorsal side of the otolith. Side (C) is the distal side of the otolith. The TL of individual (1) was 709 mm and the OL and OW were 19.7mm and 11.0mm, respectively. The TL of individual (2) was 393mm and the OL and OW were 12.6mm and 7.7mm, respectively. The TL of individual (3) was 169mm and the OL and OW were 7.4mm and 5.2mm, respectively.

APPENDIX B

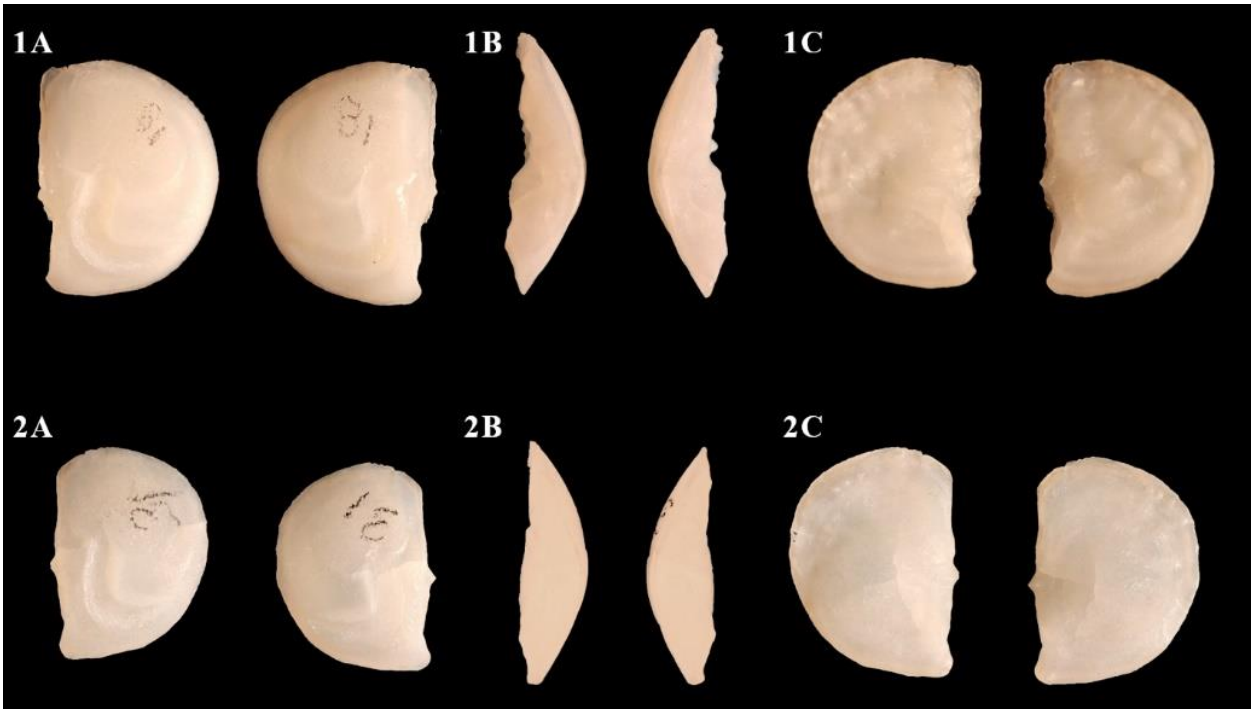

Figure 38. Black drum sagittal otoliths. Highlighting variance in otolith shape, structure, and development of protuberances. Side (A) is the proximal side of the otolith. Side (B) is the dorsal side of the otolith. Side (C) is the distal side of the otolith. The TL of individual (1) was 482mm and the OL and OW were 14.1mm and 11.2mm, respectively. The TL of individual (2) was 235mm and the OL and OW were 9.1mm and 7.2mm, respectively.

APPENDIX C

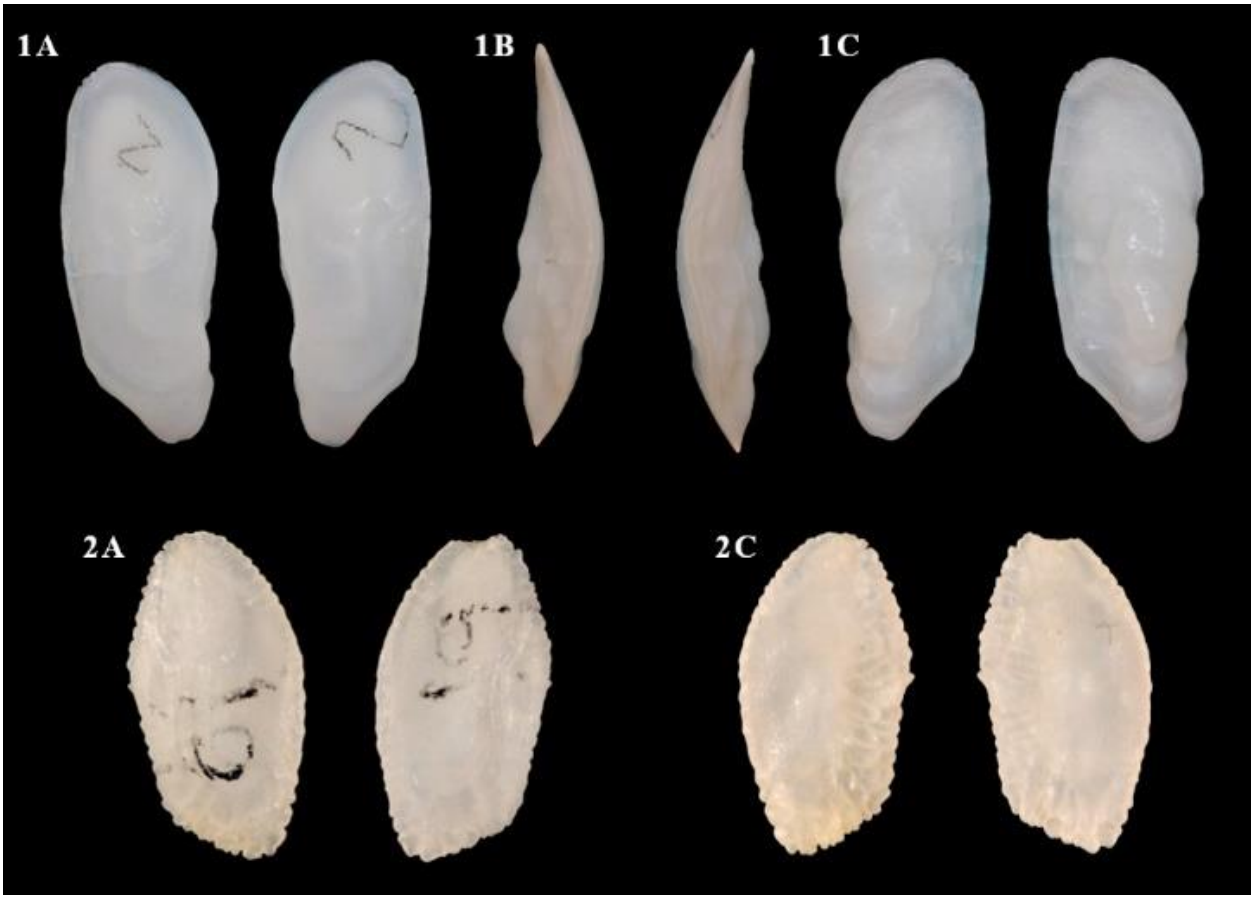

Figure 39. Spotted seatrout sagittal otoliths. Highlighting variance in otolith shape, structure, and development of protuberances. Side (A) is the proximal side of the otolith. Side (B) is the dorsal side of the otolith. Side (C) is the distal side of the otolith. The TL of individual (1) was 347mm and the OL and OW were 16.0mm and 6.2mm, respectively. The TL of individual (2) was 80mm and the OL and OW were 4.3mm and 2.3mm, respectively.

APPENDIX D

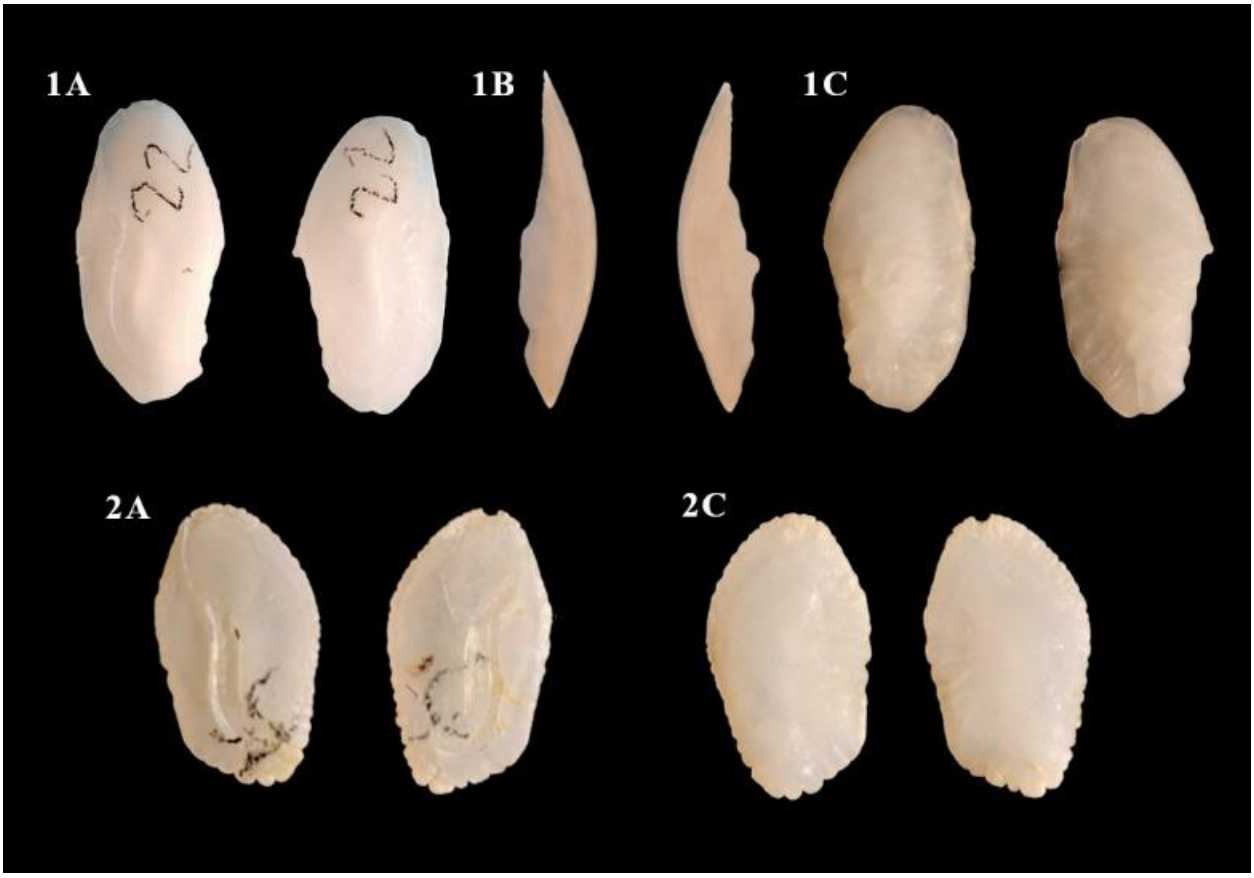

Figure 40. Sand seatrout sagittal otoliths. Highlighting variance in otolith shape, structure, and development of protuberances. Side (A) is the proximal side of the otolith. Side (B) is the dorsal side of the otolith. Side (C) is the distal side of the otolith. The TL of individual (1) was 209mm and the OL and OW were 10.8mm and 5.0mm, respectively. The TL of individual (2) was 68mm and the OL and OW were 3.8mm and 2.2mm, respectively.

APPENDIX E

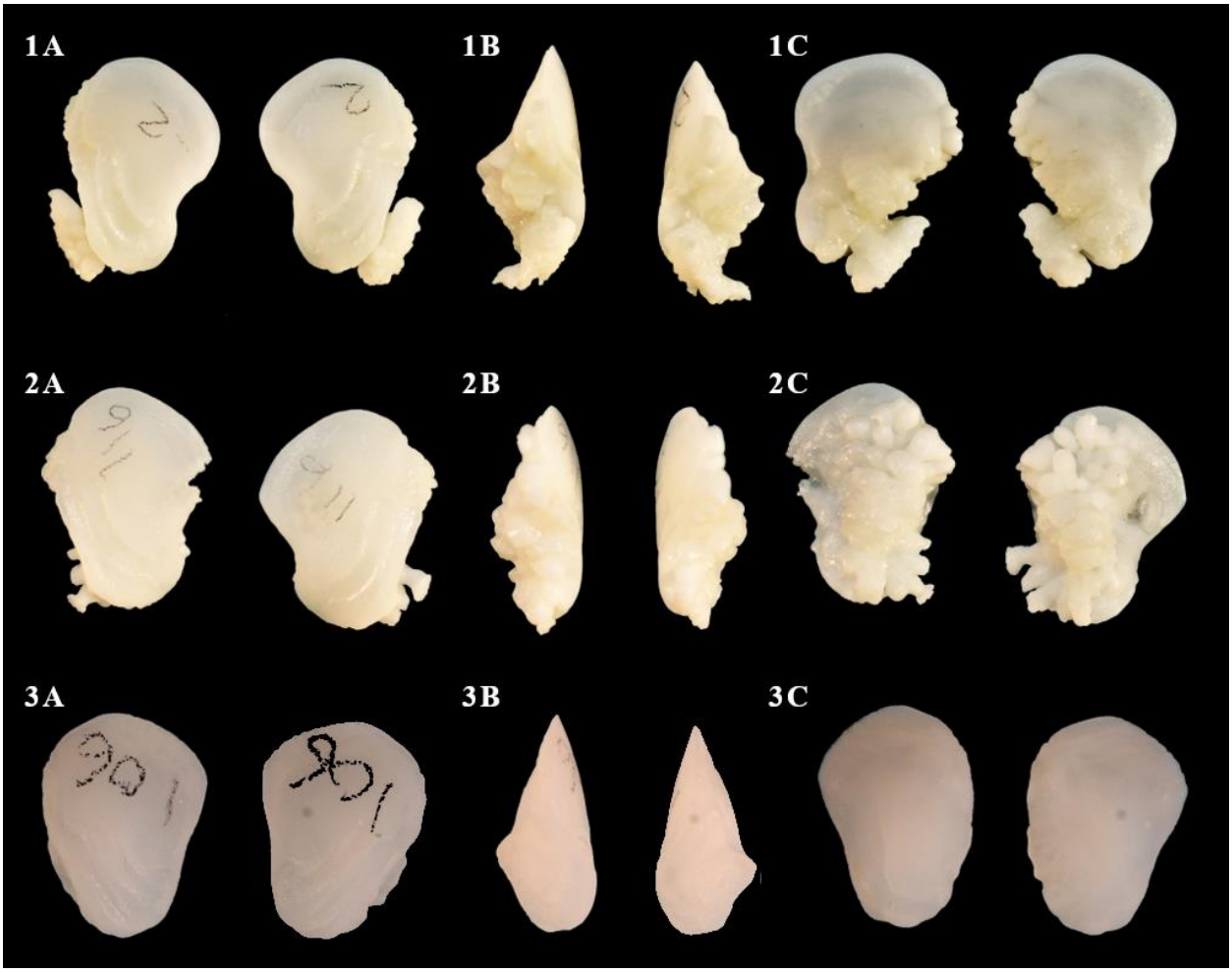

Figure 41. Atlantic croaker sagittal otoliths. Highlighting variance in otolith shape, structure, and development of protuberances – notably the development of the accessory growth center seen in individual (1) and (2). Side (A) is the proximal side of the otolith. Side (B) is the dorsal side of the otolith. Side (C) is the distal side of the otolith. The TL of individual (1) was 290mm and the OL and OW were 14.1mm and 10.8mm, respectively. The TL of individual (2) was 270mm and the OL and OW were 12.3mm and 9.4mm, respectively. The TL of individual (3) was 118mm and the OL and OW were 6.0mm and 4.4mm, respectively.

APPENDIX F

Figure 42. Spot sagittal otoliths. Highlighting variance in otolith shape, structure, and development of protuberances. Side (A) is the proximal side of the otolith. Side (B) is the dorsal side of the otolith. Side (C) is the distal side of the otolith. The TL of individual (1) was 231mm and the OL and OW were 7.9mm and 4.0mm, respectively. The TL of individual (2) was 60mm and the OL and OW were 2.8mm and 2.1mm, respectively.